Characterization of FHL2 Gene and Its Role in Human Hepatocellular Carcinoma

NG, Chor Fung

A Thesis Submitted in Partial Fulfillment

of the Requirements for the Degree of

Doctor of Philosophy

in

Biochemistry (Medicine)

The Chinese University of Hong Kong

January 2011

ProQuest LLC.
789 East Eisenhower Parkway
P.O. Box 1346
Ann Arbor, MI 48106 - 1346

Thesis Assessment Committee

Professor Shaw Pang Chui (Chair)

Professor Tsui Kwok Wing (Thesis Supervisor)

Professor Tsang Suk Ying (Committee Member)

Professor Chan Siu Yuen (External Examiner)

Abstract of thesis entitled:

Characterization of FHL2 Gene and Its Role in Human Hepatocellular Carcinoma

Submitted by NG, Chor Fung

for the degree of Doctor of Philosophy

at The Chinese University of Hong Kong in December, 2010

Abstract

Our results show that *FHL2* mRNA is downregulated in the majority of hepatocellular carcinoma (HCC) patients. The aim of this project was to assess the potential role of the *FHL2* gene and the underlying mechanisms of the aberrant gene expression in HCC. Using stable overexpression clones of FHL2 in Hep3B cells, we show that FHL2 may mediate antiproliferative effect through inhibition of the G1 to S cell cycle transition as evident from the decreased expressions of survivin and cyclin D1, as well as an increased expressions of cyclin-dependent kinase inhibitors p21 and p27. FHL2 overexpression also inhibits migration and invasion of HCC cells through epithelial-mesenchymal transition (EMT)-mediated pathway, as shown by reduction of mesenchymal marker vimentin and induction of epithelial marker E-cadherin. Surprisingly, we also demonstrated an antiapoptotic function for FHL2 overexpression with increased resistance to doxorubicin-induced apoptosis, which indicates the separation of antiproliferative and antiapoptotic role of FHL2. In summary, our findings suggest that the loss of expression of the candidate tumor suppressor gene FHL2 may be associated with HCC.

We proceed to characterize the mechanisms underlying transcriptional regulation of *FHL2* gene. We analyzed the 5'UTR of different alternative spliced variants and the expressed sequence tags. A novel transcript variant was identified and shown to be expressed in many cell lines and tissues. The two different promoters utilized by *FHL2* indicated there may be tissue-specific regulation of *FHL2*. To further elucidate the mechanism for aberrant transcription of *FHL2*, the potential promoter region as well as its methylation status was investigated. *FHL2* itself was not regulated by methylation. To explore the regulation of promoter, we generated a series of deletions mutants of the 5' flanking region of *FHL2* gene and showed that the fragment from -138 to +292 in the promoter have positive regulatory effect. The bioinformatic analysis identified putative binding sites of five transcription factors. Of these TFs, Pax-5 and ZF5 expression was downregulated and correlated with the FHL2 expression in HCC tumor samples, indicating a possible role for these transcription factors in the regulation of *FHL2* expression.

We further performed microarray analysis of the FHL2 knockout mice to identify new target genes of FHL2. Our data illustrate that FHL2 affects various genes involved in cell adhesion and motility, immune function, and transcription regulation. Of these genes, Lcn2, Bcl-6 and Creld2 belong to the category of cancer-related genes. We performed analysis of gene expression in clinical samples to identify genes relevant to human cancer and we identified the altered expression of Bcl-6 and Creld2 genes in HCC.

In addition, we also demonstrated the downregulation of FHL1 expression in HCC and showed that histone deacetylation may be involved in the repression of the *FHL1* gene in HCC. In summary, the research presented in this project provides further evidence in support of the tumor suppressing functions of FHL1 and FHL2 in HCC.

摘 要

有研究顯示 FHL2 基因在癌症中扮演重要的角色。我們的研究表示，FHL2 基因在肝細胞癌（HCC）組織的表達明顯下降。我們於是對 FHL2 在癌症中的作用及其表達調控方面進行進一步研究。利用過量表現基因，我們證實 FHL2 能抑制肝癌細胞 Hep3B 增殖，可藉由抑制 Cyclin D1 及 Survivin 表達水平以及提高細胞周期抑制蛋白 p21 和 p27 的表達，阻滯細胞由 G1 進入 S 期。此外，我們發現 FHL2 明顯抑制癌細胞遷移和侵入能力。FHL2 過度表達促使 vimentin 蛋白表達下降，E-cadherin 蛋白表達上升。所以它可能是通過調控 EMT 抑制腫瘤侵襲轉移。於此同時我們也發現，在 FHL2 高表達時具有抗凋亡的作用，FHL2 可能通過不同機制導致了細胞的生長抑制和抗凋亡作用。根據以上結果，FHL2 基因的表達下調也許與腫瘤的發生和發展中有著密切關聯。

我們進一步研究 FHL2 基因表達調控的作用機制。我們首先透過 FHL2 基因 5’ UTR 區及 EST 序列分析，對其基因轉錄變異體進行鑒定。我們對 FHL2 轉錄變異體的表達情況進行了研究。結果發現，它們可能與組織類型有密切相關。我們之後探討 FHL2 調控如何出現異常。DNA 甲基化與基因表達異常有關，但是本研究未檢測到 FHL2 基因的異常甲基化。還有通過啓動子區的克隆對表達調控進行研究，鑒定出啓動子區 1 個活性區起正調控作用(-138~+292)。我們根據生物信息學，進行預測啓動子區和轉錄因子結合位點的分析。結果顯示，這個

活性區域含有多個轉錄因子結合位點，包括 SP-1、 AP-2A、ZF5 和 Pax-5。我們發現，ZF5 和 Pax-5 基因在肝癌組織中的表現量明顯減少，以及它們與 FHL2 表達呈正相關性，表明這兩個轉錄因子有可能參與肝癌中 FHL2 的表達調控。

我們還利用基因芯片分析，對正常小鼠和 FHL2 基因敲除小鼠進行了比較，篩選出受 FHL2 調節的下游基因。結果顯示，受 FHL2 影響的基因，包括了一些與細胞黏附和移動、免疫反應、及與轉錄因子相關的基因。Lcn2、Bcl6 及 Creld2 是一些可能的腫瘤相關的基因。我們之後測定了這些基因在人肝癌樣本的表達水平，結果顯示，肝癌組織中 Bcl6 和 Creld2 表達水平均低於正常組織。它們可能是一些在人類肝癌病變過程中的新基因。

我們的研究結果還顯示 FHL 家族的另一成員 FHL1 在肝癌組織中也是低表達。我們發現 HDAC 抑制劑有效上調 FHL1 基因表達，這說明了它可能是一個受 HDAC 調控的腫瘤抑制基因。綜合而言，這些研究結果支持 FHL1 及 FHL2 可能爲肝癌相關之抑癌基因。

DECLARATION

The following people were acknowledged for their collaborative contributions to the work described in this thesis: The migration and invasion assay were performed by Dr. Judy Yuet Wa Chan; The statistical analysis of clinical data was performed by Dr. Sunny Yue Sun Cheung; The pathway enrichment analysis with Metacore was performed by Prof. Shen Bairong; Data of the glycemic control in the FHL2 knockout mice was provided by Prof. Yiu Wah Kwan and Prof. Xu Gang; Prof. Vivian Wai Yan Lui for initial help in Western blot experiments with stable cell lines.

ACKNOWLEDGEMENTS

I would like to express my sincere thanks to my supervisor, Prof. Kwok Wing Tsui, for his patient guidance, invaluable advice, and continuous support and encouragement throughout the entire period of study. Without his unstinting support, it is impossible to finish up my research work.

I want to express my special thanks to Dr. Kwok Shing Ng, a postdoctoral fellow in my laboratory for his kindly help, valuable advice and patient guidance throughout the project. My sincere thanks also go to a group of colleagues and friends from Room 610 in Mong Man Wai Building, The Chinese University of Hong Kong, for their opinions, technical support and care.

I would also like to thank the following people for their advice and great assistance with this project: Prof. Vivian Wai Yan Lui, Department of Clinical Oncology for generously providing us the antibodies and valuable advice on writing the manuscripts; Dr. Yuet Wa Chan and Prof. Kwok Pui Fung, for help with the migration and invasion experiments; Prof. Yuen Keng Ng and Prof. Bo San Lai, Department of Surgery, for providing us the primary human HCC samples and valuable comments and suggestions to the issues addressed in this dissertation; Dr. Sunny Yue Sun Cheung, Prince of Wales Hospital, for performing the statistical analysis of clinical data; Prof. Shen Bairong for performing the pathway enrichment

analysis; Dr. Patrick Ng and Dr. Wayne Zhou for their assistance with bisulfite sequencing and RT-PCR analysis of variants respectively.

Last but not least, I want to express my deepest gratitude to my family and friends for their greatest love, encouragement and support. They give me strength during my study and the completion of this thesis.

TABLE OF CONTENTS

CHAPTER 3 EXPRESSION AND FUNCTIONAL STUDIES OF FHL2

CHAPTER 4 STUDY OF FHL2 GENE AND TRANSCRIPTIONAL REGULATION IN HCC

LIST OF TABLES

LIST OF FIGURES

ABBREVIATIONS

General terms:

5'UTR	Five prime untranslated region
ACT	Activator of CREM in Testis
Akt/PKB	Protein kinase B
AP-1	Activator protein 1
AP-2A	Activator protein 2 alpha
AR	Androgen receptor
β-catenin	Beta-catenin
Bcl6	B-cell lymphoma 6 protein
BRCA1	Breast cancer 1, early onset
BSP	Bisulfite sequencing PCR
c-myc	myc proto-oncogene protein
c-jun	c-jun protooncogene
Cdk	Cyclin-dependent kinase
ChIP	Chromatin immunoprecipitation
CREB	cAMP response element binding protein
CREM	cAMP responsive element modulator
DRAL/FHL2	Downregulated in rhabdomyosarcoma LIM domain protein
E2F	E2F transcription factors
EMT	Epithelial-mesenchymal transition
ER	Endoplasmic reticulum
ERK2	Extracellular signal-regulated kinase 2
FHL	Four-and-a-half-LIM domain protein (-1, 2, 3)
FOXO1	Forkhead box O1
GCT	Giant cell tumor of bone
GO	Gene ontology
HAT	Histone acetyltransferases
HBV	Hepatitis B virus
HCC	Hepatocellular carcinoma
HCV	Hepatitis C virus
HDAC	Histone deacetylases

HDACi	Histone deacetylase inhibitors
IAP	Inhibitor of apoptosis protein
IL-6	Interleukin-6
IL-8	Interleukin-8
JAK	Janus kinase
Lcn2	Lipocalin 2
MAPK	Mitogen-activated protein kinase
MEF	Mouse embryonic fibroblasts
MEF-2	Myocyte enhancer factor 2
MMP-9	Matrix metalloprotein-9
NCBI	National Center for Biotechnology Information
NF-κB	Nuclear factor kappa B
NKX-2.5	NK2 transcription factor related, locus 5
Pax-5	Paired box protein 5
PI3K	Phosphatidylinositol 3-kinase
PLZF	Promyelocytic leukemia zinc finger protein
RANK	Receptor activator of NF-κB
Rb	Retinoblastoma protein
SP-1	Specificity protein 1
SRF	Serum response factor
STAT3	Signal transducer and activator of transcription 3
TF	Transcription factors
T/N	Tumor/normal counterpart ratio
TNF	Tumor necrosis factors
TNF-α	Tumor necrosis factor-alpha
TRAF6	TNF receptor-associated factor 6
TSG	Tumor suppressor genes
TSS	Transcription start site
Wnt	Wingless/Wnt signaling
WT	Wild-type
WT-1	Wilms' tumor 1
ZF5	Zinc finger protein 5

Materials and Methods:

%	percentage
°C	degree Celsius
×g	centrifugal force
A	Absorbance
cm^2	square centimeters
h	hour
mg	milligram (10^{-3} gram)
min	minute
ml	milliliter (10^{-3} liter)
mm	millimeter (10^{-3} meter)
mM	millimolar (10^{-3} molar)
ng	nanogram (10^{-9} gram)
rpm	revolutions per minute
µg	microgram (10^{-6} gram)
µl	microliter (10^{-6} liter)
µm	micron (10^{-6} meter)
µM	micromolar (10^{-9} molar)
U	unit
V	Voltage
cDNA	Complementary DNA
gDNA	Genomic DNA
rRNA	Ribosomal RNA
5-aza-dC	5-aza-2'-deoxycytidine
AJCC	American Joint Committee on Cancer
ANOVA	Analysis of variance
ATCC	American Type Culture Collection
BCA	Bicinchoninic acid
BrdU	Bromodeoxyuridine
BSA	Bovine serum albumin
C_T	Threshold cycle
CI	Confidence interval
CO_2	Carbon dioxide
CUHK	Chinese University of Hong Kong
DAVID	Database for Annotation, Visualization and Integrated Discovery

DEPC	Diethyl pyrocarbonate
DMEM	Dulbecco's modified Eagle medium
DMSO	Dimethyl sulfoxide
DOX	Doxorubicin
E. coli	*Escherichia coli*
ECL	Enhanced chemiluminescence
ELISA	Enzyme-linked immunosorbent assay
EMEM	Eagle's minimal essential medium
ES	Embryonic stem (cells)
EST	Expressed sequences tag
FBS	Fetal bovine serum
HRP	Horseradish peroxidase
IPA	Ingenuity Pathway Analysis
KO	Knockout
LB	Luria-Bertani
MTT	3-(4,5-dimethylthiazol-2-yl)-2,5-diphenyl tetrazolium bromide
NCBI	National Center for Biotechnology Information
O.D.	Optical density
PARP	Poly(ADP-ribose) polymerase
PBS	Phosphate buffered saline
PCR	Polymerase chain reaction
PDGF	Platelet-derived growth factor
PVDF	Polyvinylidene difluoride
qPCR	Quantitative real-time PCR
RIPA	Radioimmunoprecipitation assay
ROC	Receiver operating characteristics
RPMI	Roswell Park Memorial Institute
RT	Reverse transcription
SD	Standard deviation
SDS	Sodium dodecyl sulfate
SEM	Standard error of the mean
SPSS	Statistical Product and Service Solutions
TBST	Tris buffered saline with Tween 20
TSA	Trichostatin A
UCSC	University of California, Santa Cruz

Chapter 1

INTRODUCTION

1.1 Four-and-a-half-LIM protein 2 (FHL2)

FHL2 gene locates on chromosome 2q12-q14 and consists of 7 exons (Johannessen *et al.*, 2006). It is transcribed into a transcript of 1.5 kb in which the first three exons are non-coding, and eventually translated into a protein of 279 amino acids. Its cDNA sequence was first predicted by Morgan and Madgwick, 1996 and then cloned by two independent groups almost simultaneously (Genini *et al.*, 1997; Chan *et al.*, 1998). *FHL2* is expressed in a cell/tissue specific manner with the most abundance in heart (Chan *et al.*, 1998), a little lower expression level in ovary, a marginal expression level in brain, liver and lung (Tanahashi and Tabira, 2000). While it is not expressed in other tissues including spleen, thymus, blood leukocytes, skin and skeletal muscle or smooth muscle (Genini *et al.*, 1997; Chan *et al.*, 1998; Gabriel *et al.*, 2004).

Four-and-a-half-LIM protein 2 (FHL2) belongs to the four-and-a-half-LIM (FHL) domain family which consists of five members, FHL1, FHL2, FHL3, FHL4 and ACT (Activator of CREM in Testis) (Genini *et al.*, 1997). It was also known as

downregulated in rhabdomyosarcoma LIM (DRAL) domain protein which consists of four LIM domains and one N-terminal half LIM domain with a cell-specific distribution (Scholl *et al.*, 2000). The acronym 'LIM' was derived from the 3 transcription factors, Lin-11, Isl-1, and Mec-3, in which such a domain was first discovered (Taira *et al.*, 1995). In HepG2 cells, the endogenous FHL2 has been localized in both the cytoplasm and nucleus (Chu *et al.*, 2000; Li *et al.*, 2001; Du *et al.*, 2002; Hill and Riley, 2004; Labalette *et al.*, 2004), which is consistent with the fact that it passively shuttles between the cytoplasm and the nucleus possibly due to its small molecular mass (32 kDa) (Johannessen *et al.*, 2006). FHL2, which contains only LIM domains, has no DNA-binding activity but possesses an intrinsic transactivation function (Labalette *et al.*, 2004). The LIM domains of FHL2 consists of double zinc finger motifs, with the cysteine-rich consensus sequence [CX2CX16-23HX2CX2CX2CX16-21CX2-3(C/H/D)] (Fig. 1.1) which provide the protein-protein binding interfaces and allow FHL2 to interact with more than 50 different proteins including receptors, structural proteins, signal transducers and metabolic enzymes (Bach, 2000; Johannessen *et al.*, 2006). Corresponding to its universal distribution, FHL2 plays multiple roles, e.g., it serve as functional modifiers, adaptors and transcriptional co-activators for a series of transcription factors including androgen receptor (AR) (Muller *et al.*, 2000), activator protein-1 (AP-1) (Morlon and Sassone-Corsi, 2003), cyclic AMP response element binding protein (CREB), cAMP response element modulator (CREM) (Fimia *et al.*, 2000), breast cancer 1 (BRCA1) (Yan *et al.*, 2003), Wilms' tumor 1 (WT-1) (Du *et al.*, 2002), and nuclear factor-κB (NF-κB) (Stilo *et al.*, 2002; Labalette *et al.*, 2004).

Moreover, FHL2 could function as the co-suppressor for extracellular signal-regulated kinase 2 (ERK2) (Purcell *et al.*, 2004), serum response factor (SRF) (Philippar *et al.*, 2004), and forkhead box O1 (FOXO1) (Yang *et al.*, 2005). FHL2 is found to have diverse functions in cells including the regulation of many cellular processes such as cell survival, proliferation, differentiation, adhesion, motility, regulation of gene expression and signal transduction (reviewed in Johannessen *et al.*, 2006).

1.2 The Diverse Roles of FHL2 in Cancer

The role of FHL2 in cancer is particularly intriguing since FHL2 binds to different proteins and can function in a cell-type dependent fashion as transcriptional co-activators of several transcription factors, including androgen receptor, AP-1, CREB, BRCA1, WT-1 and NF-κB in various transformed cell types (Muller *et al.*, 2000; Morlon and Sassone-Corsi, 2003; Fimia *et al.*, 2000; Yan *et al.*, 2003; Du *et al.*, 2002; Stilo *et al.*, 2002) or as transcriptional co-repressors of ERK2, promyelocytic leukemia zinc finger protein (PLZF), SRF and FOXO1 (Purcell *et al.*, 2004; McLoughlin *et al.*, 2002; Philippar *et al.*, 2004; Yang *et al.*, 2005). FHL2 was first identified as being downregulated in human rhabdomyosarcoma cells, suggesting a role in tumor development (Genini *et al.*, 1997). Many recent studies have reported the differential expression of FHL2 in tumor tissues. Interestingly, FHL2 is overexpressed in breast cancer (Martin *et al.*, 2007), prostate cancer (Kinoshita *et al.*, 2005), ovarian cancer (Gabriel *et al.*, 2004), gastrointestinal cancer (Wang *et al.*, 2006), glioma (Li *et al.*, 2008) but down-regulated in liver cancer (Ding *et al.*,

2009b), making the role of FHL2 in cancer development illusive. In breast cancer, there are reports showing that FHL2 is downregulated in many breast cancer cell lines but overexpressed in mammary carcinoma tissues (Martin *et al.*, 2007; Yan *et al.*, 2003). In melanoma cells, FHL2 was found to promote cell growth (Chen *et al.*, 2003). Alternatively, FHL2 triggers apoptosis in human RD, monkey kidney COS-1 and normal mouse fibroblast NIH 3T3 cell lines (Scholl *et al.*, 2000) but plays an antiapoptotic role in glioblastoma cells (Li *et al.*, 2008). Most recently, FHL2 was found to act as a potent epithelial-mesenchymal transition (EMT) inducer by stimulating vimentin and MMP-9 expressions and causing a loss of E-cadherin in colon DLD1 cells (Zhang *et al.*, 2010) but increases the expression of E-cadherin in colon HT-29 cells but reduced activity of the transcription factor NF-κB (Amann *et al.*, 2010). The intriguing aspects of FHL2 being as oncoprotein or tumor suppressor may be related to its interaction with different partner proteins in different cell types. So far, the precise FHL2 function in liver cancer cells is still unclear.

1.3 Hepatocellular Carcinoma - HCC

Hepatocellular carcinoma (HCC) is the sixth common cancers worldwide and third leading cause of cancer-related death (Parkin *et al.*, 2005). It is often associated with cirrhosis and the main risk factors for HCC include infection with hepatitis B virus (HBV) or hepatitis C virus (HCV) (El-Serag and Rudolph, 2007; Blum, 2005), exposure to hepatocarcinogens such as aflatoxin B1 (Soini *et al.*, 1996) and alcohol (Donato *et al.*, 2002) which results in damage to liver tissue. Continuous tissue damage-regeneration process will lead to chronic liver disease (e.g. cirrhosis)

characterized by abnormal liver nodules formation and collagen deposition. The hyperplastic nodules with increased genomic instability can develop into dysplastic cells and ultimately into HCC after further genetic or epigenetic changes. Tumors with poorly differentiated cells represent the most malignant form of HCC (Fig. 1.2). The cancer is highly aggressive, which has a rapid growth and high tumor recurrence. The available therapies are chemotherapy, radiotherapy, surgical resection and liver transplantation. However, the common problems encountered are late diagnosis and treatment resistance that reduce the survival of patients (Thomas and Abbruzzese, 2005). Currently, there is no effective therapy for patients with advanced cancer or metastasis. HCC patients therefore have very poor prognosis. Molecular therapy may be useful in the future years. The increased knowledge of the molecular pathways involved in HCC pathogenesis has led to the development of new therapeutic agents. Anti-cancer agents which target the signaling pathways related to cell proliferation, differentiation, angiogenesis, invasion and metastasis have been being developed in recent years with the aim to reverse, prevent or delay tumorigenesis (Whittaker *et al.*, 2010; Pang and Poon, 2007; Aravalli *et al.*, 2008; Greten *et al.*, 2009).

1.4 Genetic and epigenetic mechanisms of HCC Development

The exact mechanism for the pathogenesis of HCC is still not clearly understood but accumulation of aberrant genetic and epigenetic changes is found to be closely associated with hepatocarcinogenesis. Mutation of oncogenes and tumor suppressor genes could be one of the mechanisms (Whittaker *et al.*, 2010). Notably, gene silencing of tumor suppressor genes (TSG) and critical cancer-related genes by DNA

hypermethylation of promoter region is one of several epigenetic mechanisms that draws much attention in recent years. DNA methylation typically occurs in the clusters of CpG dinucleotides called CpG islands which are found near the transcription start-site, which resulted in the transcriptional inactivation. The hypermethylation is thought to be an important and early event in carcinogenesis. The study of CpG hypermethylation pattern serves as useful biomarkers for screening and diagnosis of HCC patients (Lee *et al.*, 2003; Zhang *et al.*, 2007). Histone deacetylation is another epigenetic mechanism underlying the inactivation of TSG. Histone acetylation and deacetylation are dynamic processes regulated by histone acetyltransferases (HATs) and histone deacetylases (HDACs) respectively that controls chromatin structure and function and play a role in regulating gene expression (reviewed in Peterson, 2002). Histone acetylation is in general associated with open chromatin structure that enhances transcription, whereas deacetylation of histones is in general associated with inactive chromatin and transcription repression (Workman and Kingston, 1998; Hebbes *et al.*, 1998). HDAC inhibitors (e.g. trichostatin A) have been shown to have anti-tumor effect *in-vitro* and *in-vivo* by various mechanisms including cell growth arrest, apoptosis and differentiation induction (Yamashita *et al.*, 2003; Venturelli *et al.*, 2007). HDAC inhibitors were shown to activate a number of genes including the apoptosis-related proteins through increased histone acetylation (Chiba *et al.*, 2004).

1.5 FHL2 Gene Regulation

The mechanisms of the transcriptional regulation of FHL2 gene are still unknown. To better understand regulation of FHL2, we characterized the FHL2 gene and the splice variants which is a critical part of gene regulation. The transcript variants of FHL2 have never been precisely characterized. They may have a role in the differential expression of the gene in different tissues and the differential expression of various isoforms may be related to cancer. Besides, our project will investigate the mechanisms that mediate the epigenetic regulation of FHL proteins in HCC, such as DNA methylation, histone modifications which may explain their deregulated expression in HCC. Although FHL2 was indicated to be regulated epigenetically in hepatoma cells in a microarray study (Dannenberg and Edenberg, 2006), no direct evidence of DNA methylation has been available from literature. Previous studies have shown that FHL2 promoter is likely to be p53-responsive (Scholl *et al.*, 2000) and androgen could induce expression of FHL2 that is mediated by the action of serum response factor on FHL2 promoter (Heemers *et al.*, 2007). In fact, different transcription factor binding sites are mapped to the FHL2 promoter using computer prediction programs (for example, SRF, NKX-2.5, MEF-2, E2F and AP-1) (Johannessen *et al.*, 2006). The regulation of FHL2 promoter has not been extensively studied and is another aspect worth of investigation.

1.6 Mechanisms of FHL2 Involved in Carcinogenesis

FHL2 has been reported to interact with many proteins or transcription factors to modulate their activity (see references above). In fact, FHL2 may be involved in enhancing or suppressing the activation of NF-κB (Stilo *et al.*, 2002, Bai *et al.*, 2005),

although direct association of FHL2 and NF-κB has not been addressed (Qiao *et al.*, 2009), as well as coactivation with β-catenin (Wei *et al.*, 2003). NF-κB and β-catenin are transcription factors that are important in regulating cell proliferation and play important role in the aberrant signaling of HCC. In fact, some of the target genes regulated by FHL2 are involved in Wnt/β-catenin signaling (for instance the Wnt-responsive genes cyclin D1, c-myc, c-jun and IL-8) (Wei *et al.*, 2003). Previous reports show that FHL2 is able to regulate cyclin D1 expression (Labalette *et al.*, 2008; Martin *et al.*, 2002). FHL2 may regulate cyclin D1 directly by cooperating with β-catenin and occupies the cyclin D1 promoter (Wei *et al.*, 2003; Labalette *et al.*, 2004), or by binding with FOXO1 to counteract its repression at the cyclin D1 promoter (Yang *et al.*, 2005). It may also regulate cyclin D1 via indirect mechanism by negatively regulate the extracellular signal-regulated kinase (ERK) 2 and interfering the mitogen-activated protein kinase (MAPK) signaling pathways which also play important roles in regulating cell proliferation, survival and apoptosis (Purcell *et al.*, 2004). Therefore in our project, the effect of FHL2 on the cell cycle and apoptosis regulatory proteins will be investigated.

1.7 FHL2 Knockout Mice

FHL2 knockout mice have recently been generated and are viable and maintain normal cardiovascular development and function as their wild-type (WT) littermates (Chu *et al.*, 2000a), despite the fact that FHL2 is important in promoting mouse myoblast differentiation and muscle development (Martin *et al.*, 2002). The lack of cardiac phenotype in FHL2-deficient mice may be due to functional redundancy

among the FHL family members (Chu *et al.*, 2000b). However, the mice were shown to display mild phenotypes with defects in bone formation due to increased bone resorption (Bai *et al.*, 2005), impaired skin wound healing (Wixler *et al.*, 2007) and exaggerated response to cardiac hypertrophic effect following β-adrenergic stimulation in the heart (Kong *et al.*, 2001). This suggests that FHL2 may also play a role in osteoporosis and wound healing. FHL2 may also play a role in myocardial inflammation and ischemic injury as it is associated with upregulation of cytokine genes in response to cardiac injury (Wan *et al.*, 2002; Sun *et al.*, 2006).

1.8 Microarray Study of FHL2 Knockout Mice

In the paper we also conducted a novel microarray study to analyze the gene expression in liver of FHL2-deficient mice. A similar microarray study has been reported but in immortalized FHL2-/- mouse embryonic fibroblasts (MEF) (Labalette *et al.*, 2008). Interestingly, FHL2-/- cells showed a lower rate of proliferation than WT MEFs. The decreased in proliferation was associated with downregulation of several G1/S and G2/M cyclins, and impaired Rb phosphorylation together with downregulation of cyclin dependent kinase (Cdk) inhibitors. This study shows that FHL2 plays key roles in regulating cell cycle-related proteins and cell proliferation. Since FHL2 interacts with many transcription factors, it may be possible that FHL2 can affect various signaling pathways. The microarray analysis of FHL2 knockout mice could provide information of the genes that are regulated by FHL2 at the whole genome level as well as the signaling pathways mediated by FHL2. By combining the results from microarray data and expression analysis in

clinical samples, hopefully we may identify some novel target genes of FHL2 with altered expression in the HCC tumors. They may play essential roles in the tumor development.

1.9 FHL1 and FHL3 Protein

FHL1 and FHL3 also belong to the FHL family of transcription cofactors which have high homology to FHL2 (47.9% and 51.8% identical in amino acid sequence to FHL2 respectively) (Johannessen *et al.*, 2006). *FHL1* gene has at least three different isoforms (FHL1, FHLB, FHL1C) showing different tissue specificities (Lee *et al.*, 1998; Lee *et al.*, 1999; Ng *et al.*, 2001). FHL1 has the widest tissue distribution, with major expressions in heart, skeletal muscle, placenta, ovary, prostate, small intestine, colon, spleen and testis, and low expressions in brain, lung, liver, pancreas and thymus. On the other hand, FHL3 was predominantly expressed in the skeletal muscle and cardiac tissue (Morgan and Madgwick, 1999; Chu *et al.*, 2000b). FHL1 was shown to play a role in muscular dystrophies and cardiovascular disease (Shathasivam *et al.*, 2010), whereas FHL3 may play a role in myogenesis (Cottle *et al.*, 2007). Recent studies suggest that FHL1, and possibly FHL3, may also play a crucial role in cancer (Ding *et al.*, 2009b). Interestingly, FHL1 is downregulated in many types of cancers such as brain, breast, kidney, liver, lung, prostate, skin, gastric, thyroid and bladder cancers (Shen *et al.*, 2006; Xun *et al.*, 2008; Sakashita *et al.*, 2008; Bhattacharjee *et al.*, 2001; Fryknäs *et al.*, 2006; Matsumoto *et al.*, 2010). It was discovered that FHL1 can prevent cells from gaining the anchorage independence and ability to migrate during cell transformation (Shen *et al.*, 2006). In

addition, FHL1 overexpression in breast cancer cells is able to inhibit cancer cell growth (Ding *et al.*, 2009a). These studies suggest a putative TSG role for FHL1 and FHL3. Our project is also aimed at investigating the possible role of these genes in HCC development.

1.10 Projective Objectives and Long Term Significance

Understanding the molecular mechanisms of HCC is important to the development of effective agents against specific molecular targets. The previous studies support the hypothesis that FHL proteins may play a role in tumorigenesis. Our project aims to investigate the possible role of FHL2 (FHL1 and FHL3 as part of project) in HCC development. This includes studies of functional roles of FHL2, the transcriptional regulation and the target genes downstream of FHL2. The project will be beneficial to the understanding of the molecular pathogenesis of HCC as well as for the diagnosis of HCC and the development of novel targeting therapies. The specific objectives of our project are:

Study of Functional Roles of FHL Proteins

(i) Evaluation of the expression of FHL1-3 genes in liver cancer cell lines and biopsy samples from HCC patients which serves as a basis for further investigation; (Chapter 3 & 6)

(ii) Correlations between FHL1 and FHL2 gene expression and the clinical-pathological parameters to identify any possible associations. They may be useful as biomarkers for predicting the disease states or outcomes for HCC patients; (Chapter 3 & 6)

(iii) Establishment of a stable HCC cell line over-expressing FHL2 and study of the oncogenic functions of FHL2 protein in a number of *in-vitro* bioassays; (Chapter 3)

Study of the FHL2 Gene and Transcriptional Regulation

(iv) Characterization of the alternatively spliced variants of human *FHL2* gene by *in silico* and RT-PCR analysis and their expression pattern in liver cancer; (Chapter 4)

(v) Gene mutation analysis of FHL2 to identify any non-synonymous somatic mutations that could contribute to HCC carcinogenesis; (Chapter 4)

(vi) Study of the promoter regulation of FHL2 by transcription factor binding sites analysis; (Chapter 4)

(vii) Study of the mechanisms that are responsible for the epigenetic regulation the FHL genes in liver cancer cells; (Chapter 4 & 6)

Study of Downstream Genes by Microarray Analysis

(viii) Gene expression profiling of FHL2 knockout mice which aims to identify the genes regulated downstream of FHL2 and to determine whether their expressions were altered in HCC tumor. (Chapter 5)

The project aims to combine the information from both *in-vitro* assay and clinical samples to support a role of FHL proteins in HCC.

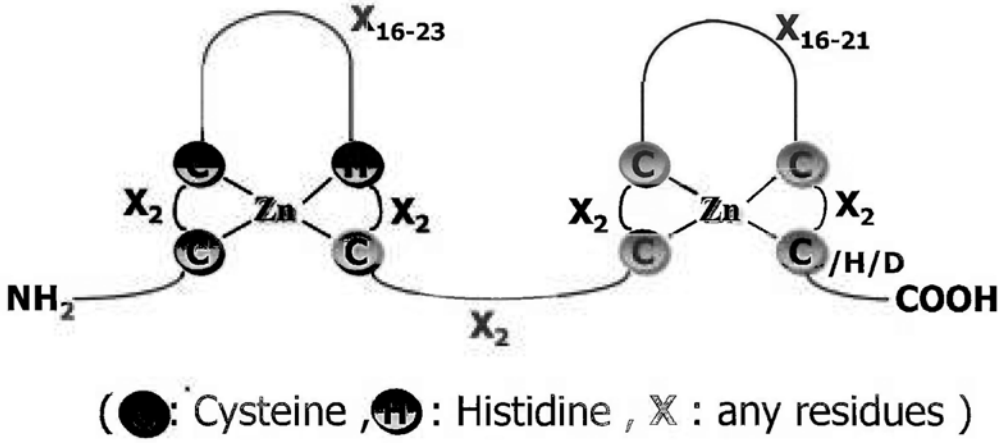

Fig. 1.1: Schematic diagram of a LIM domain, with a C_2HC and C_4 motif. (C = Cys, H = His, D = Asp, X = variable amino acid)

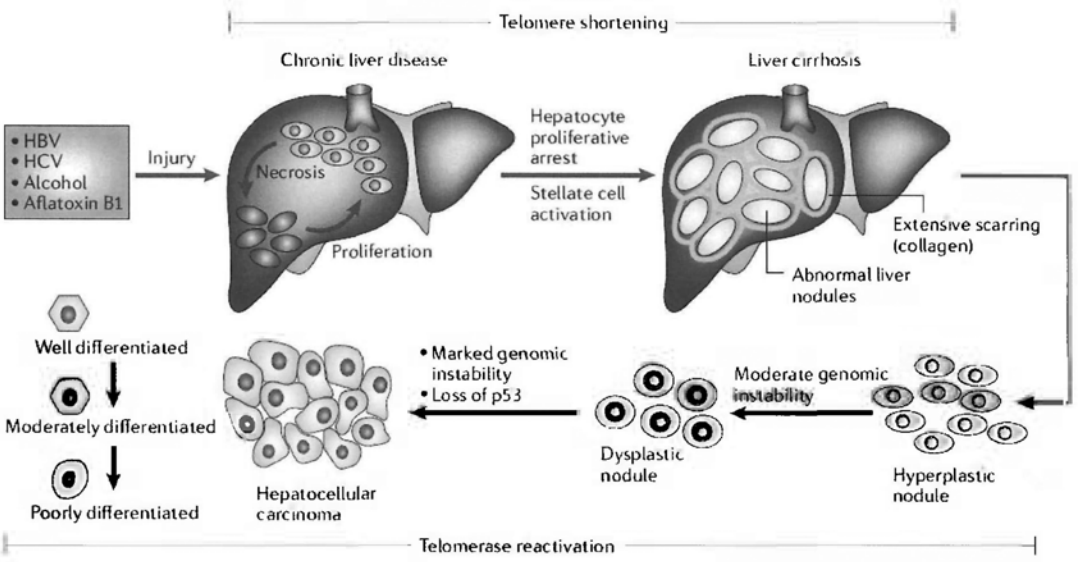

Fig. 1.2: Pathogenesis of HCC. Continuous tissue damage-regeneration process will lead to a chronic liver disease (cirrhosis) characterized by abnormal liver nodules formation and collagen deposition. The hyperplastic nodules with increased genomic instability can develop into dysplastic cells and ultimately HCC which can be further classified into well, moderate and poorly differentiated forms. (The figure is copied from Farazi and DePinho, 2006).

Chapter 2

MATERIALS AND METHODS

2.1 Cell lines and cell culture method

2.1.1 Cell lines, medium and culture conditions

Culture media, supplements, and subculturing reagents were purchased from Invitrogen. Sterile disposable culture plastic wares (Iwaki) and pipettes were used in all cell culture studies. The following cell lines were used: hepatocellular carcinoma cells (Huh7 from Japanese Collection of Research Bioresources; Hep3B from ATCC); hepatoblastoma cells (HepG2 from ATCC); immortalized normal liver cell lines (LO2 and MiHA from Cell Bank of the Chinese Academy of Sciences; WRL68 from ATCC); colon adenocarcinoma cells (Caco-2); breast adenocarcinoma cells (MCF-7); cervical carcinoma cells (Hela) and glioblastoma cells (U138MG) (all from ATCC). HepG2 and Hep3B were maintained in Roswell Park Memorial Institute (RPMI) medium-1640. Huh7, WRL68, LO2, MiHA was maintained in Dulbecco's modified Eagle medium (DMEM). Caco-2, MCF-7, Hela and U-138MG were maintained in Eagle's minimal essential medium (EMEM). All the media were supplemented with 10% fetal bovine serum (FBS), 100 U/ml of penicillin and 100 μg/ml of streptomycin. Cells were grown in 75 cm^2 culture flask and were maintained at 37°C

in a 5% CO_2 humidified incubator. They were subcultured using 0.25% trypsin every 4-5 days before reaching about 90% confluence. All the cell lines used were adherent cells.

2.1.2 Freezing Cells

Cells from confluent 150 cm^2 culture flask were washed with PBS, trypsinized and resuspended in the growth medium to inactivate trypsin. After centrifugation at 200 ×g for 5 min, the medium was aspirated and the pellet was resuspended in 3 ml complete medium with 10% DMSO (density: 3-5 × 10^6/ml). The cell suspension was transferred to cryovials and placed into Nalge Nunc slow-freeze container at -80°C overnight before storage in liquid nitrogen.

2.1.3 Thawing cells

The frozen cells were thawed quickly at 37°C and diluted in 5 ml growth medium. The cell suspension was centrifuged at 200 ×g for 5 min and the medium was aspirated. The pellet was resuspended in complete medium and transferred to 75 cm^2 flask to allow growth at 37°C/5% CO_2.

2.2 Clinical samples and sample selection criteria

Tumorous HCC tissues and adjacent non-tumor tissue (at least 1-cm distance away from the tumor edge) were collected from patients who underwent surgical resection at the Prince of Wales Hospital, Hong Kong between 1998 and 2005. Written consent was obtained from the patients prior to tissue harvesting and the

study protocol was approved by the ethics committee of the Chinese University of Hong Kong. The tissues were immediately snap-frozen in liquid nitrogen and stored at -80°C until processed for RNA extraction. Human tissue samples were randomly selected from our tissue collection. Samples with definitive demographic, clinicopathological and follow-up records were used for our analyses. All the selected tissues collected had the following characteristics:- (1) collected before any treatment; (2) with/without HBV/HCV infection; (3) age ≥ 20 years old; (4) primary HCC; and (5) non-necrotic. The characteristics of patients are listed in Table 2.1. For more details of patient characteristics, please refer to Supplementary Table S2.

2.3 FHL2 knockout mice

The FHL2 knockout (KO) mice were previously generated by homologous recombination in ES cells (Chu *et al.*, 2000a). In the knockout construct, a 300-bp deletion was made from the ATG start codon and replaced with a cDNA encoding *LacZ* and containing a pGKneo cassette. FHL2 KO mice were generated on the hybrid Black Swiss/129-SV/J background. Breeding pairs of FHL2 heterozygous mice were maintained in our laboratory and used to generate homozygous KO ($FHL2^{-/-}$) and WT littermates. Mice were weaned and genotyped at 3 weeks of age. PCR analysis was carried out on mouse tail genomic DNA using primers for the *FHL2* gene and *neo* cDNA with the following conditions: denaturation at 94°C for 4 min, followed by 31 cycles of 30 s at 95°C, 30 s at 60°C, and 1 min at 72°C. All animals were housed in the Laboratory Animal House of CUHK and maintained under standard conditions.

2.4 Oligonucleotides

All oligonucleotides were purchased from Sigma Proligo. Oligonucleotide sequences are given in Table 2.2. The primer pairs were designed using the primer design software Primer3 (http://frodo.wi.mit.edu/) or the NCBI Primer-Blast (http://www.ncbi.nlm.nih.gov/tools/primer-blast/).

2.5 General methods for DNA works

2.5.1 Recombinant DNA techniques

The *E. coli* strain DH5α was used for cloning experiments. Solid media and liquid broth of LB (Luria-Bertani) was used for culture of bacteria. Selection of insert was performed by growing cells on agar plates as well as in liquid culture at 37°C using 100 μg/ml ampillicin under vigorous shaking at 250 rpm. Procedures for DNA purification, restriction and ligation, agarose gel electrophoresis and transformation of *E. coli* by heat shock were carried out as described by Sambrook *et al.*, 1989. Restriction enzymes and ligase were purchased from New England Biolabs and used according to their protocols. Bacterial culture media were purchased from USB Corporation.

2.5.2 Plasmid DNA extraction

Plasmid DNA was extracted from bacterial cultures using either the Qiagen Plasmid Mini Kit or Qiagen Plasmid Midi Kit according to manufacturer's instructions. The former was used for small-scale preparation and the latter was used

to prepare plasmid DNA for cell transfection. The yields and quality of obtained plasmids were determined by spectrophotometry (Nanodrop ND-1000) and agarose gel electrophoresis. The purified plasmid DNA should have an $A_{260/280}$ ratio between 1.8-2.0 and an $A_{260/230}$ ratio $\geq$ 1.8.

2.5.3 Genomic DNA extraction

Genomic DNA was extracted from cells or tissues using proteinase K digestion followed by extraction with QIAamp DNA Mini Kit according to manufacturer's instructions (Qiagen). The concentration and quality of the DNA preparation was determined by a spectrophotometer. Pure DNA should have an A_{260}/A_{280} ratio of 1.7 to 1.9, indicating the absence of proteins. The A_{260}/A_{230} ratio should be 1.8 to 2.0, indicating the absence of other organic compounds or cellular contaminants. Integrity of DNA was also checked by agarose gel electrophoresis. For genomic DNA, a sharp band of large molecular weight should be observed on agarose gel.

2.6 RNA extraction

2.6.1 RNA extraction from cells

For RNA isolation, cells were grown in 60 mm dishes. Total RNA was extracted from cell monolayer by lysis with 1 ml TRIzol reagent (Invitrogen) and passing the lysates several times through a pipette. After incubation for 5 min at room temperature, 200 µl of chloroform was added and the tubes were shaken vigorously for 15 s and left at room temperature for 2 min. Following centrifugation (12,000 ×g for 10 min at 4°C), the mixture separates into the lower and upper phase. The

aqueous upper phase containing the RNA was transferred to a new tube and mixed with equal volume of 70% ethanol. The sample was then applied to the RNeasy mini column for the RNA to bind to the membrane, followed by RNA purification using the RNeasy Mini Kit (Qiagen). RNA was finally eluted in 30 µl ultra pure nuclease-free water (Gibco-BRL).

2.6.2 RNA extraction from mouse and human tissues

Standard procedures were followed when handling RNA to avoid RNase contamination. In animal experiment, the dissecting instruments and glassware used were baked in a dry oven for 6 h at 180°C. Mice were sacrificed by cervical dislocation and the livers were quickly removed and dissected into four major lobes, rinsed in cold DEPC-treated PBS to remove blood, and immediately snap-frozen in liquid nitrogen and stored at -80°C until RNA extraction. Frozen human liver samples were retrieved from the tissue bank of Department of Surgery. To perform RNA extraction, tissues were quickly cut into small pieces (<30 mg) with a sterile razor blade and placed into each 2 ml eppendorf tube with 0.6 ml of TRIzol reagent on ice. The samples were homogenized at short intervals of about 30 s using a tissue homogenizer (Ultra-turrax T25, IKA). The tubes were kept on ice to prevent overheating and RNA degradation. After complete lysis, the total RNA was extracted by the TRIzol and RNeasy methods as mentioned above. The purified RNA was eluted in 50 µl RNase-free water.

2.6.3 RNA quantification and quality analysis

The RNA concentration (ng/μl) and quality were determined with a Nanodrop ND-1000 spectrophotometer (NanoDrop Technologies). Pure RNA has an A_{260}/A_{280} ratio (absorbance readings at 260 nm/280 nm) of 1.9 to 2.1. The $A_{260}/_{230}$ ratio for RNA should be greater than 2.0 (a ratio lower than that indicates the presence of contaminants in RNA). The integrity and overall quality of RNA was also checked by 1% agarose gel electrophoresis and ethidium bromide staining. Intact RNA should give sharp ribosomal bands of 28S rRNA and 18S rRNA (the ratio being approximately 2:1) without any smearing of bands.

2.7 Reverse Transcription

Aliquot of 1 μg total RNA was used for reverse transcription (RT) using QuantiTect Reverse Transcription Kit (Qiagen). Briefly, the RNA sample was treated with gDNA wipeout buffer at 42°C for 2 min to remove contaminating genomic DNA and then reverse transcribed into cDNA using the Quantiscript RT buffer and a RT primer mix containing oligo-dT and random hexamers, and the reactions were carried out for 30 min at 42°C in a thermocycler. The reverse transcriptase was inactivated by incubation at 95°C at 3 min. The cDNA was stored at -20°C until use.

2.8 Quantitative real-time PCR

Real-time PCR analysis of gene expression was performed with ABI 7500 Fast Real-time PCR system (Applied Biosystems). Real-time PCR was performed in 96-well optical plates and the real-time PCR mixtures (final volume 10 μl) consists of 2 μl cDNA (diluted 1:10 in nuclease-free water), 5 μl Power SYBR Green PCR

Master Mix (2×) (Applied Biosystems) and 125 nM forward and reverse primers. All samples were analyzed in triplicates and no-template controls were included for every experiment. The PCR cycling conditions included an initial step of 50°C for 2 min and initial denaturation at 95°C for 10 min, followed by 40 cycles of amplification at 95°C for 15 s and 60°C for 1 min. Dissociation analysis was performed at the end of each run to check the specificity of PCR reaction. PCR product was also checked by gel electrophoresis. The comparative C_T method ($2^{-\Delta\Delta C_T}$) was used to calculate the relative amounts of each mRNA between samples, normalized to the endogenous housekeeping gene β-actin according to the following equation:

Relative expression (ratio of sample A/ sample B)

$=2\text{^-}[(C_T \text{ target} - C_T \text{ β-actin})_{\text{sample A}} - (C_T \text{ target} - C_T \text{ β-actin})_{\text{sample B}}]$

C_T value represents average of the triplicate C_T values.

2.9 Clinical Correlation Study

The clinical record and pathologic information of each patient was analyzed. The information includes sex, age, tumor size, tumor number, clinical staging, HBV/HCV infection, pathological grade of tumor, tumor characteristics, etc. The tumor staging was classified according to the American Joint Committee on Cancer (AJCC) system that was based on TNM classification with regard to tumor size (T), degree of invasion to local lymph node (N) or distant metastasis (M). A summary of clinical characteristics of the HCC patients were shown in Table 2.1. The clinicopathological correlation study was conducted in 47 patients. Box plot was

used to show the distribution of the values and tests of differences between groups were performed using the Mann-Whitey *U* test or Kruskal-Wallis test with a significance level set at 0.05. All statistical analyses were performed using SPSS software (SPSS Inc, Chicago).

2.10 Survival analysis

36 patients were included in the survival analysis (some patients were excluded from analysis because of post-operative mortality which would affect the analysis). Survival analysis was performed using a Cox proportional hazard model which calculates the risk of death (hazard ratio) given by the Exp(B) value and its 95% confidence interval (CI). For construction of survival curves, Kaplan and Meier survival analysis was performed and the differences between two groups were compared by the log-rank test. The cutoff level for FHL2 expression was determined by receiver operating characteristics (ROC) curve analysis. All statistical analyses were performed using SPSS Software.

2.11 Cloning of FHL2 expression vector

The open reading frame of FHL2 was amplified by polymerase chain reaction (PCR) by the primers FHL2cDNA-for and FHL2cDNA-rev (Table 2.2). PCR was carried out in 20-μl reaction mixtures containing 1x Phusion GC buffer (Finnzymes), 200 μM of each of dNTP, 250 nM of each primer, and 0.5 U Phusion High-Fidelity DNA polymerase (Finnzymes). PCR conditions were 98°C 1 min, and then 30 cycles of denaturation at 98°C for 15 s, annealing at 60°C for 30 s, and extension at 72°C

for 45 s, and a final extension at 72°C for 10 min. The PCR fragment (840 bp) was recovered from the agarose gel, and cloned into *Eco*RI and *Xho*I sites of pcDNA3.1(+) empty vector (Invitrogen) to obtain the pcDNA3.1-FHL2 expression vector. The identity of the clone was confirmed by restriction analysis of plasmid DNA and sequencing analysis.

2.12 Establishment of FHL2 stable cell lines

1×10^5 Hep3B cells were plated per well in 6-well plate (at 60-70% confluence) and transfected 24 h after plating with 2 μg linearized plasmid DNA in Opti-MEM medium (Invitrogen) using Lipofectamine Plus Reagent (Invitrogen). Plasmids were linearized by *Bgl*II enzyme digestion, followed by gel purification with a gel extraction kit (GE Health Care). Medium was replaced with complete growth medium 4 h after transfection. Forty-eight hours later, transfected cells were split at a ratio of 1:15. Selection was then performed by administration of G418 antibiotics (Invitrogen) in the medium at a concentration of 400 μg/ml for 21 days. Medium was replenished every 3 to 4 days. The G418 concentration used for selection was determined by establishing a dose-response curve on the non-transfected cells using MTT assay. The G418-resistant colonies were isolated by a limited dilution approach and the clones were analyzed for expression by real-time PCR and Western blot analysis. They were expanded as stable cell lines and maintained in regular growth medium containing 200 μg/ml of G418 selection agent.

2.13 Trypan Blue Exclusion Assay

Cell proliferation was determined by cell counting. Stable clones of Hep3B cells were plated in 6-well plates at a density of 5×10^4 cells per well in 2 ml complete growth medium and incubated at 37°C. Cells were harvested by trypsin/EDTA dissociation at various time points. The cell pellet was resuspended in 100 µl of growth medium and mixed with the same volume of 0.4% trypan blue (Sigma). The number of trypan blue-excluded cells was counted using a standard hemocytometer.

2.14 BrdU Incorporation Assay

The assay was performed using the colorimetric bromodeoxyuridine (BrdU) kit (Roche Diagnostics) according to the manufacturer's instructions. Stable clones of Hep3B cells were plated in 96-well culture plates at a density of 1,500 cells/100 µl medium per well and incubated at 37°C. Cells were labeled with BrdU reagent for the final 20 h and labeled cells were detected by a horseradish peroxidase (HRP)-conjugated anti-BrdU antibody. The wells were washed four times with wash buffer to remove unspecific binding of antibody. Substrate solution was added to develop the reaction for 30 min. The absorbance at 450 nm after blank correction (cell-free medium control subtracted) is proportional to the number of proliferating cells.

2.15 Migration and Invasion Assay

A Transwell Boyden chamber assay system was used to assess cell migration and invasion activity (Fig. 2.1). Transwell inserts with 8 µm pore size (SPL Life Sciences) were placed into individual well of a 24-well culture plate. The day before

the experiment, cells were seeded into flasks with medium containing 1% FBS. 1×10^5 cells were seeded in 300 µl FBS-free medium in the upper compartment of each well. The lower chamber was filled with 600 µl of complete medium containing the chemoattractant platelet-derived growth factor (PDGF)-BB (10 ng/ml). Cells were allowed to migrate through the microporous membrane for 7 h. At the end of incubation, cells on the upper side of the membrane were removed by gently wiping with a cotton swab and the cells that were migrated on the lower surface of the membrane were fixed with 2% paraformaldehyde, stained with hematoyxlin, and counted manually on photographs taken with a magnification of 200x. A total of five random fields were counted for each well. The invasion assay was performed using the same system except that the Transwell filter was pre-coated with 50 µl Matrigel basement membrane matrix (BD Biosciences) and 1×10^6 cells/well were allowed to migrate for 42 h.

2.16 Protein extraction and protein quantification

Cells were seeded at about 50% confluency in 100mm dishes (1×10^6/dish) and grown overnight. The cells were washed twice with cold PBS, collected by scrapping and lysed in 400 µl of cold Radio-Immunoprecipitation Assay (RIPA) buffer (Millipore) (50 mM Tris-HCl (pH 7.4), 150 mM NaCl, 0.25% deoxycholic acid, 1% NP-40 and 1 mM EDTA) supplemented freshly with a cocktail of protease inhibitors (Roche, Complete-Mini tablets). The cell extracts were incubated on ice for 30 min with occasional vortexing every 10 minutes. Cell debris was removed by centrifugation at 14,000 ×g for 10 min at 4°C and the supernatant was collected and

frozen in aliquots at -80°C. The protein concentration was determined by a bicinchoninic acid (BCA) protein assay. Briefly, 5 μl of samples or BSA standards (bovine serum albumin) were added with 200 μl of BCA working reagent (a 50:1 mixture of bicinchoninic acid (Sigma) and 4% copper (II) sulfate solution). The microplates were incubated at 37°C for 30 min. Absorbance was determined at 540 nm with an ELISA plate reader. After subtraction of the blank value, a BSA standard curve was constructed from the known concentrations of BSA (serial dilutions from 0.156 mg/ml to 2.5 mg/ml) and the protein concentration of samples was determined using the standard curve.

2.17 Western Blot Analysis

An equal amount of protein (20 or 30 μg) was mixed with 5× loading buffer (containing 250 mM Tris-HCl (pH 6.8), 10% SDS, 50% glycerol, 10% β-mercaptoethanol and 0.05% bromophenol blue), which was boiled for 4 min at 95℃ and subjected to SDS polyacrylamide gel electrophoresis. After that, the proteins were transferred onto a polyvinylidene difluoride (PVDF) membrane (Immobilon P, Millipore) at 15V for 1 h using a semi-dry transfer system (Biorad) or by wet transfer at 100V for 90 min. The membrane was blocked with 5% non-fat milk in TBST (10 mM Tris-HCl, 150 mM NaCl, 0.1% Tween-20) for 1 h, probed with primary antibody overnight at 4°C under gentle agitation, followed by incubation with secondary antibody (1:3,000-1:5,000) (Biorad) for 1 h at room temperature. The membrane was washed several times in TBST and then developed with ECL chemiluminescent detection system (Millipore) and autographed on X-ray

film using a film processor. The following primary antibodies were used in the Western blot analysis: mouse monoclonal anti-FHL2 (F4B2-B11) (1:1000), rabbit polyclonal anti-Bcl-xL (M-125) (1:500), rabbit polyclonal anti-Mcl-1 (S-19) (1:1000), rabbit polyclonal anti-p21 (C-19) and anti-p27 (C-19) (1:2000), mouse monoclonal anti-E-cadherin (67A4) (1:2000), mouse monoclonal anti-p53 (DO-1) (1:1000, all from Santa Cruz Biotechnology), rabbit polyclonal anti-survivin (1:1000), rabbit polyclonal anti-STAT3 and anti-p-STAT3 (Tyr750) (1:2000) and rabbit polyclonal anti-AKT and anti-p-AKT (Ser473) (1:2000; all from Cell Signaling Technology), rabbit monoclonal anti-cyclin D1 (clone SP4) (1:1000; Thermo Scientific), mouse monoclonal anti-Bcl-2 (clone 124) (1:500; Dako Corporation), and mouse monoclonal anti-vimentin (clone V9) (1:2000; Sigma Aldrich) and mouse monoclonal anti-β-actin (1:10,000; Calbiochem). Anti human β-actin was used for normalization. Densitometry analysis was performed using ImageJ (NIH, Bethesda, MD).

2.18 Cell Viability Analysis

Colorimetric MTT assays were used to determine the cell viability after treatment with doxorubicin (DOX) (Sigma Aldrich). The cells were seeded in 96-well plates at 8,000 cells per well in 100 µl volume of complete growth media and allowed to adhere at 37°C for 4 h. They were treated with 100 µl medium containing different concentrations of DOX or the vehicle for 48 h. After the incubation period, 20 µl MTT solution (5 mg/ml) was added to each well and the cells were cultured at 37°C for 48 h. The supernatant was aspirated and 100 µl

dimethyl sulfoxide (DMSO) was added to all wells to solubilize the purple formazan crystals under gentle shaking for 10 min at room temperature and absorbance at $O.D._{540}$ was determined. Absorbance reading was blanked against DMSO and the cell viability was expressed relative to vehicle control, which was set as 100%.

2.19 Detection of apoptosis by Western blot analysis

Cells were plated on 60 mm dishes at the same density (6×10^5 cells/dish) as in the MTT assay and treated with respective concentrations of DOX for 48 h. At the end of incubation period, both floating (dead) cells and the attached cells were collected. The floating cells were collected by centrifugation at 500 ×g for 5 min and washed once with PBS, while the attached cells were collected from the culture dishes by scrapping, combined with the floating cells and lysed with 200 µl of RIPA buffer supplemented with protease inhibitors. Western blot analysis of apoptosis-related proteins was performed using the following antibodies: anti-caspase-3 mouse monoclonal antibody (1:1000, Cell Signaling Technology), which detects both full-length and cleaved caspase-3, and anti-cleaved PARP (Asp214) rabbit polyclonal antibody (1:1000, Cell Signaling Technology).

2.20 *In silico* analysis of *FHL2* splice variants

Expressed sequences tag (EST) sequences were retrieved from the NCBI EST sequence database (http://www.ncbi.nlm.nih.gov/projects/dbEST/) and were aligned using the UCSC genome browser (http://www.genome.ucsc.edu/). Those 5'-EST sequences were selected for analysis of the 5'UTR of FHL2 gene. Multiple sequence

alignments were then performed using ClustalW v.1.83 from GenomeNet, the online database from Kyoto University, Japan (http://align.genome.jp/) to identify the splice variants of the *FHL2* gene. The tissues from which the ESTs were derived were also analyzed for the tissue distribution properties. TSS and first exon of the gene was predicted using the web-based program FirstEF (First Exon Finder) (Davuluri, 2003) (http://rulai.cshl.org/tools/FirstEF/).

2.21 Identification of *FHL2* multiple transcripts by reverse transcription PCR

Total RNA was extracted from cell line and clinical sample using Trizol reagent and purified using RNAeasy kit (Qiagen) and 1 μg was used for reverse transcription. Real-time PCR was performed in a 20 μl final reaction volume containing 2 μl of 10 × PCR buffer (Promega), 0.4 μl 10 mM dNTP, 0.6 μl of 10 μM forward and reverse primers and 20 ng of cDNA. Thermal cycling program started with an initial denaturation at 95°C for 5 min, followed by 30 cycles (95°C for 30 s, 60°C for 30 s and 72°C for 45 s) of amplification. PCR products were separated in 2.5% agarose gel followed by DNA purification and DNA sequencing (service provided by BGI).

2.22 Cloning of FHL2 promoter and deletion mutants

The 5' flanking region of the human FHL2 gene (~2.2 kb) was amplified by PCR from genomic DNA using the primers P2268luc-F and P2268luc-R and cloned into the *Kpn*I/*Nhe*I sites of pGL4.10 empty luciferase vector (Promega) to generate the full-length FHL2 promoter luciferase reporter construct. PCR was performed in

20 μl mixtures containing 1x Phusion GC Buffer (Phusion), 200 μM of each dNTP, 0.5 μM of each primer, 3% DMSO, and 0.5 U Phusion High Fidelity DNA polymerase. PCR conditions were 98°C for 5 min, five cycles of 98°C for 30 s for denaturation, 65°C for 30 s for annealing, 72° for 2 min for extension, followed by 25 cycles where the annealing step was adjusted to 60°C, and a final step at 72°C for 10 min. For the construction of deletion mutants, different lengths of the 5'-flanking region were amplified from the reporter plasmid by PCR using the same reverse primer and the forward primers listed in Table 2.2, followed by subcloning into the same restriction enzyme sites of pGL4.10. All clones were verified by restriction enzyme digestion and DNA sequencing.

2.23 Transient transfection and dual luciferase reporter assay

Huh7-cells were plated at 2×10^4 cells in 0.5 ml antibiotic-free medium per well in 24-well plates at 60-80% confluence. Twenty four hours later, cells were transfected with 0.4 μg of deletion constructs and 40 ng of pSV-Ruc, the *Renilla* luciferase vector per well using FuGENE 6 Transfection Reagent (Roche). A ratio of 1 μg DNA to 3 μl FuGENE 6 reagent ratio was used. After 48 h of transfection, dual luciferase assay (Promega) was performed to study the promoter activity following manufacturer's protocol. Briefly, cells were washed twice with PBS, and lysed in 100 μl 1X Passive Lysis Buffer by gently rocking on orbital shaker at room temperature for 15 min. A 75 μl aliquot of the lysate was incubated with 75 μl of firefly luciferase substrate (LAR II) at room temperature for 30 min, and the firefly luciferase activity was measured in a luminometer (Perkin Elmer EnVision 2101).

The reaction was quenched and *Renilla* luciferase activity was determined by addition of 75 µl of the Stop & Glo reagent, followed 30 min later by luminescence measurement. The promoter activity was expressed as arbitrary units normalized to *Renilla* luciferase activity to control the transfection efficiency for each well.

2.24 Promoter analysis and transcription factor binding site prediction

Ensemble (http://www.ensembl.org) was used for multiple sequence alignment of *FHL2* 5' flanking region of different eukaryotic species to identify conserved nucleotide sequences that may be functionally important regions in different genomes. Transcription factor binding sites in the promoter region were predicted by computational programs MatInspector (Genomatix) (http://www.genomatix.de) and TRANSFAC (Biobase) (http://www.biobase.de).

2.25 5-aza-dC and TSA treatment

5-aza-dC and TSA were used to block the DNA methylation and histone deacetylation, respectively. Cells were seeded at 1×10^5 cells per well in 6-well plates 24-h before treatment. Cells were treated either with 0, 2 and 5 µM of 5-aza-dC (Sigma) for 4 days or 0.1, 0.3 and 0.5 µg/ml of TSA (Sigma) for 24 hour. Drugs and medium were refreshed every day during treatment. The cells were harvested in 0.5 ml TRIzol and processed for RNA isolation. Real-time PCR was used to determine the gene expression after treatment of each cell lines with 5-aza-dC and TSA.

2.26 Bisulfite treatment and bisulfite sequencing

Hepatoma cells were analyzed for the promoter methylation status by bisulfite sequencing. Genomic DNA was subjected to sodium bisulfite treatment with the EZ DNA Methylation-Gold kit (Zymo Research) according to manufacturer's protocol. Twenty nanograms of treated DNA were used as template for PCR amplification at the relevant genomic regions using the primers listed in Table 2.2. Methyl Primer Express v1.0 (Applied Biosystems) was used to identify CpG islands in the FHL2 and FHL1 promoter region and design primers that amplify these regions. PCR products were cloned into pGEM-T Easy vector (Promega). A total of 5 individual clones were sequenced and the sequencing data were visualized using CpGviewer software (University of Leeds, UK) (Carr *et al.*, 2007).

2.27 FHL2 cDNA sequencing in HCC samples

Primers were designed to amplify (from cDNA) a 965-b.p. product that covers the entire coding region of FHL2 gene in HCC patient samples. The primers were designed against sequences common to all the transcript variants. The cDNA prepared from the tumor tissues of HCC patients were used as template for PCR. Each PCR reaction consisted of a total volume of 25 μl consisting of 5 μl of 10 x diluted cDNA, 12.5 pmol of each primer, 200 μM of dNTPs, 1x Phusion HF PCR buffer (Finnzymes), and 0.5 U of Phusion Hot Start DNA polymerase (Finnzymes). The PCR conditions were as follows: initial denaturation at 98°C for 30 s, 35 cycles of amplification consisting of a 10-s denaturation step at 98°C, a 30-s annealing step

at 60°C and a 35-s extension step at 72°C, followed by a final 10 min extension at 72°C. The PCR products were checked by 1 % agarose gel electrophoresis and were sequenced directly using the same primers used for amplification.

2.28 Sample Preparation and Microarray Analysis

RNA extracted from the left lobe of the liver was used in microarray analysis. RNA fractions from three animals per group ($FHL2^{-/-}$ and WT) were pooled and sent to Gene Company Hong Kong for gene chip processing and data analysis. High-quality intact RNA samples were required as the starting materials. For gene expression profiling, Affymetrix GeneChip Mouse Gene ST 1.0 Array which contains probe sets for >28,000 mouse genes was used (one microarray for each sample). Briefly, 300 μg of total RNA was reverse transcribed, labeled and hybridized to the arrays according to the Affymetrix GeneChip Whole Transcript Sense Target Labeling Assay protocol. Following hybridization, the arrays were washed and stained using the GeneChip fluidics station 450 (Affymetrix) and scanned using GeneArray scanner 3000 (Affymetrix) as described in the protocol. The data was then extracted from the scanned images and checked for quality control with Affymetrix Expression Console software v.1.0. The intensity data between gene chips was normalized by RMA normalization method and expression data analysis was further performed using Partek Genomics Suite v.6.4.

Quantitative real-time PCR (qPCR) was used to validate the microarray gene expression results as to confirm the differential expression of specific genes. The primer sequences used for validation are listed in Table 2.2.

2.29 Microarray data analysis

2.29.1 Functional annotation clustering

Genes associated with enriched biological theme were identified using the Database for Annotation, Visualization and Integrated Discovery (DAVID) (Huang *et al.*, 2007; Huang *et al.*, 2009) (http://david.abcc.ncifcrf.gov/). The gene list with at least 2-fold change in gene expression was analyzed using the DAVID Gene Functional Classification Tool to generate a summary of the enriched annotation terms ordered by the enrichment *P*-value (Ease score). Functional clustering was also performed using DAVID.

2.29.2 Ingenuity Pathway Analysis (IPA)

The list of genes was also uploaded to IPA 3.0 application. The software is a powerful tool which computes the relevant networks and searches for biological functions and diseases by using a proprietary database, and would be useful for understanding the molecular and cellular mechanisms.

2.29.3 Pathway enrichment analysis

To find the possible pathways regulated by FHL2, pathway enrichment analysis was performed using MetaCore^{TM}, a commercial integrated software suite developed

by GeneGO Company which enables the identification and prioritization of the most relevant pathways.

2.30 Statistical Analysis

The results shown represent mean ± S.D. from triplicates and three independent experiments unless otherwise specified. The expression levels in normal and tumor tissues were compared by one sample Student's *t*-test or a Wilcoxon signed rank test. For other experiments, statistical significance between groups was analyzed by One-Way ANOVA followed by Dunnett's test for multiple comparisons. $P<0.05$ is considered to be statistically significant. Graphical representation and statistical analysis were performed by using GraphPad Prism 4 software (GaphPad Software Inc, San Diego).

Table 2.1. Clinical features of HCC patients. The patients were categorized according to their sex, age, tumor size, differentiation status, tumor stage, HBV infection and cirrhosis status.

	N (%)
Sex	
Male	31 (73.8)
Female	11 (26.2)
Age (y)	
<57	21 (50.0)
>=57	21 (50.0)
*Tumor size (cm)**	
< 5	20 (48.8)
>= 5	21 (51.2)
Differentiation	
Well	4 (9.5)
Well to moderate	7 (16.7)
Moderate	26 (61.9)
Moderate to poor	3 (7.1)
Poor	2 (4.8)
*AJCC Staging**	
Stage I	30 (73.2)
Stage II	3 (7.3)
Stage III	8 (19.5)
HBV (HBsAg)	
Positive	33 (78.6)
Negative	9 (21.4)
Cirrhosis	
Positive	20 (47.6)
Negative	22 (52.4)

*record of one patient sample is missing

Table 2.2. List of oligonucleotide primers used in this study.

Oligonucleotide Name	**Forward (F) and Reverse (R) primer sequence (5'-3')**	**Product size (bp)**
A. Primers for genotyping FHL2 knockout mice		
neo1	F-GGATCGGCCATTGAACAAGATG	350
neo2	R-GAGCAAGGTGAGATGACAGGAG	
FHL2-P2	F-AGCATGACTGAACGCTTTGACT	405
FHL2-P3	R-GGTAACCAGAACAGGGAGAGTG	
B. Primers for cloning of FHL2 gene into pcDNA3.1 expression vector		
FHL2cDNA-F	TAGGGCGAATTCATGACTGAGCGCTTTGACTG	864
FHL2cDNA-R	TAGGGCGTCGACTCAGATGTCTTTCCCACAGT	
C. Primers for cloning of deletion mutants of the FHL2 proximal promoter		
Forward Primers:		
P-2268luc-F	TAGGGCGGTACCTCCACAATCCATGGCTGATA	2584
P-1320luc-F	TAGGGCGGTACCAGGGTGGCCTTAACTCAGGT	1636
P-395luc-F	TAGGGCGGTACCGCATCTGCAGGGTAAGAAGG	711
P-138luc-F	TAGGGCGGTACCGAGGGCACGAAGAAAGGAG	454
P+4luc-F	TAGGGCGGTACCCGAGGCGTGCATCTCCTTAT	322
P+37luc-F	TAGGGCGGTACCTTTCTCGAGGGCGGGAGCTG	280
Reverse Primer:		
P-2268luc-R	TAGGGCGCTAGCTGCTCTCCTCTCACCAGTCTC	
D. Primers used for PCR on bisulfite-treated DNA		
PCR on FHL2 gene:		
FHL2_340BSP	F-AAGAAAGGAGTTTTGGTAAATAAAGGGTA	340
	R-CGAACCCTAATAACTAAACCCCTC	
PCR on FHL1 gene:		
FHL1_195BSP	F-TATATAGTTTTCGTGTAGTGGGTAGAG	195
	R-GAGGGGGTTTAGTTCGTAGTCGT	
FHL1_426BSP	F-TTCGGCGGAGGGGGTTTAGT	426
	R-GATTAAGAGGTAGTGGGGTGGAG	

E. Primers used to co-amplify the transcript variants of FHL2		
FHL2exon1b-4	F-TCCAGCCCCGTCCGGGAGTC R-GTGGCAGTCAAAGCGCTCAGT	88-267
F. Primers used for mutation analysis of the *FHL2* gene (PCR and direct sequencing)		
FHL2cDNAseq	F-GGTTGCTGAAAAGCCAGGAG R-ATGTGGCTGGAAGAAACCAG	965
G. Primers for quantitative real-time PCR		
Primer pairs specific for human genes:		
FHL2	F-CTGGTTTCTTCCAGCCACAT R-ATTTGGGTGTGCCTTACTCG	177
FHL2CDS	F-CCCATCAGCGGACTTGGTGGC R-GGGGCACAGGATGTCGTCCCT	141
FHL1	F-CTGCGTGGATTGCTACAAGA R-GTGCCAGGATTGTCCTTCAT	115
FHL3	F-CAGGACTGTGGCTCCTTTTC R-TCAGGGAGTACCAGTTTGGG	125
AP-2A	F-CTGTCCAAGTCCAACAGCAA R-GAAGACTTCGTTGGGGTTCA	90
SP-1	F-CAAGCCCAAACAATCACCTT R-CAATGGGTGTGAGAGTGGTG	85
Pax-5	F-GGGAAGGAGAGCTTGCTTTT R-GCAGTCTTCTCAGTCGGACC	93
ZF5	F-GGACTTAAGGCAGTGCTTGG R-GGAGAGAGGTGCTTACTGGG	132
Bcl-6	F-AGGAAAGGCCGGACACCAGG R-TGGCATGGCGGGTGAACTGG	114
Creld2	F-CGCACACCCAGCCAGGCTAC R-CCCACTTCACACTCGCCGCA	121
Beta-actin	F-AGAGCTACGAGCTGCCTGAC R-AGCACTGTGTTGGCGTACAG	184
Primer pairs specific for mouse genes:		
FHL2	F-GAAGCAGCTATCTGGGCAAC	116

	R-GACCACTAATGGGGTTGGTG	
FHL2ATGexon2	F-TGACTGAACGCTTTGACTGC R-CAGTGTGGGTTCTCCTCCTT	82
Lcn2	F-GCCTTGCCCTGCTTGGGGTC R-CGCTCCGGAAGTCTGGCTGC	108
Bcl6	F-GCCAGCCAAGAGCCCCACTG R-CCTGCTCAGAGCCCTCGGGT	107
Ccnd1	F-AGAGGGCTGTCGGCGCAGTA R-GGCTGTGGTCTCGGTTGGGC	119
Saa2	F-CCCTGCTCCTGGGAGTCTGC R-GCCCCTTGGAAAGCCTCCCC	64
Onecut1	F-CCTGAATGCCCAGGGCCACG R-GCCGGTCACCGAAGGGTTGG	67
Inhbe	F-CTGGCACGCCCTGACTCTGC R-GTCCCGCAGCGGTGCTGTTA	110
Meg3	F-TTCCTTCACAGCCCCGGCTTC R-GGCCTGAGCGAGAGCCGTTC	127
Creld2	F-GCAGTTCTCGGTGGGTCGCC R-GTCCACCAGCGTCCGGCATC	147
Ppp1r10	F-CCGCCACCACCTCCATTCCG R-CGGTGCCCACCACCTCCAAC	110
Beta-actin	F-AGAGGGAAATCGTGCGTGAC R-CAATAGTGATGACCTGGCCGT	138

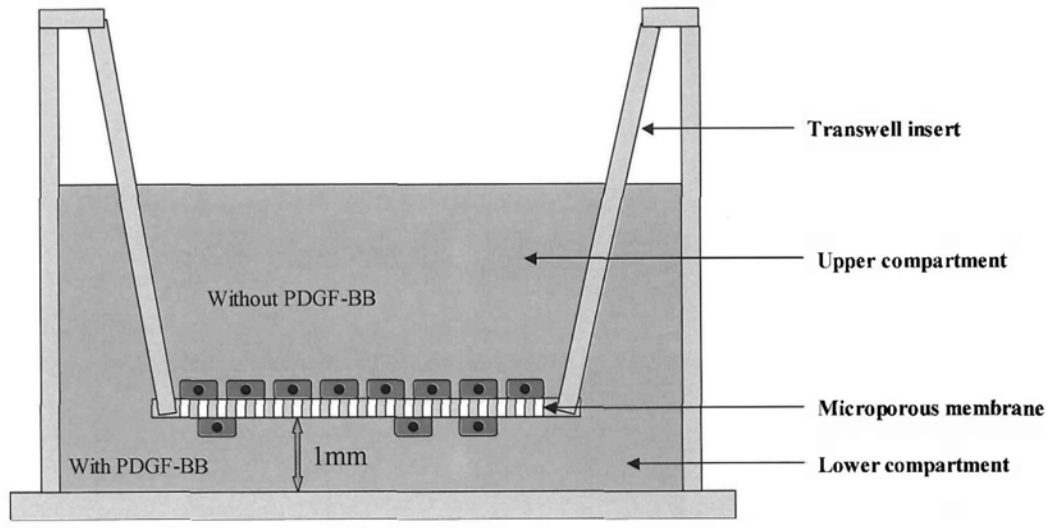

Fig. 2.1: Transwell (Boyden Chamber) was used for measuring the migration and invasion of tumour cells. The chambers contain porous filter (8 μm pore size). Matrigel was added to the filter as an indicator to study the cell invasion ability.

Chapter 3

EXPRESSION AND FUNCTIONAL STUDIES OF FHL2

3.1 Introduction

While FHL2 has been implicated in many forms of cancers, its role is particularly intriguing since its effect seems to be cell-type specific. So far, the precise function of FHL2 in liver tumorigenesis remains unclear. Here, we demonstrated that FHL2 overexpression inhibits the proliferation of human HCC cells Hep3B through cell cycle regulation by decreasing cyclin D1 expression while increasing the expressions of cyclin-dependent kinase inhibitors p21 and p27. FHL2 overexpression also inhibits migration and invasion of Hep3B cells through epithelial-mesenchymal transition (EMT)-mediated pathway, as shown by reduction of mesenchymal marker vimentin and induction of epithelial marker E-cadherin. The tumor-suppressor function for FHL2 is supported by the finding of reduced FHL2 expression in HCC cell lines and tumorous tissues. Surprisingly, we also demonstrated an antiapoptotic function for FHL2 overexpression with increased resistance to doxorubicin-induced apoptosis, which indicates the separation of antiproliferative and antiapoptotic role of FHL2. Taken together, we demonstrate a

dual function for FHL2 which may explain its contradictory roles in different types of cancers.

3.2 Results

3.2.1 Expression of FHL2 in HCC cell lines and tumor tissues

Initially, we intended to evaluate the expression status of FHL2 in HCC cell lines and tumorous tissues. The mRNA and protein levels of FHL2 in four liver cell lines were determined by real-time PCR and Western blot analysis, respectively. Real-time PCR analysis showed that the *FHL2* mRNA levels were much lower in the three HCC cell lines (Huh7, HepG2 and Hep3B) compared with the normal hepatocyte line WRL68 (Fig. 3.1A). Western blot showed that FHL2 protein was expressed in WRL68, but undetectable in the three HCC cell lines (Fig. 3.1B). Similarly, we employed real-time PCR method to measure *FHL2* mRNA expression in HCC tumorous tissues of 47 patients in comparison to the adjacent normal tissue. The results showed that *FHL2* mRNA levels were downregulated by >2-fold in 29 of 47 tumors (62%) compared to that of the corresponding non-tumor tissue (Fig. 3.2A). Only four of 47 tumors (9%) showed >2-fold increased *FHL2* expression. On average, there was about 30% loss of *FHL2* mRNA expression in tumor tissues versus the corresponding normal tissue (Fig. 3.2B). In summary, these findings revealed a downregulation of FHL2 expression in HCC.

3.2.2 Relationship between FHL2 expression and clinicopathologic features

To investigate the significance of FHL2 expression in HCC, correlation with different clinicopathologic parameters was analyzed in HCC patients. No significant difference in expression was found for multiple tumors, tumor size, clinical stages, degree of differentiation and vascular invasion (P>0.05) (Table 3.1A). The expression levels of FHL2 seem to differ only in HCC with moderate or poor differentiation compared with well-differentiated HCC, but not statistically significant (Fig. 3.3). The relationship between FHL2 and survival was also studied. We performed the survival analysis using the Cox proportional hazard model (Table 3.1B). The gene expression did not seem to affect survival (the hazard ratio Exp(B) close to 1 indicates no difference). The survival analysis was also performed by applying the Kaplan-Meier method. We tried to analyze difference between two survival curves by dividing two groups with a cutoff value of 0.35 for FHL2 expression, but the result was not statistically significant (P=0.194) (Fig. 3.4). Both methods failed to identify the association with survival.

3.2.3 Overexpression of FHL2 in human HCC cell line Hep3B and establishment of FHL2 stable transfectants

To study the functional role of downregulation of FHL2 in HCC, the consequences of FHL2 overexpression in HCC cells were investigated. The FHL2 expression plasmid pcDNA3.1-FHL2 containing the open reading frame and the control vector pcDNA3.1 were transfected into Hep3B cells. After transfection, cells were selected by G418 antibiotics for 3 weeks and three independent clones were picked out. Western blot confirmed the re-expression of FHL2 protein in these three

clones, and the two clones with the highest level (clone 1 and clone 3) were selected for further study (Fig. 3.5).

3.2.4 Effect of FHL2 overexpression on cell proliferation and cell cycle

To further characterize the role of FHL2 in HCC cells, we performed functional *in-vitro* assays with the FHL2 protein expressing cell clones in comparison to the vector transfected cells. Cell proliferation was measured by cell counting following Trypan Blue staining or by a BrdU incorporation assay. As shown in Fig. 3.6A, the growth rate of FHL2 stable cell clones was reduced compared with the vector control cells. Results obtained from BrdU assays also demonstrated the FHL2 expressing cell clones exhibited impaired proliferation compared to the vector control cells (Fig. 3.6B). In order to gain further insights into the mechanism by which FHL2 suppresses HCC cell proliferation, we examined whether FHL2 overexpression affected the cell cycle. Cell lysates prepared from Hep3B cells stably expressing FHL2 were subjected to Western blot analysis. As shown in Fig. 3.7, lower protein levels of cyclin D1, and higher protein levels of p21 and p27 were observed in HCC cells expressing FHL2 compared with cells expressing empty vector. This suggests that FHL2 plays a role in the regulation of cell proliferation.

3.2.5 Effect of FHL2 overexpression on cell migration and invasion and regulation of epithelial-mesenchymal transition

The effect of FHL2 overexpression on HCC cell migration and invasion was examined using a Boyden chamber system. In the migration experiment, it was

found that fewer cells migrated to the lower surface of membrane in FHL2 expressing cells compared with the vector control cells (Fig. 3.8). In the invasion experiment, similarly, we found that the number of invaded cells observed was significantly lower in the FHL2 expressing cell clones compared with control cells (Fig. 3.9A). To examine whether FHL2 could decrease cell motility and invasiveness through epithelial-mesenchymal transition (EMT), we evaluated the expression of EMT-related proteins by Western blot analysis. Results as shown in Fig. 3.9B demonstrated that the expression of mesenchymal marker vimentin was reduced while that of the epithelial marker E-cadherin was elevated in FHL2 expressing stable clones. The results suggested that FHL2 may play a role in the regulation of EMT.

3.2.6 Effect of FHL2 overexpression on apoptosis

The effect of FHL2 overexpression on the apoptosis-related proteins was also investigated by Western blotting to determine its effect on HCC cell apoptosis. Surprisingly, higher levels of antiapoptotic Bcl-2 and Bcl-xL were detected in HCC cells expressing FHL2 compared with the vector control cells (Fig. 3.10). To identify whether there was any role of FHL2 in the antiapoptotic signaling pathways, we further evaluated the expression of phosphorylated AKT (p-AKT) and phosphorylated STAT3 (p-STAT3) in the FHL2 stable cells, but no significant changes were observed. Among other antiapoptotic proteins we studied, the expression of Mcl-1 was slightly increased while the expression of survivin was

significantly reduced in FHL2 expressing cells. In summary, the results suggested FHL2 may play a role in the regulation of apoptosis.

Furthermore, the Western blot results demonstrated that the effect of FHL2 on the apoptosis-associated proteins observed in clone 3 was consistently stronger than that in clone 1, although FHL2 expression was similar in these two clones. Since the clone was originated from single cell, it is possible that the two clones display different sensitivity to FHL2's effect. However, it might also be caused by variation in the integration site of the FHL2 gene.

3.2.7 Effect of FHL2 overexpression on doxorubicin-induced cytotoxicity and apoptosis in Hep3B cells

Since Bcl-2 and Bcl-xL have been shown to mediate antiapoptosis in many cancer cells, we next studied whether elevation of Bcl-2 and Bcl-xL in FHL2 expressing HCC cells would protect cell from apoptosis. Cells were induced to undergo apoptosis by treatment with doxorubicin (DOX) for 48 h. DOX was known to trigger apoptosis at concentrations ranging from 0.05 to 5 μM but cell death was not likely due to apoptosis at elevated drug concentrations (reviewed in Gewirtz *et al.*, 1999). The effect of FHL2 overexpression on DOX-induced cytotoxicity was first evaluated by MTT viability assay. As shown in Fig. 3.11A, DOX induced a dose-dependent cytotoxic effect in HCC cells. Interestingly, DOX caused a significantly lower cytotoxicity in the FHL2 expressing cell clones (clone 3 < clone 1) compared with the case of vector control cells at the concentrations of 0.5, 1, 2.5,

5 and 10 μM respectively. In agreement to the trend obtained from the results of MTT assay, microscopic evaluation of the stable cells confirmed that highest viability (least cell death) was observed in clone 3, followed by clone 1 and lowest viability was observed in vector control after treatment with 2.5 μM DOX (Fig. 3.11B).

In summary, the results suggested that FHL2 overexpression confers the resistance to apoptosis induced by DOX in HCC cells and protects cell death from apoptosis. Interestingly, our study showed that the antiapoptotic effect of FHL2 in the two FHL2 clones was shown to correlate with the protein expression of Bcl-2 and Bcl-xL. Therefore, we believed that Bcl-2 and Bcl-xL mediated the antiapoptotic effect of FHL2 against DOX-induced apoptosis.

3.3 Discussion

Identification of the differences in the genetics of cancer cells and normal cells and exploration of those genes associated with carcinogenesis are important for the development of targeted therapies in cancer treatment. In this study, we examined the potential role of FHL2 in liver carcinogenesis. Our examination of the effects of overexpression of FHL2 in Hep3B cells has revealed an interesting finding of the dual functions of FHL2 in liver carcinoma cells. On one hand, it behaves as a potential tumor suppressor, which inhibits the tumor cell growth as well as cell invasion and motility. On the other hand, it possesses antiapoptotic function and that overexpression in cancer cells confers resistance to apoptosis towards an apoptotic stimulus induced by doxorubicin. Each of these findings will be discussed below.

3.3.1 Expression of FHL2 and clinical significance in HCC

Studies on FHL2 in the past few years have implicated the possible role of FHL2 in cancers. Altered expression of FHL2 is seen in many cancers and difference in the expression pattern was observed among different cancers (Scholl *et al.*, 2000; Kinoshita *et al.*, 2005; Gabriel *et al.*, 2004; Wang *et al.*, 2007; Martin *et al.*, 2007; Ding *et al.*, 2009b). FHL2 displays tumor promoting or tumor suppressing activities depending on the types of tumor cells, but the mechanism of how FHL2 is involved in tumorigenesis remains unclear (reviewed by Kleiber *et al.*, 2007). This led us to investigate the role of FHL2 in hepatocellular carcinoma (HCC) which has been one of the most prevalent and lethal cancers worldwide. From the gene expression analyses using real-time RT-PCR, we demonstrated that FHL2 was downregulated in

all three HCC cell lines used and in most of the clinical tumor samples. In accordance with our data, an earlier report has demonstrated a reduced expression of FHL2 in HCC tumors compared with the adjacent normal tissues (Ding *et al.*, 2009b). It has also been reported that FHL2 was overexpressed in hepatoblastoma (Wei *et al.*, 2003). The differential gene expression among the two types of liver tumors may be related to the different roles of FHL2 in different kinds of tumor. In our study, in addition to the assessment of gene expression, we also studied the clinical relevance of FHL2 expression level in HCC. We further conducted clinicopathological correlation study in HCC patients but we failed to find significant correlation between FHL2 expression and any clinical variables.

3.3.2 The effect of FHL2 expression on cell proliferation, invasion and metastasis

We subsequently evaluated the function of FHL2 in Hep3B, a human HCC cell line, by construction of the stable transfectants expressing FHL2 proteins. We confirmed that overexpression of FHL2 significantly suppressed the HCC cell proliferation. This is in agreement with the findings of a previous study which demonstrated that FHL2 suppress the HepG2 hepatoma cells growth through a TGF-β-like signaling pathway (Ding *et al.*, 2009b). Moreover, our present study reported a novel finding that FHL2 exhibits anti-migratory and anti-invasive activity in HCC cells, as demonstrated using Boyden Transwell chamber assay system. We further showed that the inhibitory action of FHL2 on cell migration and invasion is associated with the regulation of EMT. Cell invasion and metastasis play a central

role in the process of tumor progression. It has been shown that EMT, a process whereby cells undergo a transition from an epithelial to mesenchymal phenotype, results in an ability to detach from the neighboring cells and then invade and metastasize to a distant tissue/organ from the primary tumor sites (Thiery, 2002). We noticed that overexpression of FHL2 in Hep3B cells resulted in a reduced expression of the mesenchymal marker vimentin and upregulation of the epithelial marker E-cadherin. Loss of E-cadherin and gain of vimentin are well-established hallmarks of EMT associated with progression to metastasis (Thiery, 2003; Acloque *et al.*, 2009). Our findings suggested that the inhibitory effect of FHL2 on HCC invasion may be associated with a modulation of the EMT process. To the best of our knowledge, there are only two reports just published documenting the involvement of FHL2 in the regulation of EMT in cancer (Zhang *et al.*, 2010; Amann *et al.*, 2010). FHL2 was shown to be closely correlated to invasion and migration potential of colon cancer and act as a potent inducer of EMT for invasion/metastasis of colon cancer cells by stimulating vimentin and suppressing E-cadherin (Zhang *et al.*, 2010). This is the first time we show that FHL2 could inhibit liver cancer cell migration and invasion through regulation of EMT markers.

3.3.3 Effect of FHL2 expression on cell cycle and apoptosis regulatory proteins

In order to gain more insights into the mechanisms by which FHL2 suppresses cell proliferation in HCC cells, we determined the effect of overexpression of FHL2 on cell cycle and apoptosis. Cell cycle regulators are known to play a key role in cell

proliferation control and the aberrant expression of these regulators has been associated with the development of many cancers. One recent study proposed a TGF-β-like pathway in which FHL2 interacts with Smad proteins resulting in regulation of the target proteins p21 and c-myc and subsequently suppression of proliferation (Ding *et al.*, 2009b). Here, we demonstrated that overexpression of FHL2 inhibited the protein expression of cyclin D1, an important regulator of G1 to S phase transition, and induced the expression of $p21^{CIP1/WAF1}$ and $p27^{KIP1}$, inhibitors of G1 cyclin-dependent kinases in Hep3B cells, suggesting that the growth inhibitory effect of FHL2 on HCC cells is likely due to regulation of cell cycle progression from G1 to S phase. Furthermore, from the results of Western blot analysis of apoptosis-related proteins, we observed surprisingly that, overexpression of FHL2 leads to the activation of the antiapoptotic Bcl-2 family proteins Bcl-2 and Bcl-xL. Since PI3K/Akt and JAK/Stat3 signaling pathways could mediate the activation of these antiapoptotic proteins (Catlett-Falcone *et al.*, 1999; Kusaba *et al.*, 2007; Gangavarapu *et al.*, 2008), we evaluated the Akt and Stat3 phosphorylation in the stable cells expressing FHL2 by Western blotting. However, no significant change in Akt and Stat3 activation was observed. Among other antiapoptotic proteins within these signaling pathways, the expression of Mcl-1, another Bcl-2 antiapoptotic member, was slightly increased while the expression of survivin was found to be significantly reduced. Survivin is a member of inhibitor of apoptosis protein (IAP) family that plays a role in the inhibition of cell death and suppression of apoptosis but it is regarded as a bifunctional protein since it also regulates cell proliferation (Zhang *et al.*, 2010; Olie *et al.*, 2000; Johnson and Howerth, 2004; Dai *et al.*, 2005).

Survivin has been shown to play a more important role in controlling cell proliferation than apoptosis in HCC (Ito *et al.*, 2000). The contrasting effect of FHL2 observed on these antiapoptotic molecules is a topic that will require further research to clarify.

3.3.4 FHL2 exerts anti-apoptotic functions independent of growth suppression

In order to clarify if there is any proapoptotic/antiapoptotic role of FHL2, we next studied the consequences of overexpression of FHL2 on HCC cell apoptosis induced by an apoptotic stimulus doxorubicin in Hep3B cells. Doxorubicin was known to induce apoptosis via the activation of caspases and disruption of mitochondrial membrane potential (Gamen *et al.*, 2000). Doxorubicin caused cytotoxicity was shown to be associated with DNA damages, free-radical formation and damage of cell membrane (Gewirtz, 1999). In our study, overexpression of FHL2 itself did not remarkably induce apoptosis in Hep3B cells, as demonstrated by Western Blot analysis of expression of apoptosis proteins, activated caspase-3 and PARP. However, we discovered that overexpression of FHL2 significantly inhibited doxorubicin-induced cytotoxicity and prevented cells from undergoing apoptosis. The antiapoptotic effect of FHL2 may be attributed to the increased expressions of Bcl-2 and Bcl-xL, which is a known mechanism to confer resistance to apoptosis cancer cells (Chun and Lee, 2004). Bcl-2 and Bcl-xL were shown to have inhibitory effect on HCC apoptosis induced by different factors (Takehara *et al.*, 2001; Guo *et al.*, 2002). In our study, overexpression of FHL2 was found to increase the

expression of Bcl-2 and Bcl-xL, which may contribute to the antiapoptotic effect towards doxorubicin-induced apoptosis in HCC cells.

FHL2 has been shown to suppress FOXO1 activity and inhibit FOXO1-induced apoptosis in prostate cancer cells through the interaction with FOXO1 with SIRT1 (Yang *et al.*, 2005). Furthermore, FHL2 was found to inhibit the cyclin D1 gene expression regulated by FOXO1. Here, our study provides evidence that FHL2 regulates cyclin D1 expression and exerts antiapoptotic effect against doxorubicin in HCC cells. Interestingly, FOXO transcription factors are known to be involved in doxorubicin-mediated apoptotic signaling (Yu *et al.*, 2008; Lüpertz *et al.*, 2008). Although the situation may vary, it is worthwhile to further investigate in the future whether the interaction of FHL2 and FOXO1 would also occur in HCC cells and whether such interaction would contribute to the antiapoptotic effect of FHL2 and the regulation of cell cycle mediators.

3.3.5 Summary

In conclusion, we have constructed stable transfectants of FHL2 expressing proteins and demonstrated for the first time a bifunctional role of FHL2 in HCC cells. Collectively, our results indicated that FHL2 acts as tumor suppressor which inhibits HCC cell proliferation through regulation of cell cycle progression and cancer cell migration/invasion through the regulation of EMT. The tumor-suppressor function for FHL2 was supported by the finding of reduced FHL2 expression in HCC cell lines and tumorous tissues. Alternatively, we have demonstrated what we believe to

be a novel antiapoptotic function of FHL2 in HCC. Indeed, these two effects are not necessarily contradictory since FHL2 was shown to inhibit tumor growth by cell cycle regulation rather than apoptosis. The antiapoptotic role could be another aspect of FHL2 in relation to interference with the apoptosis signaling pathway that promotes cell survival against apoptotic stimuli. The balance between cell proliferation and cell survival/death therefore determines the overall effect of FHL2. We believed that the dual function revealed for FHL2 may account for its contrasting expression and effects observed in different types of cancers.

3.4 Limitations and Future Perspectives

This study relies solely on an overexpression strategy. Although this is important for understanding the function of a protein in cell, studying the loss of FHL2 may be more relevant to what is happening in HCC. Re-expression of this gene does not directly address its physiological role in liver cancer since it is missing in liver cancer cells. In the future study, the effect of gene knockdown in a normal liver cell line will be investigated.

Moreover, knockdown of FHL2 will be necessary to confirm whether the effects observed in cell lines were caused by FHL2 overexpression. Besides, more studies are needed to support the conclusions, e.g. knockdown of E-cadherin or overexpression of vimentin should be performed to determine whether this would abrogate FHL2 effects on migration or invasion.

The study provides data for the role of FHL2 in cell proliferation, cell motility and apoptosis. However, more studies are required to explore the mechanism underlying these effects.

Reduction of FHL2 in tumor specimens is a critical piece of evidence that support the rationale of the studies. FHL2 protein levels should also be determined between tumor and normal tissues.

The cell line WRL68 may not be a suitable normal control for comparison of gene expression since it is of embryonic origin. Other adult human normal liver cell lines will be used in future experiments.

Moreover, the number of overexpressing clones analyzed in cell assays may not be sufficient. The future experiments should also include the pool of overexpressing cells in addition to single cell clones to exclude the effect of clonal variation.

Table 3.1: Correlation between FHL2 expression and clinical features

A: Correlation of FHL2 with the various parameters

Variables	Test Statistics		Significance
Multiple Tumour	Mann-Whitney U Asymp. Sig. (2-tailed)	0.4438	NS
Vascular Invasion	Mann-Whitney U Asymp. Sig. (2-tailed)	0.7762	NS
Size >=5cm	Mann-Whitney U Asymp. Sig. (2-tailed)	0.5038	NS
AJCC Staging	Kruskal Wallis ANOVA Asymp. Sig.	0.4456	NS
Tumour Differentiation	Kruskal Wallis ANOVA Asymp. Sig.	0.6861	NS

B: Survival Analysis using Cox-proportional Hazard Model

Variable	B	SE	Wald	df	**Sig.**	Exp(B)	95% CI Exp(B)
FHL2	-0.0536	0.3035	0.0312	1	0.8597	0.9478	0.5229-1.7180

A

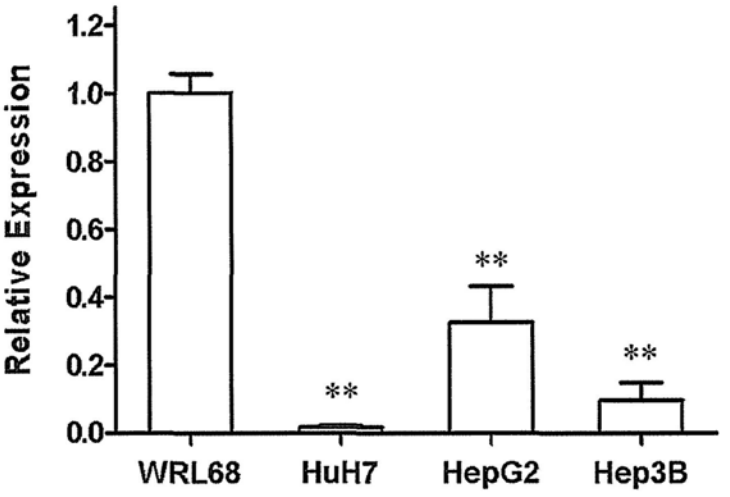

B

Fig. 3.1: Expression of FHL2 in HCC cell lines. **(A)** *FHL2* mRNA levels in four liver cell lines were determined by quantitative real-time PCR with β-actin as an endogenous control. Results shown as mean ± S.D. of 3 independent experiments. $^{**}P<0.01$ compared with WRL68. **(B)** Western blot analysis showing the expression of FHL2 protein in liver cell lines.

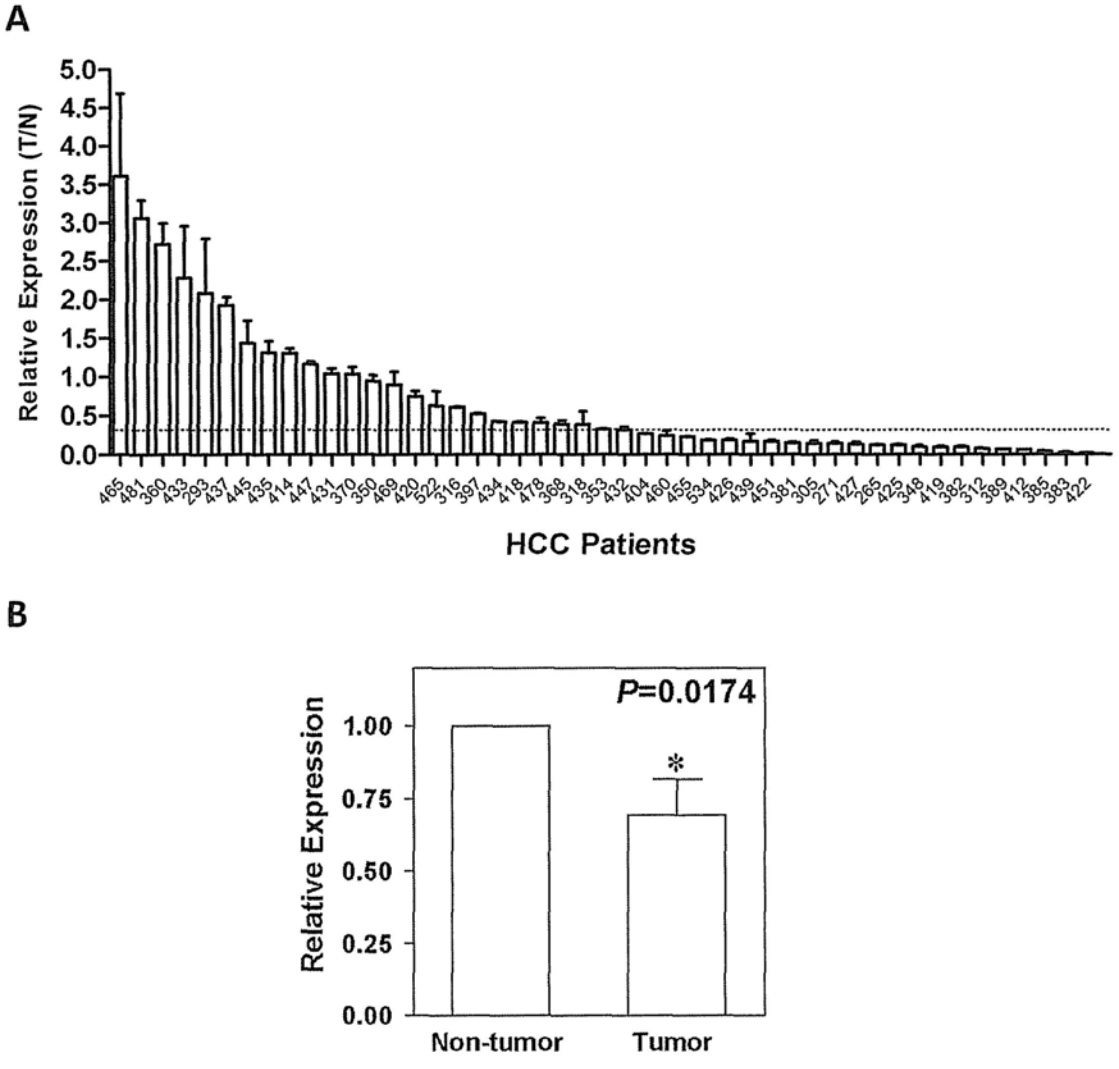

Fig. 3.2: Expression of FHL2 in HCC tumors. **(A)** The mRNA expression of *FHL2* in HCC patients was determined by real-time PCR. The data was analyzed by a comparative Ct method and a T/N ratio which denotes the relative gene expression in tumor tissue (T) compared with the adjacent non-tumor tissue (N) was calculated. *X*-axis: HCC patients analyzed. The dotted line represented the median expression. **(B)** Comparison of average expression of *FHL2* in tumor tissues and the corresponding non-tumor tissues in 47 patients. Error bar represents SEM. *Indicates significant difference compared to non-tumor tissues ($P<0.05$).

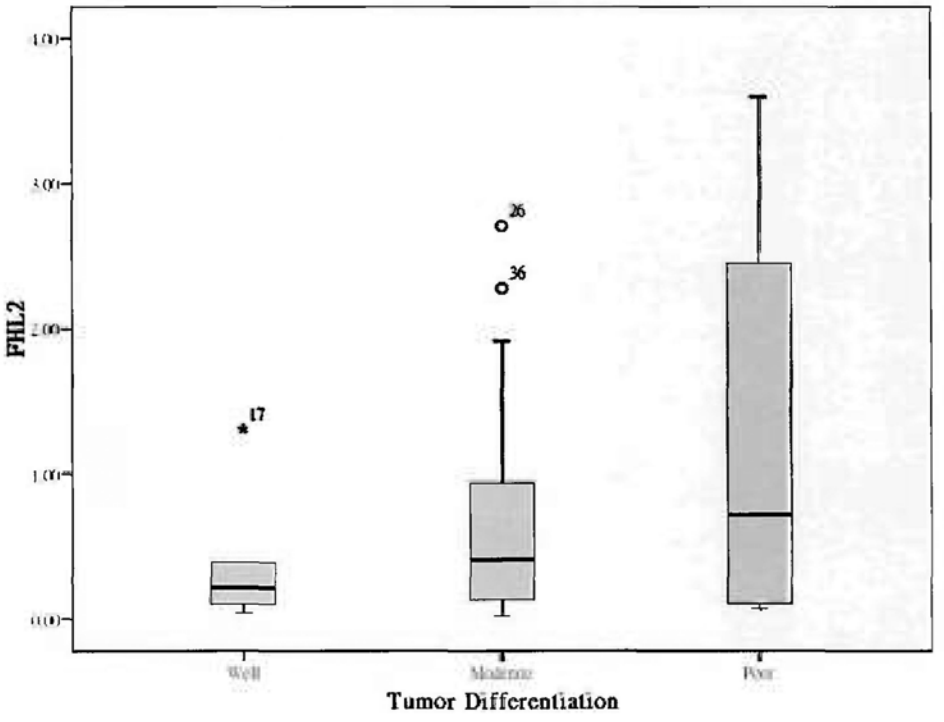

Fig. 3.3: Box plot of the expressions of FHL2 in relation to the degree of tumor differentiation. No statistically significant differences were observed between the groups.

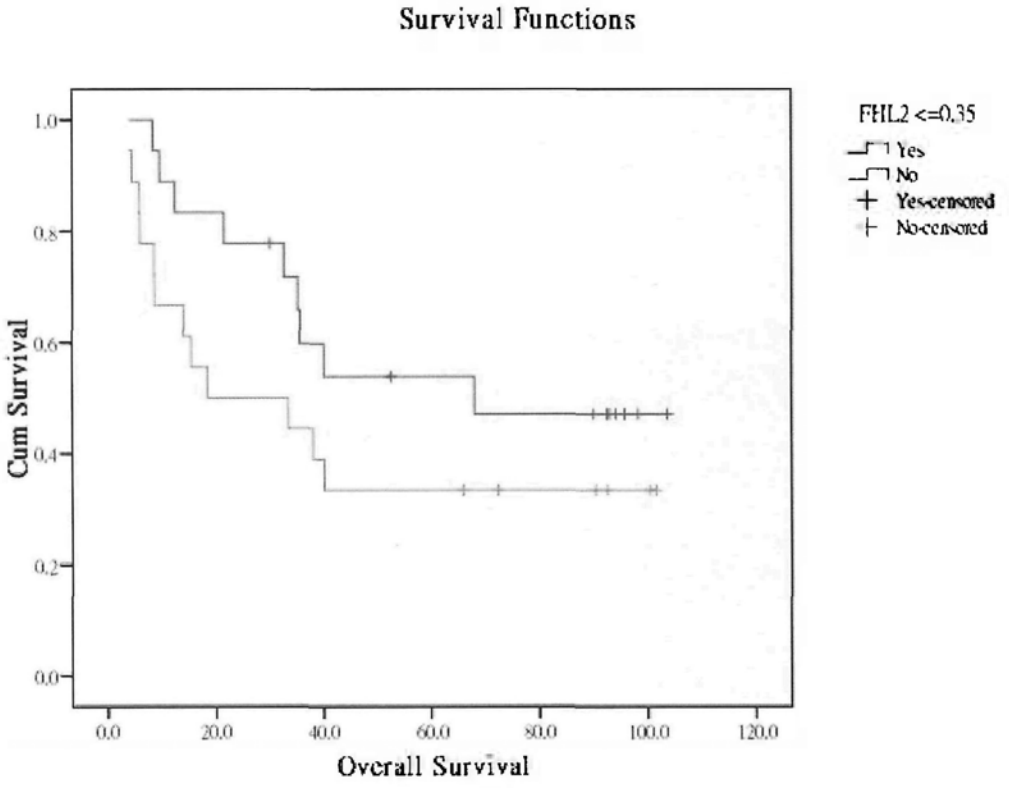

Fig. 3.4: Kaplan-Meier survival analysis for comparing patients with low (below median) and high expression (above median) of FHL2. P-value was determined by log-rank test. Patients with low FHL2 expression (T/N≤0.35) showed a slight but insignificant trend for better survival.

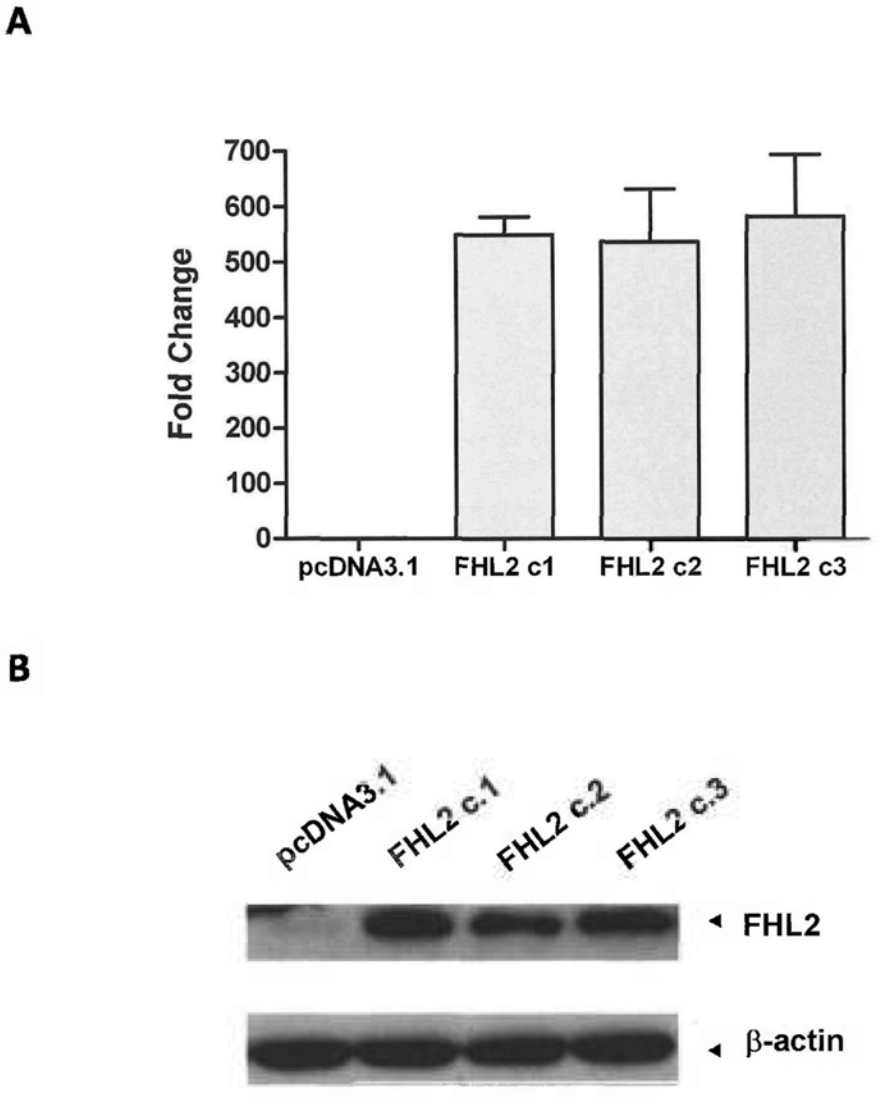

Fig. 3.5: Establishment of FHL2 stably expressing Hep3B cell lines. The expression of FHL2 in individual stable clones was analyzed by **(A)** real-time PCR and **(B)** Western Blot analysis. Results confirmed the re-expression of FHL2 protein (a single band at 32 kDa observed using a mouse monoclonal FHL2 antibody) in the three clones that were picked out (c.1: clone 1, c.2: clone 2 and c.3: clone.3).

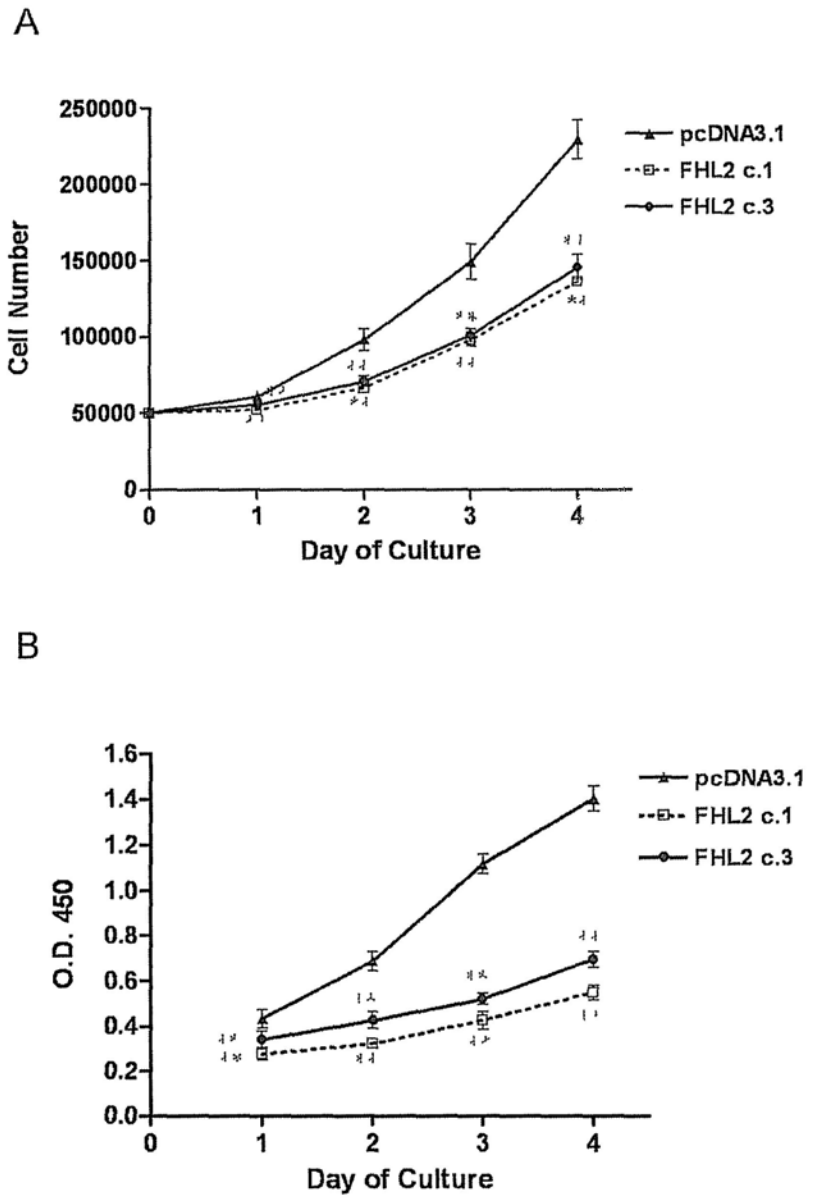

Fig. 3.6: Effect of FHL2 overexpression on cell proliferation in HCC cells. **(A)** Cell proliferation of FHL2 stably expressing cells (clone 1 and clone 3) was determined by counting viable cells as determined by Trypan Blue exclusion assay. **(B)** Proliferation of cells was also determined using an ELISA-based BrdU incorporation assay. BrdU incorporation was evaluated by measuring the absorbance at 450 nm over 4 days after cell seeding. Results represent mean ± S.D. of 3 independent experiments. **Indicates significant differences compared to pcDNA3.1 control at each time point. ($P<0.01$).

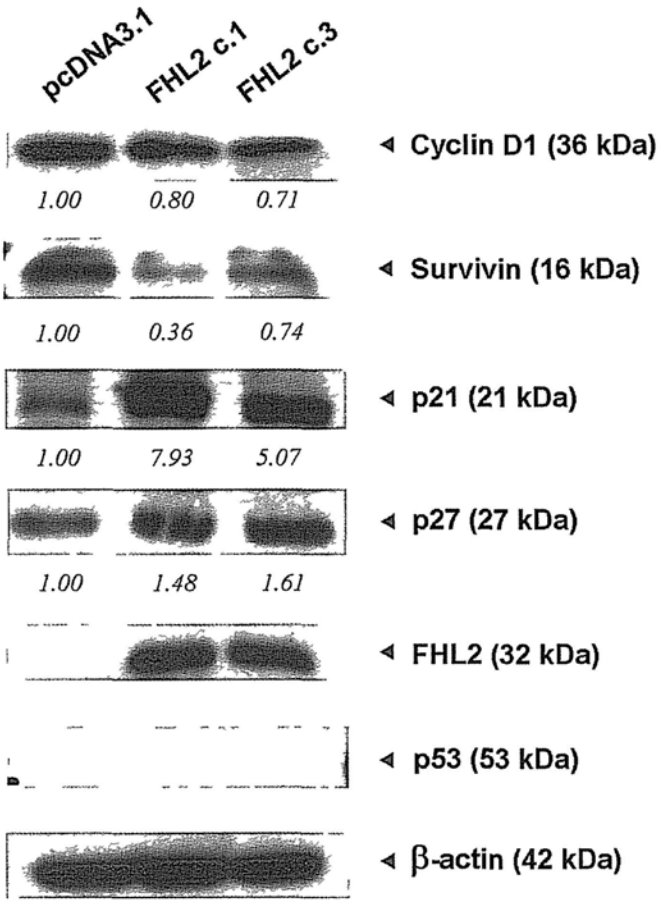

Fig. 3.7: Western blotting analysis of the cell cycle regulators in the stable cell lines. The relative intensities were quantified by densitometry. Results shown are from a single experiment and representative of three independent experiments.

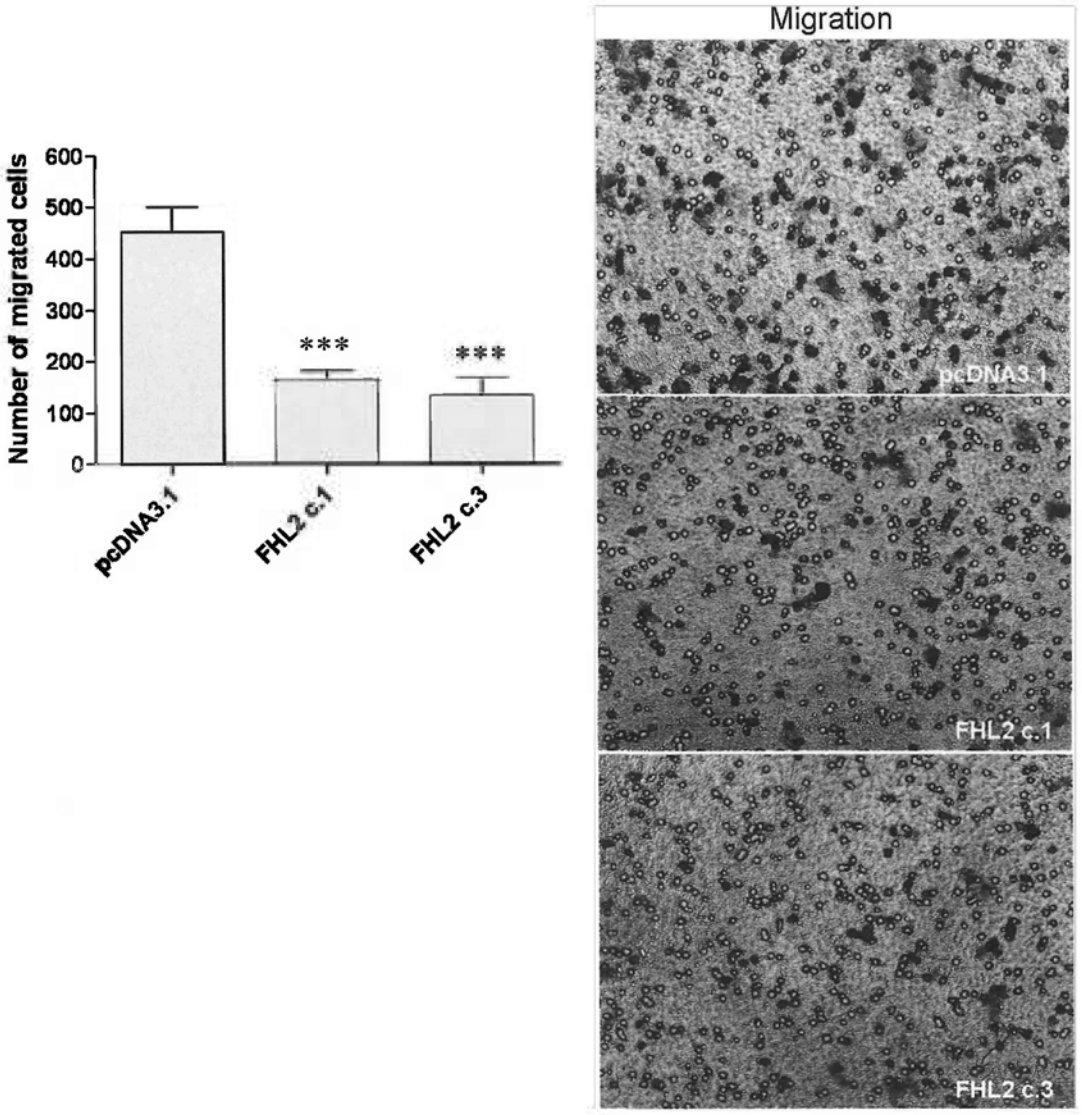

Fig. 3.8: Effect of FHL2 over-expression on cell migration. The FHL2 stably expressing cells (clone 1 and clone 3) were examined for migration activity using the Boyden chamber system. Results represent mean ± S.D. of 3 independent experiments. $^{**}P<0.01$; $^{***}P<0.001$ compared to empty vector. *Right Panel*: Photographs of one representative experiment out of three are given (magnification x200). Filter pores of transwell appear as white circles.

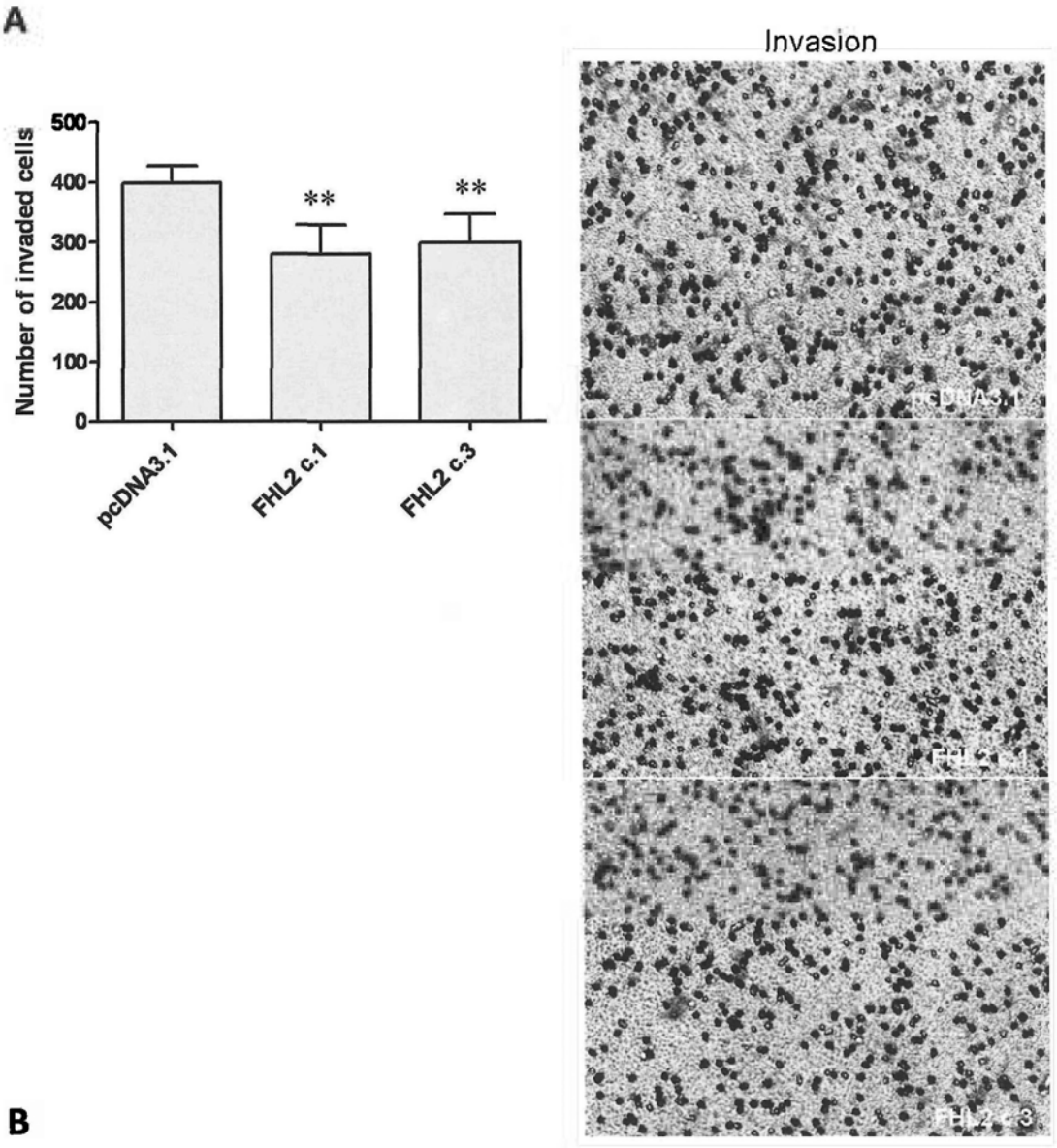
A
Invasion
Number of invaded cells
500
400
300
200
100
0
**
**
pcDNA3.1
FHL2 c.1
FHL2 c.3
B
pcDNA3.1
FHL2 c.1
FHL2 c.3
E-cadherin (120 kDa)
1.00
1.33
1.37
Vimentin (58 kDa)
1.00
0.79
0.72
β-actin (42 kDa)

Fig. 3.9: **(A)** Effect of FHL2 over-expression on cell invasion. The FHL2 stably expressing cells (clone 1 and clone 3) were examined for invasion activity using the Boyden chamber system. Results represent mean ± S.D. of 3 independent experiments. $^{**}P<0.01$; $^{***}P<0.001$ compared to empty vector. *Right Panel*: Photographs of one representative experiment out of three are given (magnification x200). Filter pores of transwell appear as white circles. **(B)** Western blotting analysis of protein expression of the vimentin and E-cadherin in the stable cell lines. The relative intensities were quantified by densitometry. Results shown are from a single experiment and representative of three independent experiments.

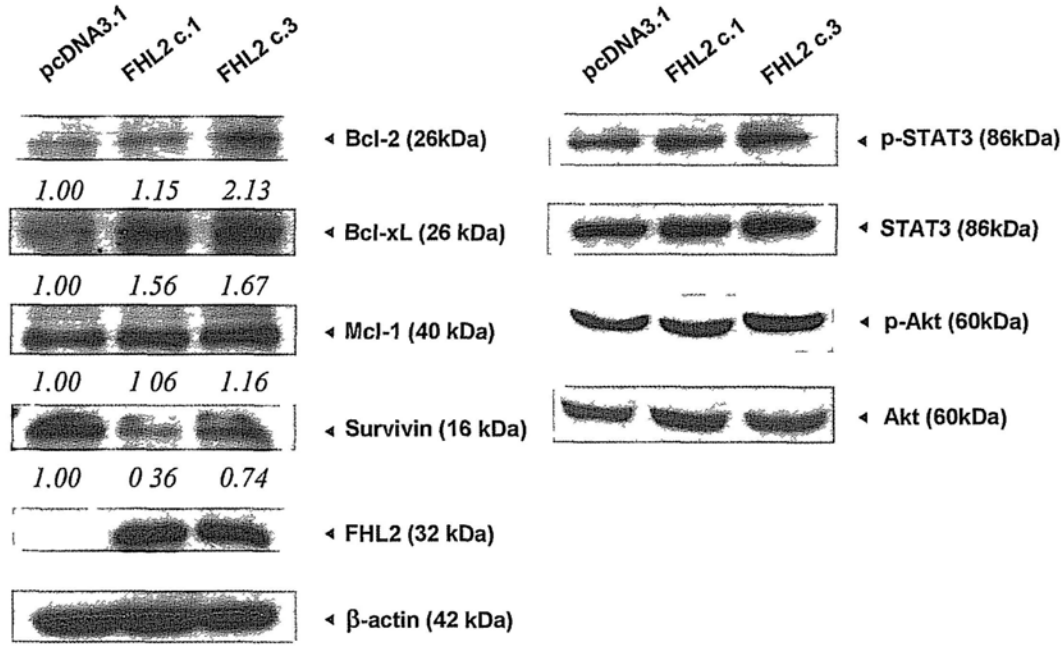

Fig. 3.10: Western blot analysis of a panel of apoptosis-related proteins in Hep3B cell lines stably expressing FHL2 (clone 1 and clone 3) and vector control cells. Thirty micrograms of total cellular protein from each sample was analyzed. Beta actin was used as loading control. The relative intensities were quantified by densitometry. Results shown are from a single experiment and representative of three independent experiments. The increase in expression of Stat3 and Akt in clone 1 and clone 3 was not consistent between experiments.

A

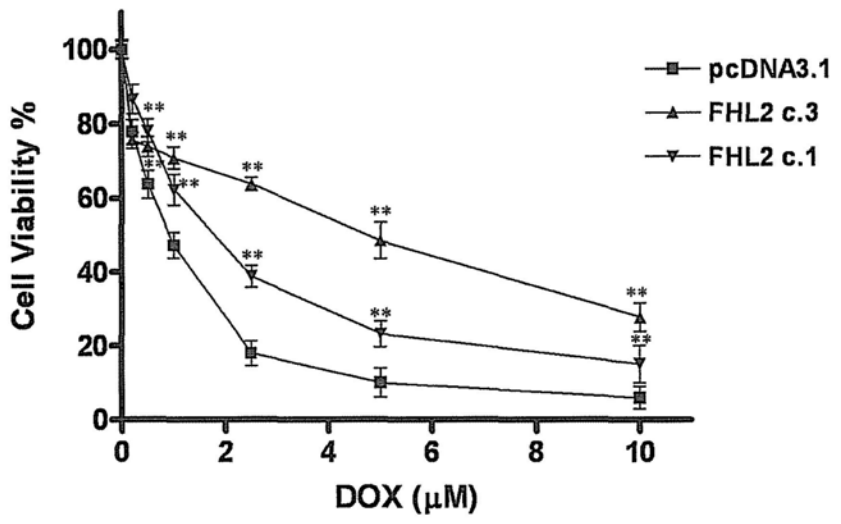

B

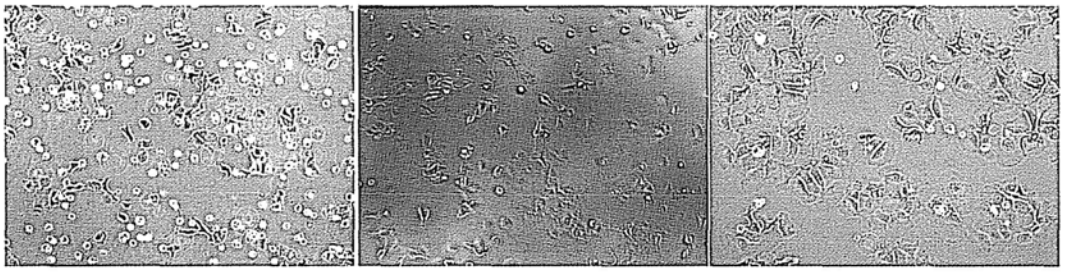

Fig. 3.11: Effect of FHL2 over-expression on doxorubicin (DOX)-induced cytotoxicity and apoptosis in HCC cells. **(A)** The FHL2 stable (clone 1 and clone 3), and control cells were treated with the tested concentrations of DOX for 48 h. The cytotoxicity effect was evaluated by the MTT assay. $^{**}P<0.01$ compared with vector control. Results represent mean ± S.D. of quadruplicate cultures from 3 independent experiments. **(B)** Representative microscopic images of these stable transfectants after treatment with 2.5 μM DOX (magnification x100).

C

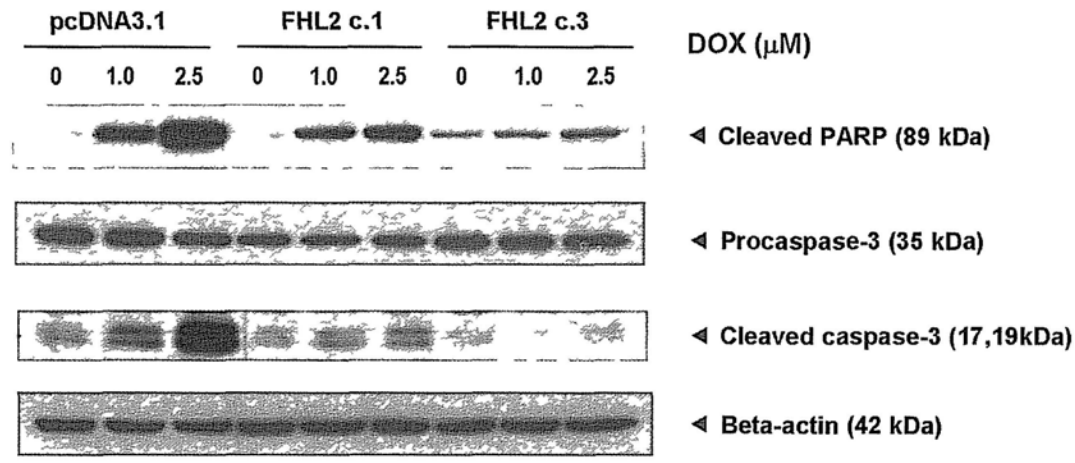

Fig. 3.12: **(C)** Expression of cleaved caspase-3 and poly(ADP-ribose) polymerase (PARP) proteins were analyzed by Western blotting analysis following treatment with 0, 1 and 2.5 μM DOX for 48 h (20 μg cellular protein was loaded per lane). Results shown are from a single experiment and representative of three independent experiments.

Chapter 4

STUDY OF FHL2 GENE AND TRANSCRIPTIONAL REGULATION IN HCC

4.1 Introduction

The FHL2 was originally identified to be expressed abundantly in the heart, as well as in a wide range of tissues demonstrated in various studies. The human *FHL2* gene expresses different transcripts which are known to differ only in the 5' UTR region. However, little is known about the functional role of the different variants and the mechanism of gene regulation. In the present study, we characterized the different alternative spliced transcripts of *FHL2* by *in silico* analysis and RT-PCR analysis. A novel transcript variant was identified. The *FHL2* gene produces transcripts by different 5' exons, which may be responsible for tissue-specific regulation. Our study revealed a reduced expression level of *FHL2* mRNA in a majority of the HCC tissues. However, this was not associated with a change in isoform-specific expression. To study the mechanism of gene regulation, the potential promoter region as well as its methylation status was investigated. *FHL2* itself was not regulated by methylation, although the downregulated expression was reactivated upon demethylation treatment. Deletion mutation analysis of 5' flanking

region showed that the fragment from -138 to +292 in the promoter region has positive regulatory effect. We identified the binding sites of paired box gene 5 (Pax-5)/ Zinc finger protein 5 (ZF5) in this region and found that Pax-5 and ZF5 expression in HCC tumor samples had a significant positive correlation with FHL2 expression, indicating a possible role for these transcription factors in the regulation of *FHL2* expression.

4.2 Results

4.2.1 *In Silico* analysis of *FHL2* splice variants

It is known that the splice variants of *FHL2* differ only in their 5'UTR region. The actual variants are studied by analyzing the EST sequences. Among the 407 EST sequences matched to *FHL2* gene, 123 sequences were selected for analysis in the 5'UTR region (See Table 4.1). By multiple sequence alignment, the selected EST can be categorized into five splice forms, which are different in the first 1-3 exons (designated by 1a/1b, 2 and 3). They were named as *FHL2* transcript variant 1 to 5 (3 being a novel transcript variant). Two alternative 5' exons exist for *FHL2* gene. Exon 1a, which is found only in variant 4, lies 40 kb upstream of exon 1b. The combinations of exon 1b, 2 and 3 constitute the other isoforms. According to the information in the databases from National Centre for Biotechnology Information of the National Institute of health, USA, there were different sizes of exon 1b (255 and 149 bp respectively). By EST blast search, exon 1b was predicted to be 149 bp. Moreover, the transcription start site (TSS) prediction for the 5' terminal exon was consistent with this observation. To summarize, the *FHL2* gene should consist of 6-8

exons. The last 5 exons contain the coding sequences for 280 amino acids. Fig. 4.2A is a summary of the five alternative splice variants for *FHL2* (which contained exons as shown), and the exon/intron arrangement is depicted in Table 4.2. The tissue distribution analysis of EST sequences shows that *FHL2* transcript variant 4 is found mainly in the heart, while the other transcripts are distributed in a wide variety of organs (Fig. 4.1 and Table 4.1).

4.2.2 RT-PCR analysis of *FHL2* transcript variants

To validate the results obtained from analysis of EST data, primers were designed to amplify the cDNA region between exon 1b and 4 from giant-cell tumor of bone (GCT cells). The RT-PCR products which show four bands in agarose gel were verified by DNA sequencing to be the four transcript variants from our prediction (Fig. 4.2B and 4.3). The largest-sized product (267 bp) which encompasses exons 1b and 4 corresponds to transcript variant 2. The 215-bp and 138-bp PCR products which correspond respectively to transcript variants 1 and 5, were found to have exons 3 and 2 missing respectively compared to the longest variant. A novel transcript, designated as *FHL2* variant 3, was identified. This variant contained exon 1b as the only exon in the 5'UTR region, corresponding to the smallest PCR product of 88 bp in size. Additional analysis showed that the *FHL2* multiple transcripts were detected in WRL68, MCF7, Caco-2, Hela, U-138MG and HepG2 cell line despite their different origins, as well as in the clinical HCC samples (Fig. 4.3, upper and lower). Interestingly, no obvious switch in isoform expression was detected in all samples (Fig. 4.3). It was noted however, that variant 1 and 2

seem to occupy a higher ratio in both HepG2 cancer cells and tumor tissues when compared to the normal cell line, WRL68 and normal tissues.

4.2.3 Mutation analysis of the FHL2 gene

We also performed mutation analysis of the FHL2 gene for detection of mutations that cause the functional change of the protein. The transcribed regions of FHL2 gene were analyzed. We analyzed eleven HCC tumor tissues (patient no. 305, 312, 318, 350, 404, 425, 437, 447, 455, 465 and 534) but we did not detect any mutations in these tumors. The results indicate that somatic mutation of FHL2 was not present and therefore probably not a cause of functional alterations in tumor cells.

4.2.4 Study of promoter methylation in HCC cells

To further explore whether the reduced expression of *FHL2* in HCC is due to promoter hypermethylation which leads to transcription silencing, the effect of demethylation treatment with 5-aza-2'-deoxycytidine (5-aza-dC) on *FHL2* expression was investigated. The results showed that the expression of *FHL2* was significantly increased in Hep3B, MiHA, L02 and HepG2 cell lines upon treatment with 5-aza-dC (Fig. 4.4). Meanwhile, *FHL2* expression level was correlated with the concentration of 5-aza-dC in these cell lines, which demonstrated about 2-5 fold induction of mRNA expression.

Next, the methylation status of *FHL2* promoter was evaluated by bisulfite genomic sequencing. The Methyl Primer Express software identified a CpG island located in the -1435/+1015 region of *FHL2* gene, using the conventional criteria for CpG island prediction as defined by Gardiner-Garden and Frommer (1987) (length ≥ 200 bp; %GC ≥ 50%, observed CpG/expected CpG ≥ 0.6) (Fig. 4.5, top panel). Primers were used to amplify a 340 bp region from -129 to +211 to analyze the CpG methylation sites (+1 defined as transcription start site). The results showed that there was almost a total lack of methylation in all the cell lines, indicating that the *FHL2* promoter was poorly methylated in these cells (Fig. 4.5B), which was inconsistent with their responsiveness towards 5-aza-dC treatment. These observations indicated that the decreased expression level of *FHL2* was probably due to the DNA methylation of those genes which function as the upstream regulators of *FHL2* instead of the promoter of *FHL2* itself.

4.2.5 Effect of TSA treatment on FHL2 expression

We also examined the effects of TSA on the expression of *FHL2* in liver cancer cells. Our result showed that the expression level of *FHL2* was significantly reduced in HepG2, Hep3B and WRL68 cells (Fig. 4.6). However, it increased significantly in Huh7 cells. The results indicated the downregulation of FHL2 expression was not due to histone deacetylation.

4.2.6 Deletion mutation analysis of *FHL2* promoter

To identify the promoter activities of the 5'-flanking region of *FHL2* gene, a series of 5'-deletion reporter plasmids were constructed by inserting the PCR fragments of various sizes into the pGL4.10-basic vector for luciferase activity analysis. A schematic diagram of the construct is shown in Fig. 4.7, top panel. The predicted promoter region upstream of exon 1b (untranslated region) and a TATA box (TTATAT) near the putative TSS were identified in the *FHL2* gene. Construct containing 2268 bp of 5' flanking region and 292 bp exon induced a 5-fold increase in luciferase activity over pGL4.10-basic in Huh7 cells (Figure 4.7). Deletion of 5' flanking region from -2268 to -1320 did not alter the promoter activity, but further deletion to -395 resulted in a higher activity and promoter showed a highest activity upon deletion to -138, which was 10-fold higher than that of pGL4.10-basic. However, when 5' region of the promoter was further deleted to -4 and +37, the promoter activity decreased considerably, although the deletion did not completely abolish promoter activity. The results indicated the presence of negative regulatory elements in the region from -1320 to -139, while the region from -138 to +37 contains the potential positive cis-acting elements necessary for *FHL2* transcription.

4.2.7 Bioinformatic analysis of *FHL2* promoter region

To further identify the possible *cis*-regulatory elements in the promoter region of *FHL2* gene, the DNA sequences between −184 and +94 bp which showed the presence of positive regulatory activity, were analysed with both matrix search for transcriptional binding site by MATCH® program in TRANSFAC® database (Kel *et al.*, 2003) and by MatInspector program (Cartharius *et al.*, 2005). These programs

used a weight matrix-based method to search for specific transcription factor (TF) binding sites. The common transcription factor binding sites were further subjected to alignment among multiple species with Ensembl Genome Browser (Stenger *et al.*, 2005). The most evolutionary conserved regions among different species were highlighted (Fig. 4.8), which may be functional regions in gene regulation. Five transcription factors which interact with the putative binding sites within the evolutionary conserved region were chosen for further investigation. The five transcription factors including ZF5, Activator protein-2 (AP-2), Specificity protein 1 (SP-1), Pax-5 and Serum response factor (SRF) as well as their putative binding sites are indicated in Fig. 4.7 and 4.8.

4.2.8 Expression analysis of TFs in HCC tissues

It remains unclear which transcription factors are responsible for regulation of *FHL2* transcription. To further investigate whether the predicted TFs are involved in the regulation of *FHL2*, the expression levels of these TFs were measured by quantitative real time PCR in 10 pairs of primary HCC and adjacent non-tumor tissues. The results showed that there were no significant differences in gene expression of AP-2A and SP-1 between tumor and normal tissues ($P>0.05$), indicating that these TFs were unlikely to contribute to the regulation of *FHL2* (Fig. 4.9). We found that ZF5 expression was downregulated in most tumors compared to their normal tissues (Fig. 4.10A). There was a significant difference in ZF5 expression between tumor and normal tissues (T/N =0.77, P=0.0008, Wilcoxon signed rank test) (Fig. 4.10B). On the other hand, a gender difference in Pax-5

expression was observed among these patients. Although not significant, the expression of Pax-5 tends to be lower in male HCC patients and it was downregulated in 7 out of 10 males (P=0.08) but upregulated in 4 out 9 female patients (Fig. 4.10A). Besides, the results also indicate that the expression of Pax-5 was correlated to that of *FHL2* in the male patients, which was shown to be downregulated to the same extent as *FHL2* level (Fig. 4.10C). In addition, we found that the expression of ZF5 in tumor tissues was also correlated with FHL2 expression in male patients. Given a greater susceptibility of men than women to HCC development, Pax-5 and ZF5 may be potentially involved in HCC pathogenesis in a gender-specific fashion. The results suggested that they may function as the upstream regulator of *FHL2* modulating its expression and its downregulation may lead to the decreased expression of *FHL2* in HCC.

4.3 Discussion

4.3.1 Characterization of human *FHL2* transcript variants

The human *FHL2* gene expresses different transcript variants which are known to differ only in the 5'UTR. In this study, we examined the variations in the different *FHL2* transcripts and characterized the promoter regulation of *FHL2* in HCC cells. Using EST analysis and RT-PCR, we identified different transcript variants of *FHL2* and characterized their exon sequences. We showed that the first three exons constitute the different isoforms of *FHL2*, with only two different first exons existed (defined as "1a" and "1b"). Comparing to the NCBI sequences, there were different variants of exon 1b (shorter and longer) for *FHL2* transcript variant 1 and 5. By EST analysis, exon 1b was identified to be 149 bp instead of 255 bp. However, the 5' end of the transcript will need to be determined by 5' RACE in future study. According to the NCBI, transcript variant 2 contains an extra 121-bp exon between exon 3 and 4. By means of the analysis of the amplified products, we find that all identified transcript variants do not contain this exon.

FHL2 gene produces transcripts by using two promoters with alternative 5' exons. The function of this alternative promoter has not been clearly established. In the EST analysis, we found that transcript variant 4 which contained exon 1a, was expressed preferentially in the heart tissue. It was observed that exon 1a lies approximately 40 kb upstream of exon 1b in genomic sequences. Since *FHL2* protein was known to be expressed abundantly in the heart and related to heart development and function, the promoter region flanking exon 1a may have a

tissue-specific regulation and transcriptional role in the tissue development. This promoter was not characterized in the present study. Further investigation will be needed to understand the importance of this isoform-specific regulation of promoter in heart functions.

Unlike transcript variant 4, all other variants were widely distributed in different organs shown by the EST analysis. Identical results were obtained from the RT-PCR analysis. Primers were selected specifically to amplify the exons between 1a and 4, as well as 1b and 4, respectively. We were unable to detect variant 4 in our samples (data not shown) which was explained by its tissue-restricted expression pattern. On the other hand, the other variants were found to be expressed in a variety of cell lines from different sources. In the present study, we have identified five alternative variants of *FHL2* including a novel splice variant, designated variant 3, which contains exon 1b only in the 5'UTR. This transcript was expressed at high levels in most cell lines and was present at similar levels to other transcripts in human liver tissues. Although multiple transcript variants existed for *FHL2*, the different expression levels of these *FHL2* transcripts have not been investigated previously. This may be because all transcripts were usually detected using a pair of primers. As well as measuring the *FHL2* gene expression, the isoforms expression pattern was analyzed in the HCC tissues and adjacent normal tissues. Tumor samples showing different expression levels of *FHL2* were examined for the isoform-specific expression. Although there was not an obvious dominant transcript among the four spliced forms of *FHL2*, slight changes in proportion of these transcripts was

observed in certain samples. There seems to be a higher proportion of the longest variants (variant 1 and 2) in both liver cancer cells and tumor tissues compared to the normal ones. However, there was no a clear trend with regard to switching transcripts among these samples. According to the nucleotide sequences of these *FHL2* transcripts, they were generated from different combinations of the first three non-coding exons and predicted to be translated into the same protein products. Since the length of 5'UTR could affect the translation of the resultant transcript, the different expression levels of these four transcript isoforms may result in the different translation efficiencies. Therefore, these multiple transcript isoforms may participate in the regulation of *FHL2* protein expression in human liver, however, the exact molecular mechanism remains to be investigated.

4.3.2 Mutation analysis of FHL2 gene

Besides expression studies, we also examined whether somatic mutation of *FHL2* gene could contribute to the HCC cancer phenotype. A previous study showed that eleven out of 14 prostate cancer samples had a missense mutation in nucleotide 154 in exon 4 (which results in the substitution of lysine into glutatmate) compared to non-diseased tissues (Teigan and Molund, 2004). In the present study, we did not find any mutation in the coding region of *FHL2* in the tumor samples. Therefore, the mutation of FHL2 protein was not significant in HCC, although gene mutation may be a mechanism that contributes to other cancers (e.g. prostate) by affecting the biological functions of FHL2 in cells. While our result was limited to the coding region, we cannot exclude the possibility that mutations in other regions (e.g. 5'UTR

or promoter) could also have an effect on the expression of FHL2 in HCC, but it awaits further investigation.

4.3.3 Study of the role of epigenetics in the regulation of FHL2 gene

In this study, we showed that *FHL2* were down-regulated in nine out of ten HCC tumor samples compared with that of matched normal liver tissues. This observation was consistent with the findings in a recent study (Ding *et al.*, 2009b). However, *FHL2* mRNA level were also reported being upregulated in eight out of ten liver tumors compared with matched normal tissues (Wei *et al.*, 2003). DNA methylation has emerged as an important epigenetic mechanism in the transcriptional regulation. To see whether the downregulation of *FHL2* in HCC samples were due to epigenetic inactivation, the *FHL2* expression was measured upon 5-aza-dC treatment. Our results demonstrate that the *FHL2* expression restored upon 5-aza-dC treatment in Hep3B, HepG2 and MiHA cell lines. However, bisulphite sequencing result showed that *FHL2* promoter was poorly methylated, which indicated the reduced expression of *FHL2* gene was not directly related to the methylation of its own promoter.

Moreover, TSA was shown to downregulate *FHL2* expression in a number of cell lines. TSA was a histone deacetylase (HDAC) inhibitor which can activate gene transcription by changing the acetylation status of histones. The results indicate that the loss of expression of *FHL2* in HCC did not seem to be associated with histone deacetylation. Although the general role of TSA was to induce expression, many studies indicate that TSA treatment can result in upregulation and downregulation of

a set of genes (in nearly equal ratio), and the effect seems to be gene-specific (Glaser *et al.*, 2003; Makki *et al.*, 2008, Van Lint *et al.*, 1996). The mechanism of repression of *FHL2* by TSA was unknown. We proposed that the effect of TSA on gene repression was resulted from the acetylation effect of histones which causes the activation of those repressor genes of *FHL2*.

4.3.4 Identification of transcription factors important in the regulation of the FHL2 gene

In this study, we also characterized the promoter regulation of *FHL2* gene in HCC cells. Since only the exon 1b transcripts were found in the liver and most other tissues, the *FHL2* proximal promoter region upstream of exon 1b was characterized in our study. We have identified promoter activity in the 2200 bp region upstream of the transcription start site and the presence of a TATA box near the TSS. Deletion of the region -1320/-139 resulted in a significant increase in promoter activity, indicating this region showed repressive effects on transcription due to presence of one or more negative regulatory elements. However, deletion of the region -138/+36 resulted in a drastic decrease of promoter activity, indicating this region was important in the positive regulation of *FHL2* gene, which contained the positive cis-acting elements critical for the *FHL2* transcription. In addition, we observed that a significant promoter activity was retained in the exon 1b and exon 2 regions of *FHL2* gene, which may also contain the positive cis-elements. To further characterize the *FHL2* gene regulation, the promoter region of orthologous gene was examined to identify the potential cis-elements involved in *FHL2* transcription. We

found that the region upstream of *FHL2* and exon 1b was highly conserved among different mammalian species, which indicated a possible regulatory function in transcription. By computer-based prediction, the promoter region -184 and +94 was found to contain putative binding sites for five transcription factors including ZF-5, AP-2, SP-1, Pax-5 and SRF. Two computer programs were used to identify the conserved transcription factor binding sites to provide a more accurate prediction. The results of our promoter analysis were in general agreement to the results of previous studies. One study showed that the 145-bp fragment of *FHL2* promoter was fully responsive to androgen induction as the 1570-bp fragment, which was attributed to binding of serum response factor (SRF) within the 145-bp sequence (Heemers *et al.*, 2007). *FHL2* was known to be a target gene of SRF which mediated the androgen induction of *FHL2*. Knockdown of SRF resulted in a decrease in *FHL2* expression and hampered the proliferation of prostate cancer cells. A most recent study identified another promoter region of *FHL2* (upstream of protein-coding sequence) within which Sp1 binding sites were located, and the correlation between *FHL2* and Sp1 expression in gastrointestinal cancers (Guo *et al.*, 2010). The GC-rich region of our promoter was also found to contain Sp1 binding sites. These results indicated that the regulation of *FHL2* by these transcription factors may play an important role in cancer progression.

Although the mechanism for the downregulation of *FHL2* in HCC tumors was not yet clear, the bioinformatics analysis showed that Pax-5 and ZF-5 has a conserved binding site in the proximal promoter region of *FHL2*. Furthermore, the

expression of ZF-5 showed a positive correlation with *FHL2* expression in HCC tissues. The correlation of Pax-5 was similar but was found in male patients. Therefore, it was reasonable to hypothesize that the downregualtion of *FHL2* in HCC cell lines may caused by downregulation of Pax-5/ZF5 which plays a positive function in *FHL2* transcription. However, the regulatory mechanism of Pax-5 and ZF-5 in HCC has not been explored. This prompts us to further characterize the possible role for these transcription factors in the regulation of *FHL2*.

4.3.5 Summary

In conclusion, our study has shown that the fragment between -138 and +292 bp in the 5' flanking region of *FHL2* contained positive regulatory activity. Multiple transcript variants for *FHL2* were expressed in various tissues, which may have specific roles in the regulation of *FHL2* expression through transcript switching. In addition, a novel transcript variant was identified and shown to be expressed in many cell lines and tissues. The different 5'exons found in *FHL2* transcripts indicated the presence of two distinct promoters, which may be involved in tissue-specific regulations of *FHL2*. The regulation of *FHL2* expression in HCC was believed to be the promoter regulation by upstream elements. Despite a lack of methylation in the promoter, there was a restoration of *FHL2* expression upon 5-aza-dC treatment, which was possibly linked to epigenetically silencing of those upstream genes other than *FHL2* itself. The correlation of Pax-5 and ZF5 expression with *FHL2*, together with their predicted conserved binding sites in promoter of *FHL2* supports the

possibility that these transcription factors may be involved in the regulation of *FHL2* expression.

4.4 Limitations and Future Perspectives

The study by Guo *et al.* (2010) has identified a promoter fragment which was located 1.5 kb upstream of ATG start codon in contrast to the one in our study. This indicated the existence of multiple promoters of *FHL2* gene. In our study, we have investigated the potential promoter of *FHL2* upstream of exon 1, in which significant promoter activity was detected. The CpG island was also found in the 5' region of *FHL2* gene that extends up to 1000 bp downstream of exon 1b. The results indicated the importance of the proximal promoter region (-138/+292) in the regulation of gene expression. Our data showed that the CpG island within this region was unmethylated. However, the promoter region upstream of the translation start site may be another site of gene regulation. We found that there was a CpG island located 217 bp upstream and 208 bp downstream of the starting codon. This indicated that decreased expression of *FHL2* may be due to promoter hypermethylation at other CpG islands. This would require further methylation analysis to validate our results. Besides, the different promoter regions of *FHL2* suggested that different regulatory sites (or elements) may be present that affect transcription. More studies are needed to examine the specific regulation of each of these promoters and the effect on gene transcription. Furthermore, the tissue-specific role for the transcriptional regulation of *FHL2* variant 4 and the involvement in heart development will also be investigated.

In our study, the potential regulatory elements of the *FHL2* gene were identified by computational analysis, by TFBS search and comparing genomic regions across

multiple species. However, future study will be required to confirm the binding of TFs to the specific genomic region by gel shift assay and chromatin immunoprecipitation assay (ChIP). Moreover, the conserved regions of the binding sites will be evaluated by site-directed mutagenesis analysis to confirm the specific binding of TF. The functional consequences of the transcription factor binding to promoter will also be examined by a luciferase reporter assay. Our study identified potential regulatory factors in HCC by expression analysis. Although some of them showed a correlation with *FHL2* in expression patterns, the results were limited by the small number of samples. A larger sample size was required to obtain reliable results.

A recent study showed that Pax-5 was involved in cancer. Pax-5 was identified to be a novel tumor suppressor in gastric cancer, which was shown to cause cell cycle arrest in G_0/G_1 phase and modulate the expression of the downstream targets such as p53, p21, cyclin D1 etc. The results also demonstrated the frequent epigenetic inactivation of Pax-5 in gastric tumors (unpublished data from Prof. Yu Jun). Our study showed the correlation of Pax-5 expression with *FHL2* in male HCC patients and the Pax-5 binding sites in *FHL2* promoter. Therefore, it was reasonable to hypothesize that Pax-5 function upstream of *FHL2* and may be epigenetically silenced during HCC development, which resulted in a decreased expression of *FHL2*. Moreover, the actions of Pax-5 on cancer suppression may be linked to *FHL2*. Furthermore, a previous study found that ZF5 is a downregulated gene identified in the metastatic human breast cancer cell lines overexpressing Bcl-xL (Méndez *et al.*,

2006). It showed that ZF5 is a transcriptional regulator associated with cell metastatic activity. Future investigation was needed to determine whether Pax-5 was epigenetically regulated and the possible roles of Pax-5 and ZF5 in HCC.

Table 4.1. Analysis of the 5'UTR EST sequences to identify the transcript isoforms of *FHL2*.

Accession No.	*Tissue/Organ*	*Exon * arrangement*	*Accession No.*	*Tissue/Organ*	*Exon * arrangement*
FHL2 Transcript variant 4 (NM_201557.3)					
BP259775.1	heart	1a, 4	R57505.1	heart	1a, 4
AV701652.1	adrenal gland	1a, 4	DA561967.1	heart	1a, 4
BI829702.1	brain	1a, 4	BP257466.1	heart	1a, 4
BP259904.1	heart	1a, 4	AA249230.1	heart	1a, 4
DA560402.1	heart	1a, 4	DA565357.1	heart	1a, 4
CF552311.1	muscle	1a, 4	N88051.1	heart	1a, 4
BP257640.1	heart	1a, 4	N87838.1	heart	1a, 4
AU310275.1	uncharacterized tissue	1a, 4	N56433.1	heart	1a, 4
BP260132.1	heart	1a, 4	R58049.1	heart	1a, 4
BI836901.1	pancreas, spleen	1a, 4	R57165.1	heart	1a, 4
(Total. 20)					
FHL2 Transcript variant 2 (NM_201555.1)					
DA428157.1	intestine	1b, 2, 3, 4	DA682076.1	ovary	1b, 2, 3, 4
BG326484.1	kidney	1b, 2, 3, 4	BE734330.1	placenta	1b, 2, 3, (X), 4
BI822119.1	brain, lung, testis	1b, 2, 3, 4	BE278420.1	placenta	1b, 2, 3, (X), 4
DA375986.1	brain	1b, 2, 3, 4	BI562043.1	testis	1b, 2, 3, 4
BQ070653.1	brain	1b, 2, 3, 4	AL544400.3	placenta	1b, 2, 3, 4
BI859139.1	mammary gland	1b, 2, 3, 4	BG750963.1	eye	2, 3, 4
BX397323.2	placenta	1b, 2, 3, 4	BQ671167.1	salivary gland	2, 3, 4
BX362555.2	cervix	1b, 2, 3, 4	BQ879376.1	salivary gland	2, 3, 4
AL547936.3	placenta	1b, 2, 3, 4	BG765299.1	skin	2, 3, 4
AL550363.3	placenta	1b, 2, 3, 4	CN315176.1	embryonic tissue	2, 3, 4
CB136991.1	liver	1b, 2, 3, 4	BG752058.1	eye	2, 3, 4
DA681164.1	ovary	1b, 2, 3, 4			
(Total. 23)					
FHL2 Transcript variant 1 (NM_001450.3)					
AL550367.3	placenta	1b, 2, 4	BF689796.1	skin	1b, 2, 4
BM552182.1	brain	1b, 2, 4	BM020940.1	brain	1b, 2, 4
CD245772.1	brain	1b, 2, 4	BX345763.2	placenta	1b, 2, 4
BP317193.1	heart	1b, 2, 4	BI752160.1	brain	1b, 2, 4
BQ674751.1	salivary gland	1b, 2, 4	BI768981.1	lung & spleen	1b, 2, 4
BG325700.1	kidney	1b, 2, 4	CN315180.1	embryonic tissue	1b, 2, 4
CD252183.1	brain	1b, 2, 4	BQ691655.1	pancreas	1b, 2, 4
DB058466.1	testis	1b, 2, 4	AL523628.3	uncharacterized tissue	1b, 2, 4
BQ218584.1	pancreas	1b, 2, 4	BE734708.1	placenta	1b, 2, 4
BP256716.1	kidney	1b, 2, 4	AU099359.1	uncharacterized tissue	1b, 2, 4
BM050765.1	eye	1b, 2, 4	CB150153.1	liver	1b, 2, 4
BM821704.1	stomach	1b, 2, 4	BM021037.1	brain	1b, 2, 4

(Cont'd) Table 4.1

DA897526.1	muscle	1b, 2, 4	BE279594.1	placenta	2, 4
BP261327.1	intestine	1b, 2, 4	BE408395.1	placenta	2, 4
DB027814.1	testis	1b, 2, 4	BE407750.1	placenta	2, 4
DA600757.1	connective tissue	1b, 2, 4	BE901781.1	placenta	2, 4
BP260711.1	intestine	1b, 2, 4	BM461447.1	eye	2, 4
DB264523.1	uterus	1b, 2, 4	BE900326.1	placenta	2, 4
(Total. 36)					
FHL2 Transcript variant 5 (NM_001039492.2)					
AL555196.3	cervix	1b, 3, 4	BM763421.1	stomach	1b, 3, 4
BX404505.2	uncharacterized tissue	1b, 3, 4	BX343906.2	placenta	1b, 3, 4
BX425058.2	placenta	1b, 3, 4	BI754829.1	brain	1b, 3, 4
AL583628.3	placenta	1b, 3, 4	BM559077.1	skin	1b, 3, 4
BM843999.1	lymph node	1b, 3, 4	BU506908.1	uterus	1b, 3, 4
DA430603.1	intestine	1b, 3, 4	CN315178.1	embryonic tissue	1b, 3, 4
DA893258.1	muscle	1b, 3, 4	BE733336.1	placenta	1b, 3, 4
BM807630.1	skin	1b, 3, 4	CB989635.1	placenta	1b, 3, 4
BM914664.1	skin	1b, 3, 4			
(Total. 17)					
FHL2 novel transcript (variant 3)					
DA003204.1	uncharacterized tissue	1b, 4	CN315181.1	embryonic tissue	1b, 4
AL521653.3	uncharacterized tissue	1b, 4	BX344059.2	placenta	1b, 4
BX417211.2	placenta	1b, 4	BI821099.1	brain, lung, testis	1b, 4
BP252263.1	kidney	1b, 4	BX447182.2	uncharacterized tissue	1b, 4
CB141643.1	liver	1b, 4	BG324062.1	kidney	1b, 4
BM808975.1	brain	1b, 4	BM051433.1	eye	1b, 4
BG765878.1	skin	1b, 4	BG471592.1	eye	1b, 4
BI488433.1	brain	1b, 4	BG473587.1	eye	1b, 4
BX446510.2	placenta	1b, 4	BM836767.1	ascites	1b, 4
(Total. 18)					
Miscellaneous					
BG748834.1	eye	3, 4			
CB120986.1	liver	3, 4			
(Total. 2)					
Unaligned (high error rate) or genomic contamination					
CD513350.1	pituitary gland	3, 4	DB056802.1	testis	3, 4
BI160912.1	pancreas	3, 4	AL541520.3	placenta	3, 4
BI160022.1	pancreas	4	DB010561.1	intestine	4
BQ962795.1	pancreas	4			
(Total. 7)					

*: Exons beyond exon 4 (first translated exon) was left out for simplicity.
(X): indicates an extra 121 bp between exons 3 and 4.

Table 4.2: Exon-intron analysis of the human *FHL2* gene

Exon		Splicing acceptor	Splicing donor	Intron	
Number	Length (bp)			Number	Length (bp)
1a	375	agggcagcgcAGCTGGCTGG	AAAACCACAG**gt**aagggcca	1	39,278
1b	149*	gagccgaggcGTGCATCTCC	CTGCGGTGCC	--	0
2	128	GTGAGTACCT	GGGGAGACTG**gt**gagaggag	2	2,144
3	51	ctttctct**ag**TGGCTGAGAA	TGACTTTGGG**gt**gagtcaag	3	10,106
4	180	tttttgat**ag**GTTGCTGAAA	TGACTGCAAG**gt**acctgctg	4	12,627
5	175	ggccccac**ag**GACTTGTCTT	ATCATGCCAG**gt**caggaggc	5	5,819
6	170	ctgatgac**ag**GTACCCGCAA	GTGCAAAAAG**gt**atctcaga	6	4,098
7	187	gtccctgc**ag**CCCATCACCA	CCCATCAGCG**gt**gagtgtcc	7	1,850
8	609	ctgttaac**ag**GACTTGGTGG			

*: Predicted size of exon 1b based on EST analysis.

Exon and intron sequences are shown as upper case letters and lower case letters, respectively. Bold letters represent the 5' and 3' intron donor and acceptor splice sites.

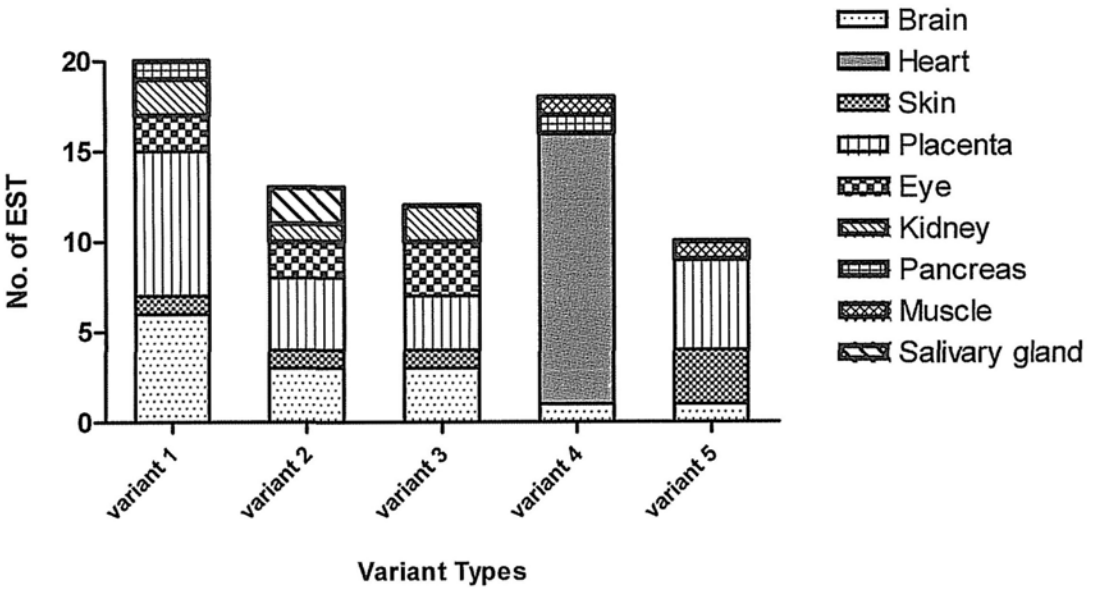

Fig. 4.1: Analysis of the tissue distribution of splice variants of *FHL2* using EST tissue information.

A

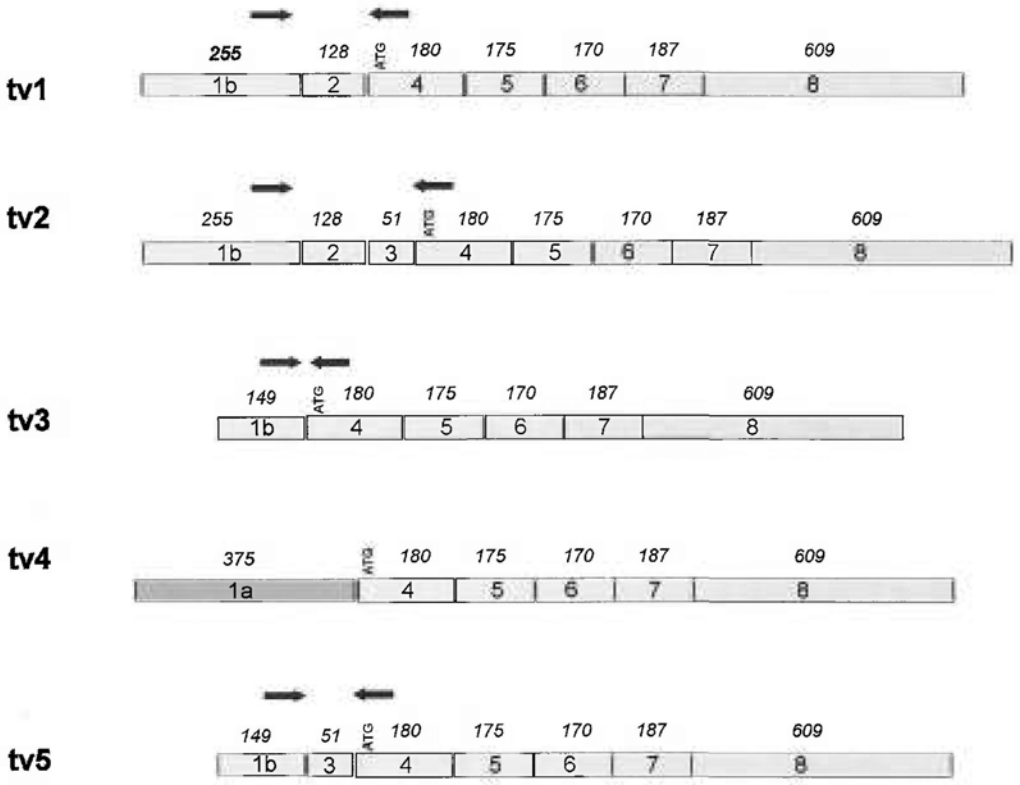
tv1
255
128
ATG
180
175
170
187
609
1b
2
4
5
6
7
8
tv2
255
128
51
ATG
180
175
170
187
609
1b
2
3
4
5
6
7
8
tv3
149
ATG
180
175
170
187
609
1b
4
5
6
7
8
tv4
375
ATG
180
175
170
187
609
1a
4
5
6
7
8
tv5
149
51
ATG
180
175
170
187
609
1b
3
4
5
6
7
8

B

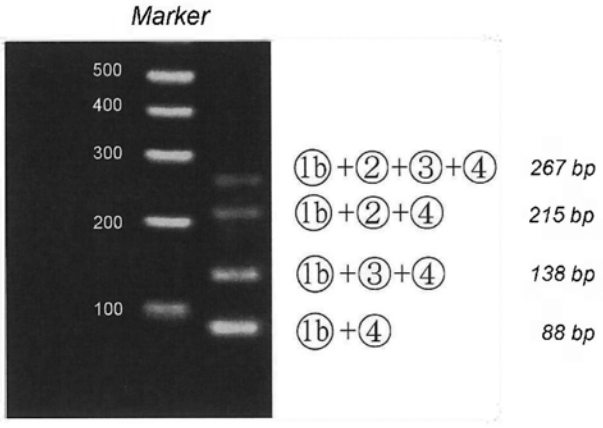
Marker
500
400
300
200
100
①b+②+③+④
267 bp
①b+②+④
215 bp
①b+③+④
138 bp
①b+④
88 bp

Fig. 4.2: Analysis of transcript variants of *FHL2*. (**A**) A schematic representation of the exon arrangement of the various splice variants. The exons were represented by boxes with numbers, whereas the length of each exon in base pairs is indicated above (in italics). (**B**) RT-PCR amplification of a fragment comprising exons 1b-4 (the location of primers is represented by arrows) from GCT cells unveils the four transcript variants of *FHL2*. The specific bands of the expected size were obtained after 30 cycles of amplifications and the identity of each band was confirmed by sequencing.

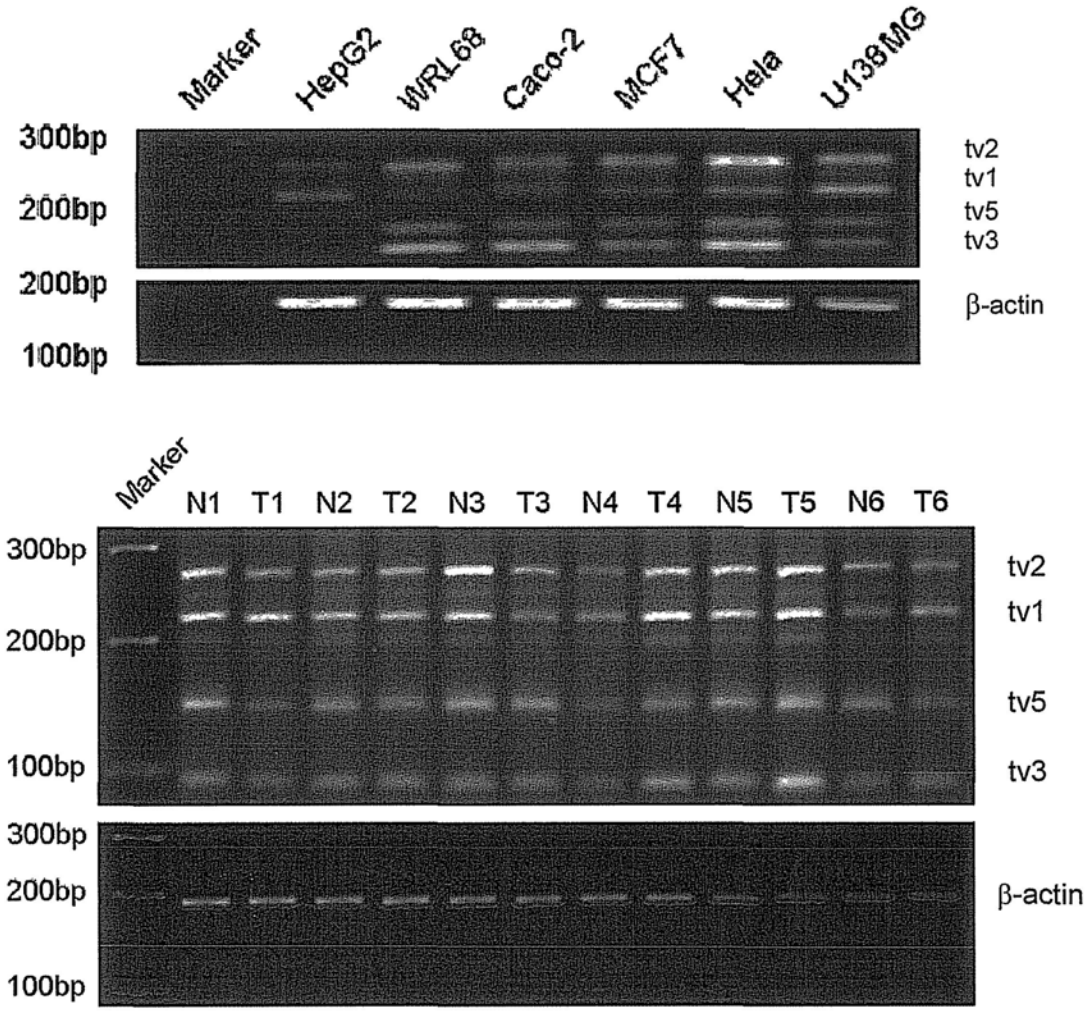

Fig. 4.3: Confirmation of the existence of FHL2 multiple transcripts in human cell lines and HCC tissue samples. Total RNA was extracted from six cell lines or HCC tumor and matched normal liver tissues as indicated on the top of the lanes, in which T represent tumor tissue, N represent normal liver tissue. Beta-actin was used as internal control. The sizes of the markers are labeled at the left of the figures. The pairs of samples are (sample code) 425, 439, 451, 293, 445 and 552 (from left to right).

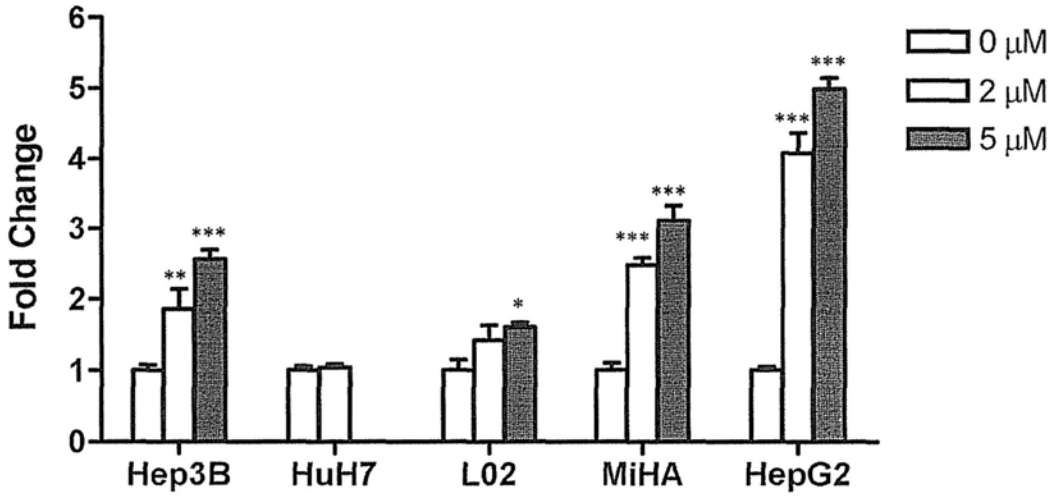

Fig. 4.4: Relative expression level of *FHL2* mRNA in HCC cell lines after 2 days of demethylation treatment with 5-aza-dC. Each bar represents the mean ± S.D. for triplicate wells. Single asterisk "*" indicates p-value < 0.05, double asterisks "**" indicates p-value < 0.01, while triple asterisks "***" indicate p-value < 0.001 with respect to control.

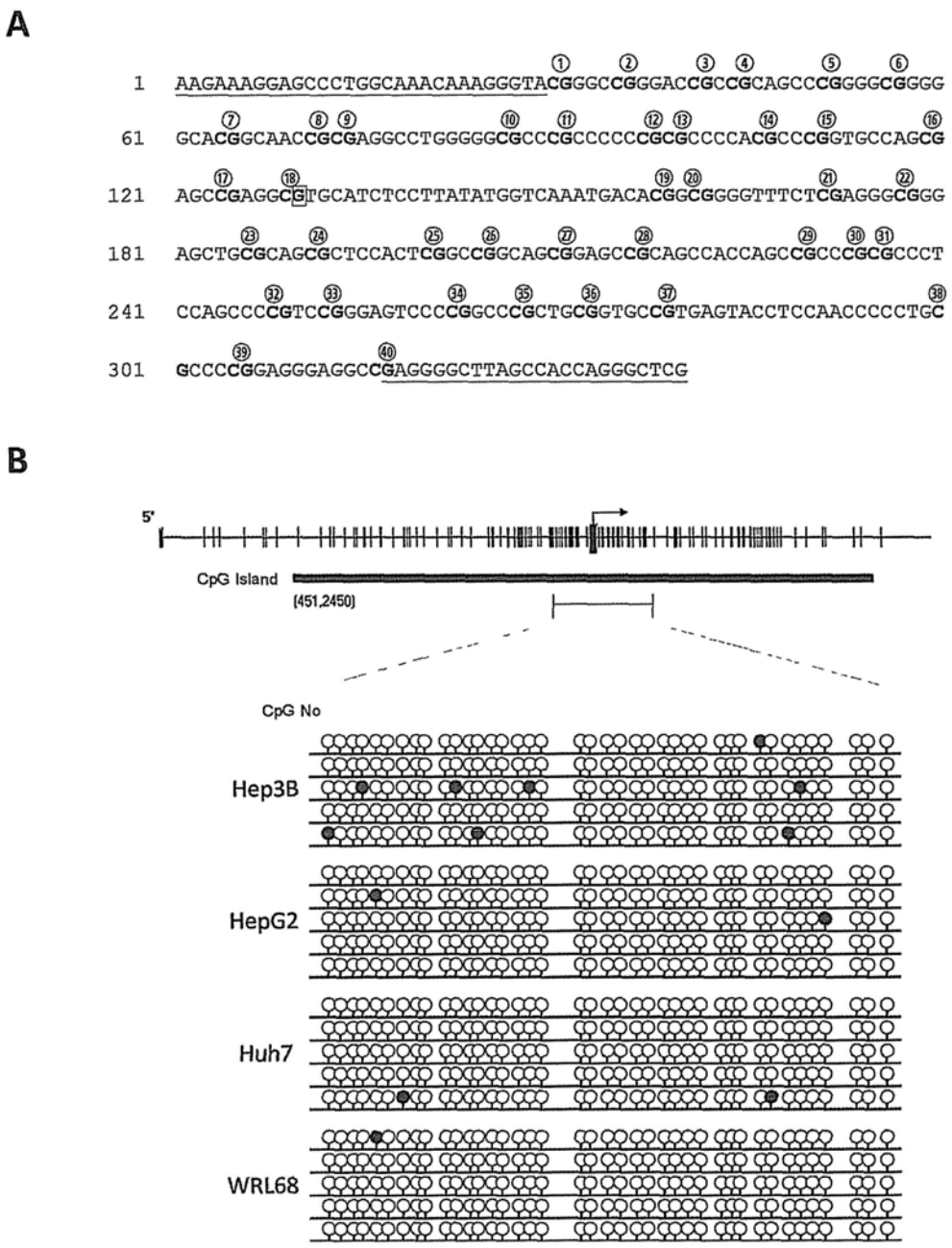

Fig. 4.5: Bisulfite genomic sequencing of *FHL2* promoter region in different cell lines. (**A**) Bisulfite sequencing was performed on the *FHL2* genomic region (-129 to +211 bp) relative to the transcription start site (TSS). Each of the CpG sites is numbered in the DNA sequence under analysis (the position of TSS was marked by a box and by an arrow in fig. B, top panel). Primers sequences for sequencing of this

region are underlined. (**B**) The methylation status of the *FHL2* promoter region in different liver cancer cell lines (Huh7, Hep3B, HepG2 and WRL68) was determined. Each row of circles represents the sequence of an individual clone. Open circles indicates unmethylated CpG dinucleotides while filled circles indicates the methylated ones.

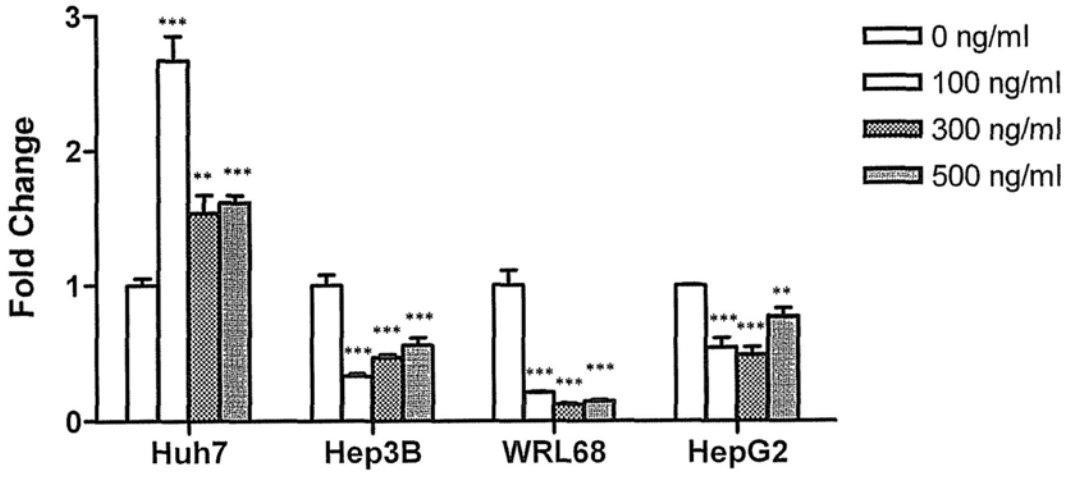

Fig. 4.6: Expression of FHL2 transcripts after treatment with TSA for 24 h. Each bar represents the mean ± S.D. for triplicate wells. Double asterisks "**" indicates p-value < 0.01, while triple asterisks "***" indicate p-value < 0.001 with respect to control.

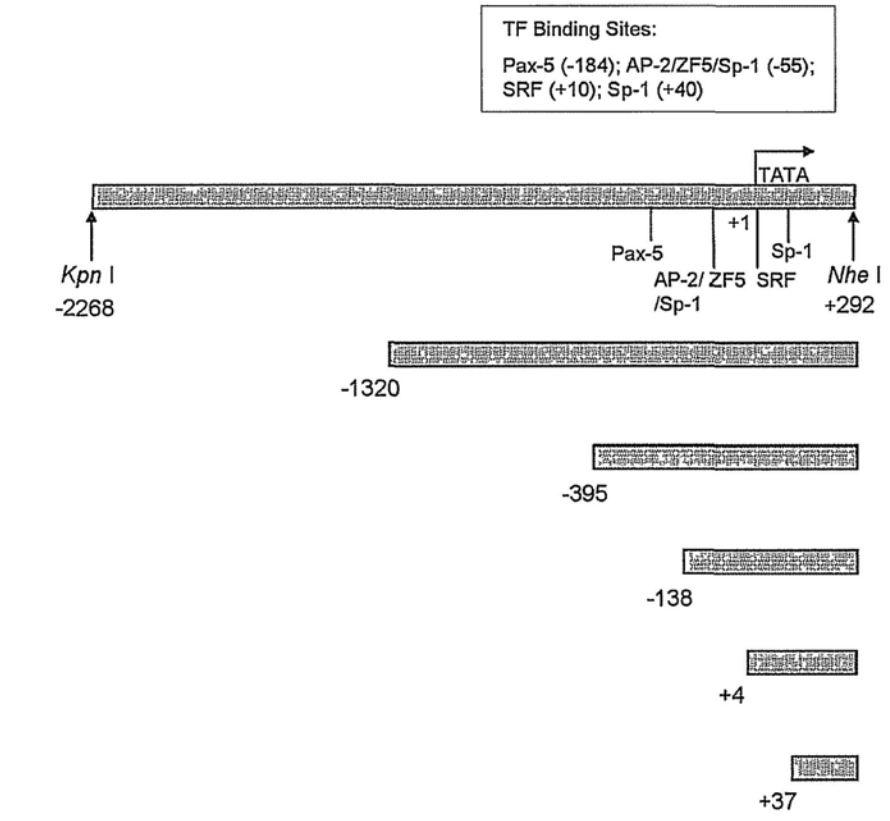
TF Binding Sites:
Pax-5 (-184); AP-2/ZF5/Sp-1 (-55);
SRF (+10); Sp-1 (+40)
TATA
+1
Pax-5
AP-2/ ZF5 /Sp-1
SRF
Sp-1
Kpn I
-2268
Nhe I
+292
-1320
-395
-138
+4
+37

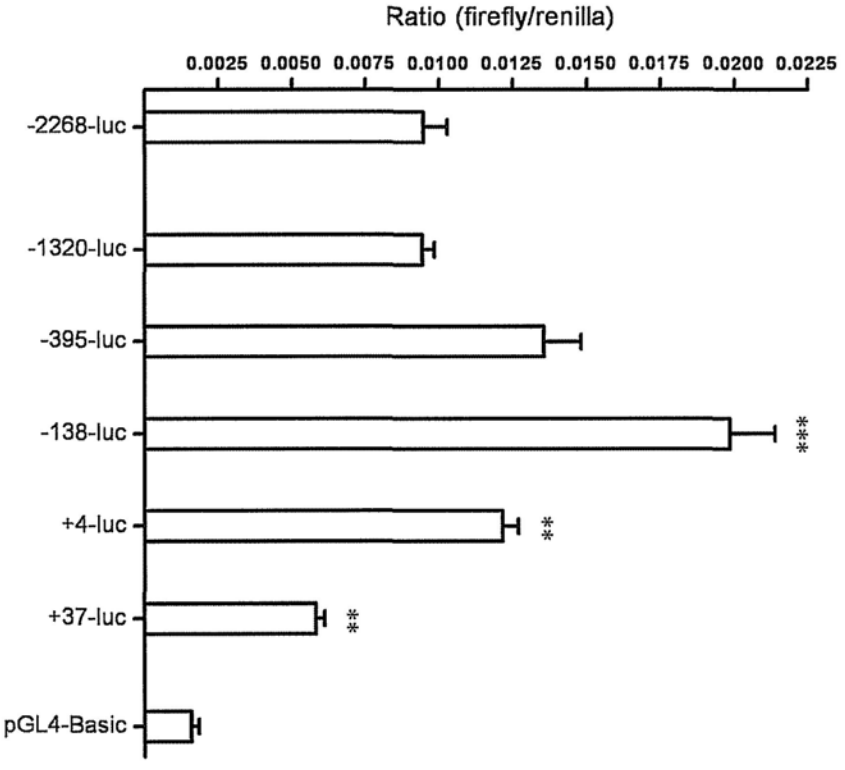
Ratio (firefly/renilla)
0.0025 0.0050 0.0075 0.0100 0.0125 0.0150 0.0175 0.0200 0.0225
-2268-luc
-1320-luc
-395-luc
-138-luc
+4-luc
+37-luc
pGL4-Basic

Fig. 4.7: Deletion analysis of the upstream sequences of *FHL2* gene. *Upper panel:* A series of truncated 5'-flanking sequences of *FHL2* were fused to the luciferase reporter gene in the pGL4.10-basic vector. Numbers indicate positions relative to the transcription start site (+1). The locations of binding sites for the transcription factors in the upstream *FHL2* promoter are described in Fig. 4.8. *Lower panel:* Promoter activities of the luciferase constructs were determined by transient transfection into Huh7 cells and dual luciferase assay. Results are presented as the ratio of *firefly* luciferase activity to the *renilla* luciferase activity. The small number was due to the high molar ratio of the *renilla* : *firefly* vector used for transfection. Data were calculated as average with S.D. from three independent experiments, each done in triplicates (n = 9). Double asterisks "**" indicates p-value < 0.01, while triple asterisks "***" indicates p-value < 0.001.

Fig. 4.8: TFs binding sites within the conserved region of *FHL2* by alignment for multiple species. By using Ensembl Browser tool, fragments spanning from -184 to +94 were aligned among different species with their names indicated on the left. The nucleotides highlighted in red are located in exons according to Ensembl database. The conserved regions (>50% of base in alignment match) are highlighted in blue shadows. The common TF binding sites predicted by MATCH and MatInspector are indicated under the aligned sequence. Basepairs marked red are important, which show a high conservation for the TF binding motif. Basepairs in capital letters denote the core sequence (usually 4) used by the MatInspector program. The transcription start site (TSS) and transcription direction are indicated as a black arrow.

AP-2A expression

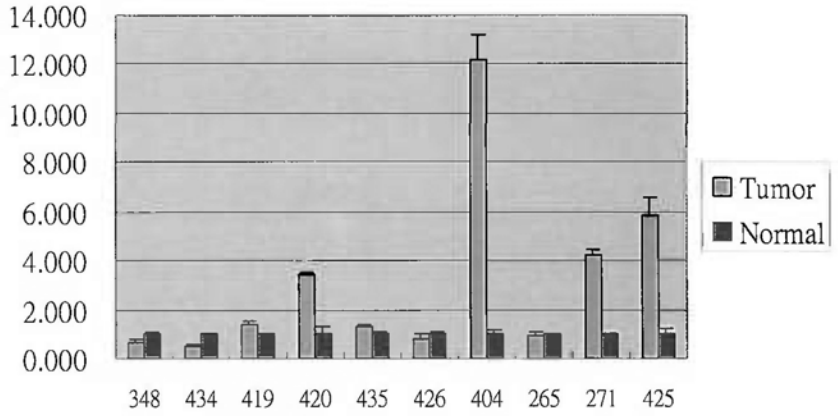

SP-1

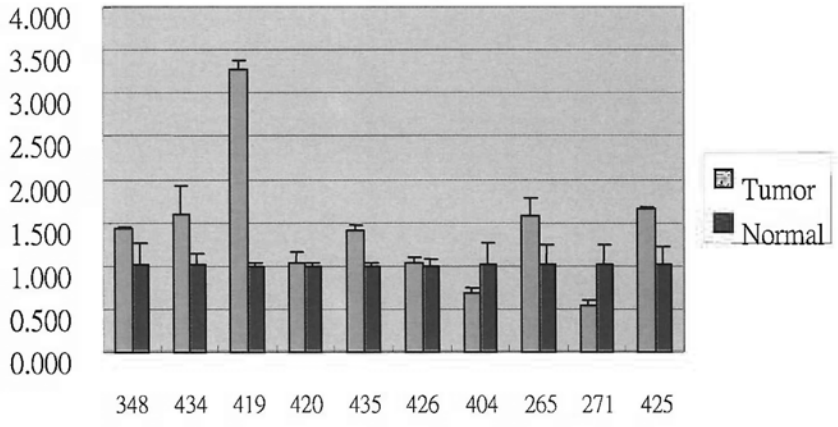

FHL2 expression

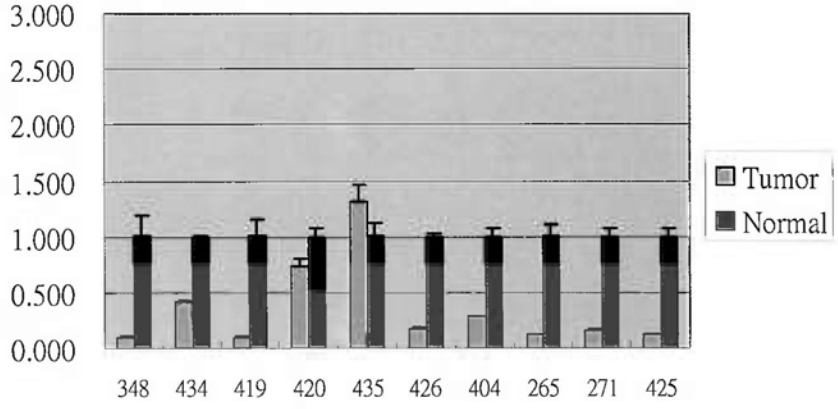

Fig. 4.9: Expression analysis of TFs in HCC tissue samples. The level of the TF gene expression of AP-2A and SP1 together with *FHL2* in tumor tissues relative to the matched non-tumor tissues were determined by quantitative real time PCR. Each bar represents the mean ± S.D. of triplicate determinations.

A

Pax-5

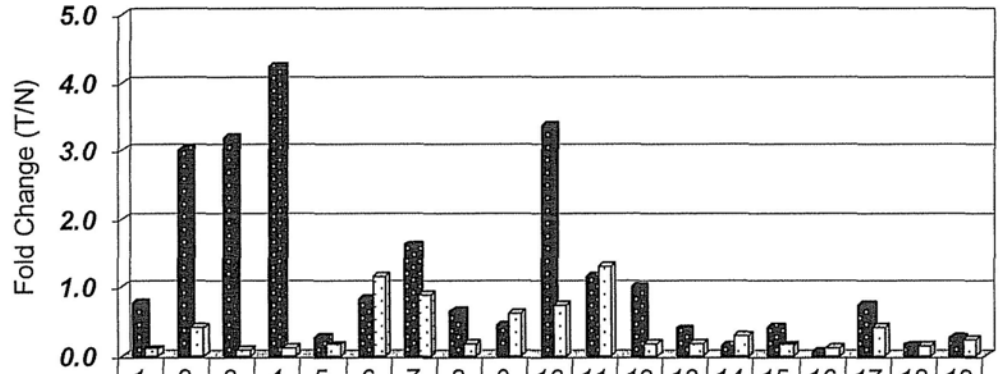

	1	2	3	4	5	6	7	8	9	10	11	12	13	14	15	16	17	18	19
Pax-5	0.8	3	3.2	4.2	0.3	0.8	1.6	0.6	0.5	3.4	1.2	1	0.4	0.2	0.4	0.1	0.7	0.2	0.3
FHL2	0.1	0.4	0.1	0.1	0.2	1.2	0.9	0.2	0.6	0.7	1.3	0.2	0.2	0.3	0.2	0.1	0.4	0.1	0.2

ZF5

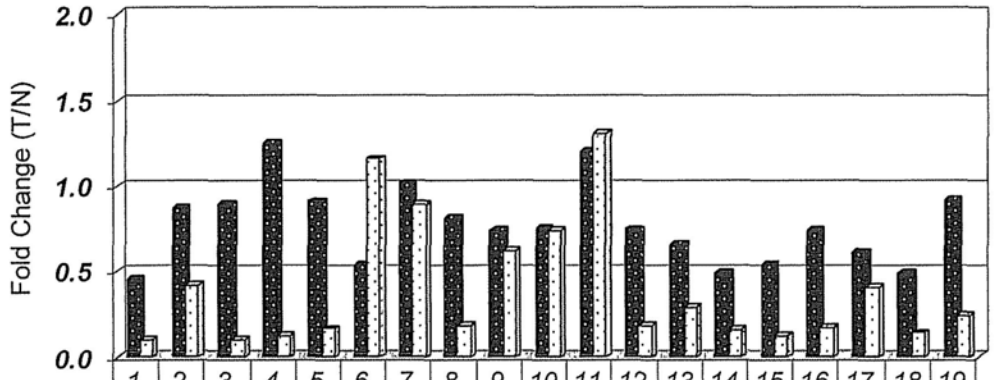

	1	2	3	4	5	6	7	8	9	10	11	12	13	14	15	16	17	18	19
ZF5	0.5	0.9	0.9	1.2	0.9	0.5	1	0.8	0.7	0.7	1.2	0.7	0.7	0.5	0.5	0.7	0.6	0.5	0.9
FHL2	0.1	0.4	0.1	0.1	0.2	1.2	0.9	0.2	0.6	0.7	1.3	0.2	0.3	0.2	0.1	0.2	0.4	0.1	0.2

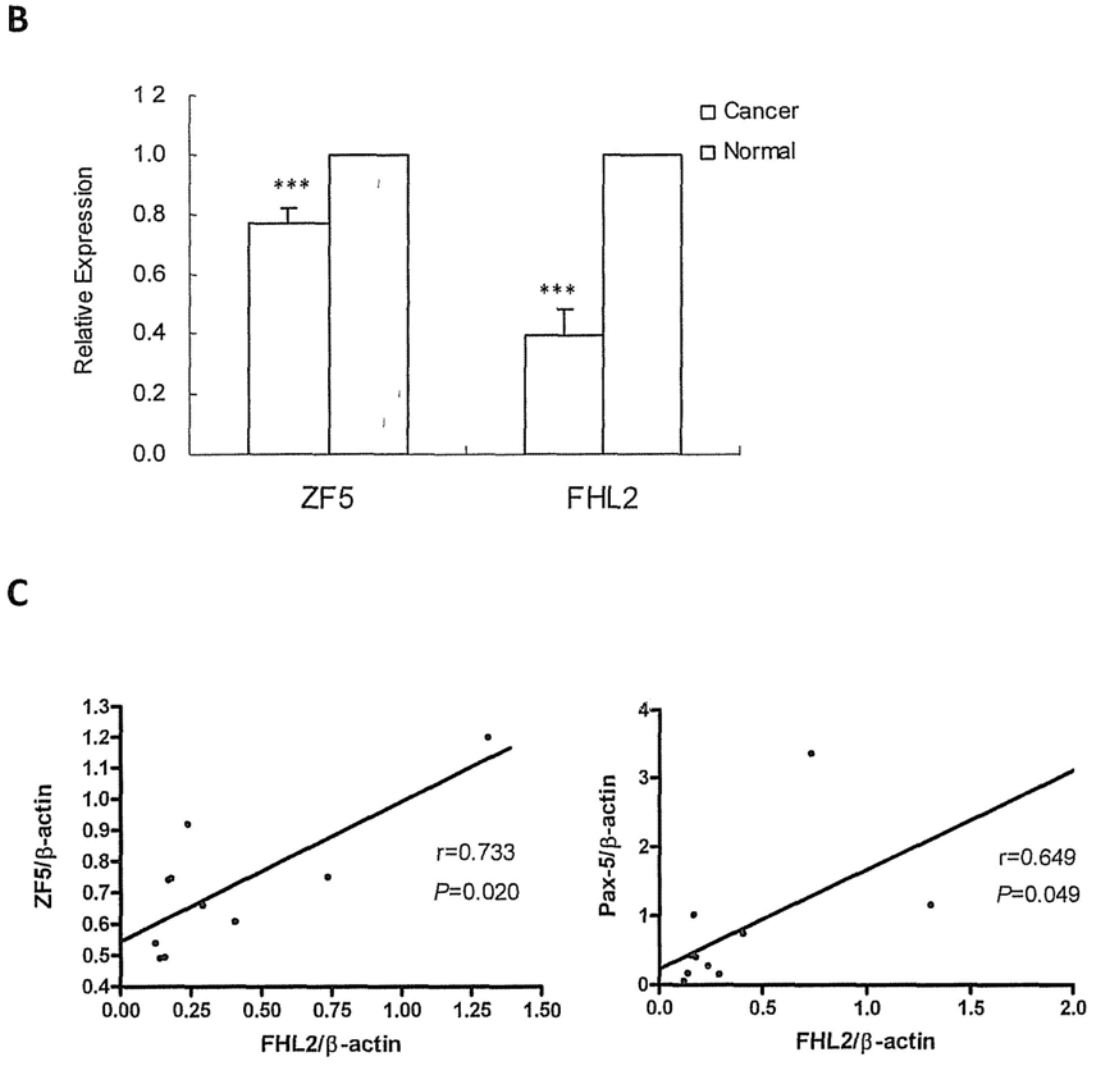

Fig. 4.10: Expression analysis of TFs in HCC tissue samples. **(A)** The expression level of Pax-5 and ZF5 together with *FHL2* in tumor tissues relative to the matched nontumor tissues were determined by quantitative real time PCR. Samples **1-9**: female patients; **10-19**: male patients. Each bar represents the mean of triplicate determinations. The error bars were omitted for clarity. **(B)** The data showed a significant difference of ZF5 expression in tumor and normal tissues (error bar: SEM, ***P<0.001 between normal and cancer) and **(C)** a positive correlation between Pax-5 and ZF5 expression and *FHL2* expression in the male patients (*P<0.05) as assessed by Spearman's correlation method (r: correlation coefficient).

Chapter 5

MICROARRAY ANALYSIS OF FHL2 KNOCKOUT MICE

5.1 Introduction

FHL2 have been shown to play a tumor suppressor function in HCC. However, the exact mechanism was poorly understood. The FHL2 knockout mice have recently been generated and they are viable and develop normally (Chu *et al.*, 2000). In the present study, microarray gene expression profiling of liver was performed to identify the genes regulated by FHL2 knockout and identify several new genes that may be involved in the pathogenesis of HCC. The microarray analysis of FHL2 knockout mice indicated the possible roles of FHL2 in immune functions and cancer. Combining the microarray expression and the clinical data from HCC tissues, Bcl-6 and Creld2 were identified to be possible target genes of FHL2 which were downregulated in HCC.

5.2 Results

5.2.1 Functional analysis of microarray data

The gene expression pattern of FHL2 knockout mice and wild-type mice was compared. We used a cut-off value of 2.0 for analysis of microarray data. There were totally 34 genes which showed 2-fold up- or down-regulation (Supplementary Table S1). The differentially expressed genes were classified according to the gene ontology (GO) information. Table 5.1 showed the genes that were classified into various functional categories (groups). In addition, the list of genes was also submitted to DAVID for functional annotation and classification. Results shown in Fig. 5.1 represent the enrichment of GO terms obtained from the functional annotation tool of DAVID and they are ordered by the enrichment *p value obtained from* statistical analysis. To further explore the functional relationship between genes, the groups of genes with common biological theme were represented by heat map diagrams (Fig. 5.2). We found that knockout of FHL2 affected the genes that were involved in:

(i) Immune response/ system - genes that may play a role in inflammatory response, e.g. Bcl6, Ighg, Chst1.

(ii) Cell adhesion and motility – genes that may be involved in tumor cell motility, e.g. Bcl6 and Onecut1.

(iii) Carbohydrate metabolism – genes involved in carbohydrate metabolism, e.g. Chst1 and Insl.

(iv) Cellular secretion into the extracellular region, e.g. Inhbe, Creld2, Lcn2, Bglap-rs1, Ins1, Ighg, Saa2.

(v) Metal ion binding - e.g. calcium ion binding in regulation of bone mineralization (Bglap-rs1), calcium binding endoplasmic reticulum gene

(Creld2), zinc binding transcription factor (Zfp42), heme/ iron binding (Cytochrome P450s Cyp26a1 and Cyp2b9).

(vi) Transcription regulation (Cluster 4) - e.g. binding to DNA or interacting with transcription factors (e.g. Bcl6, Zfp42, Ppp1r10, Onecut1).

(vii) Transmembrane proteins (e.g. Chst1, Ighg, Mfsd2) and those proteins that have been linked to signal transduction - e.g. olfactory receptor in sensory perception (Olfr172), associated with release of Ca^{2+} from sacroplasmic reticulum (Trdn).

The gene list was also analyzed using the Ingenuity Pathway Analysis (IPA) software. The full gene list was input to the IPA system for analysis. The top function classes of these genes included cancer, digestive system development and function, hematological disease, immunological response and inflammatory response (Table 5.2).

5.2.2 Pathway Enrichment Analysis

To find the possible pathways regulated by FHL2, pathway enrichment analysis was performed using MetaCore™, a commercial integrated software suite developed by GeneGO company. The gene lists for 1.5 fold, 1.6 fold, 1.7 fold and 2 fold changes were mapped into GeneGO database to do the analysis individually.

Table 5.3 shows the 10 pathways found by 2-fold expression change gene lists. The significant pathways were highlighted in bold and indicated by p-values. The

full detail of pathways for each gene list was available as spreadsheet files (not listed here). The degree of overlapping of those gene lists was presented in Venn diagram. Fig. 5.2 shows the candidate pathways' overlapping among these four lists. GeneGO's functional ontology enrichment results (Fig. 5.3) gave the 10 overlapped pathways ordered by p-value. In the figure, it used orange, blue, red and green color to represent the 2 fold, 1.5 fold, 1.6 fold and 1.7 fold condition respectively. The p-value of top 7 pathways were less than 0.05. These pathways were associated with various metabolic pathways, such as keratin sulfate metabolism and amino acid synthesis and metabolism.

5.2.3 Gene network analysis

The molecular pathway regulated by FHL2 was identified using the IPA analysis. The program identified the most significant network (with the highest score of 11) which consists of six focus genes: Alas1, Bcl6, Cabyr, Lcn2, Onecut1 and Saa2 (Fig. 5.4, top panel). The function was associated with cellular development, hematological system and development. The gene network was represented in Figure 5.4 containing all the connected genes. Red and green colour denotes the up- and down-regulated genes respectively. The results indicated that tumor necrosis factor (TNF) and interleukin-4 (IL4) may be linked to the FHL2 pathway in the regulation of the downstream genes.

5.2.4 Microarray validation

Real-time PCR was used for validating the gene expression data obtained from microarray experiment. Nine representative genes whose expression levels were remarkably changed in the microarray were further measured. The qPCR data was in good consistency with the microarray data (Fig. 5.5). The real-time RT-PCR expression data for each gene among the wild-type mice and FHL2 knockout mice was shown Fig. 5.6.

5.2.5 Gene expression pattern in clinical samples

To identify the genes which may be correlating to FHL2, the gene expression levels were also analyzed in HCC tissue samples by quantitative real-time PCR. The cancer-related genes Creld2 and Bcl-6 were selected for investigation. We found that the expression of Creld2 and Bcl-6 was downregulated in 8 out of 10 tumors and 11 out of 20 tumors respectively (Fig. 5.7 and 5.8). The median expression level of Creld2 was significantly lower in tumor tissues compared with non-tumor tissues (T/N: 0.443, P=0.032, by Wilcoxon signed rank test) (Fig. 5.7). Although not statistically significant, there was also a trend for lower expression of Bcl-6 mRNA in tumor tissues compared with non-tumor tissues (T/N: 0.868, P=0.142) (Fig. 5.8). No significant correlation with the expression of FHL2 was detected for both genes. The results indicated that Bcl-6 and Creld2 may be novel target genes of FHL2 in HCC.

5.3 Discussion

5.3.1 Identification of downstream targets of FHL2 by microarray

Microarray was used to study the gene expression pattern in the FHL2 knockout mice. This study attempted to identify specific genes regulated by FHL2 that could be responsible for the mechanisms for cancer.

In the knockout mice, we found significant changes in expression of a number of genes that were involved in immune function, inflammatory response, hematological function and transcription regulation. Interestingly, a class of cancer-related genes was identified (Cy26a1, Lcn2, Bcl6). For example, lipocalin 2 (Lcn2), a secreted glycoprotein, was a tumor marker recently identified that is abnormally expressed in many types of cancers (Shi *et al.*, 2008; Leng *et al.*, 2009; Cho and Kim, 2009). In breast cancer cells, Lcn2 enhances tumor growth and metastasis by protecting MMP-9 degradation and increasing angiogenesis (Fernández *et al.*, 2005). Interestingly, Lcn2 (or oncogene 24p3) was found to be the most upregulated gene after the induction of liver tumors using three tumor mice models, which suggests a role in hepatocarcinogenesis (Meyer *et al.*, 2003). Moreover, the results show that some of the affected genes were involved in a number of cellular metabolic pathways (Fig. 5.3). Although the specific pathways were unknown from these data, there was some indication of the roles played by FHL2. Using a lower threshold (1.7-fold) in the microarray analysis, we also found that FHL2 affected genes involved in glucose metabolic process (Ins1, Onecut1, predicted gene EG629081, Pfkfb3) and have links to insulin signaling pathways. Previously, we performed

experiments in knockout and wild-type mice and they showed difference in glucose-induced insulin release (data not shown). Moreover, the difference of glucose tolerance was demonstrated between the two groups of mice in a preliminary experiment (data not shown). Therefore, FHL2 may play a role in regulating glucose metabolism and the pathogenesis of diabetes.

From the microarray analysis, we found that cyclin D1 (Ccnd1) was also linked to the FHL2 pathway. Cyclin D1 has cell cycle regulatory function. The expression was downregulated in the $FHL2^{-/-}$ mice compared to control mice. The change in cyclin D1 expression was different from that in FHL2 overexpression study. FHL2 was known to interact with β-catenin and the activation of β-catenin was implicated in the development of cancer (Wei *et al.*, 2003). Although cyclin D1 was known to be activated by FHL2 which was dependent on β-catenin, the significance of gene regulation in liver tissue awaits further investigation.

The network analysis predicted that the FHL2 effect may be mediated by TNF and IL-4. In fact, FHL2 has been shown to be related to the production of the pro-inflammatory cytokines such as TNF-α, IL-6, IL-8 that was implicated in myocardial injury following cardiopulmonary bypass (Wan *et al.*, 2002) and cancer (Martin *et al.*, 2007). FHL2 was also found to inhibit the RANK (member of TNF family receptor) signaling through association with TRAF6 which was activated in osteoclastogenesis (Bai *et al.*, 2005). The results suggested that TNF-α may be related to the signaling of FHL2, which merits further study.

5.3.2 Identification of novel downstream targets of FHL2 which showed altered expression in HCC

The microarray was also used to identify the genes that were correlated with FHL2 in HCC. We studied whether the gene expression was altered in HCC samples. We found that the expression of Creld2 was significantly downregulated in most of tumors compared to adjacent normal tissue. Although not significant, there was also a trend for Bcl-6 to be downregulated in tumors with low FHL2 expression. They may be functionally related to FHL2. Bcl-6, a gene involved in cell cycle and apoptosis, was induced by FOXO transcription factors which could suppress the level of antiapoptotic Bcl-xL (Lam *et al.*, 2006; Fernandez de Mattos *et al.*, 2004). Bcl-6 may play a role in proliferation of cancer cells. Our results also showed that the expression of Bcl-6 was significantly down-regulated in the FHL2 overexpressing stable cells compared to the control cells (shown in Fig. 5.8B), suggesting that Bcl-6 may be regulated by FHL2. Bcl-6 showed a complex expression patterns in cancers. A recent study showed that there was a loss of expression of Bcl-6 oncoprotein during breast cancer progression (Pinto *et al.*, 2009). Creld2 was first identified to be a novel endoplasmic reticulum (ER) stress-induced gene (Oh-hashi *et al.*, 2009). ER stress was linked to the onset and progression of many diseases including neurodegenerative diseases, cancer, diabetes, etc. Recently, Creld2 was found to be a novel target gene of androgen receptor (AR) in pancreatic cancer that mediates disease progression (Jariwala *et al.*, 2007). Interestingly, FHL2 was known to be a co-activator of AR (Muller *et al.*, 2000) and thus Creld2 should

also be responsive to FHL2 similar to AR. However, further evidence was needed to prove a relation between these genes and FHL2 as well as their roles in HCC.

In conclusion, the microarray together with some preliminary data indicates the roles of FHL2 in immune functions and cancer. We also identified Bcl-6 and Creld2 as novel markers which may be related to FHL2 in the pathogenesis of HCC. They may be tumor suppressor genes associated with HCC.

5.4 Limitations and Future Perspectives

The microarray did not clearly show the significant changed gene sets and the magnitude of change in gene expression in the FHL2-/- mice was not high. This may be because the gene knockout of FHL2 can affect virtually any process in the organism. To identify the mechanism related to FHL2 in cancer, a future study would be investigating the gene expression profiling after the tumor was induced. The tumor animal model can be performed by administration of a chemical N-nitrosodiethyl-amine (DEN) into the mice. First, the study would address the question whether FHL2 knockout mice would be more or less susceptible to tumor development. This serves as an evidence of the role of FHL2 in liver cancer. Second, the microarray will be able to identify the genes responsible for the tumor suppressive or activating effect of FHL2.

Moreover, the protein expression of FHL2 will be measured to confirm the existence of FHL2 protein in the normal liver tissues. The deletion of the protein in knockout mice will also be confirmed by Western blot analysis.

Table 5.1: Results obtained from GO term enrichment analysis using the DAVID Functional Annotation Chart. Below presents a summary of enriched annotation terms which were ordered in terms of their p-value.

Term	Genes	Count	P-Value	Genes
regulation of cell-matrix adhesion		2	1.8E-2	Bcl6, Onecut1
Cor1/Xlr/Xmr conserved region		2	2.5E-2	Xlr3b, Xlr4b/4c
Secreted		6	3.2E-2	Balap-rs1, Creld2, Inhbe, Ins1, Lcn2, Saa2
Maturity onset diabetes of the young		2	3.6E-2	Ins1, Onecut1
cleavage on pair of basic residues		3	3.7E-2	Balap-rs1, Inhbe, Ins1
regulation of cell-substrate adhesion		2	5.2E-2	Bcl6, Onecut1
positive regulation of cell motion		2	5.3E-2	Bcl6, Onecut1
PIRSF000045:cytochrome P450 CYP2D6		2	5.6E-2	Cyp26a1, Cyp2b9
B cell differentiation		2	5.9E-2	Bcl6, Onecut1
extracellular region		6	6.7E-2	Balap-rs1, Creld2, Inhbe, Ins1, Lcn2, Saa2
carbohydrate metabolism		2	9.0E-2	Chst1, Ins1
Retinol metabolism		2	9.1E-2	Cyp26a1, Cyp2b9
B cell activation		2	9.6E-2	Bcl6, Onecut1

Cluster 1

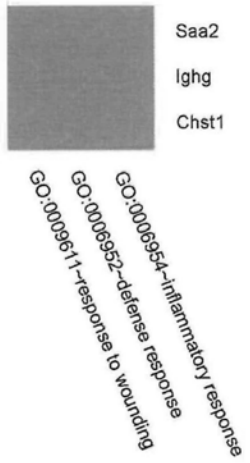

Cluster 2

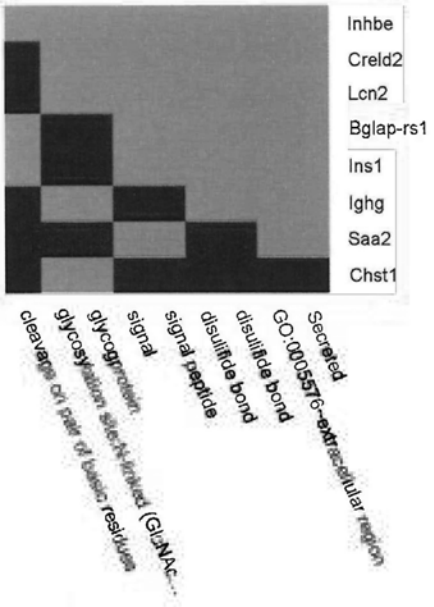

Cluster 3

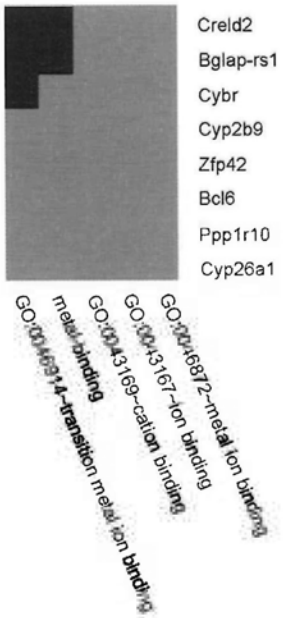

Cluster 4

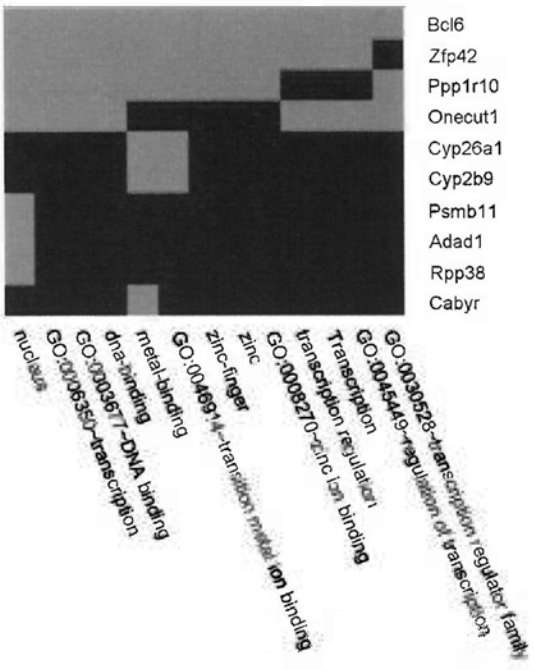

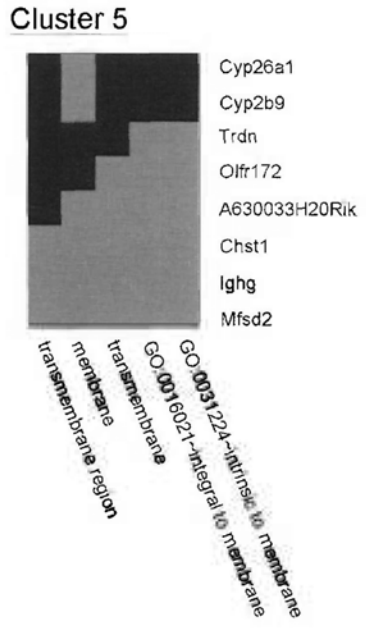

Fig. 5.1: Heat map representation of the results obtained with DAVID functional annotation tool. The heat map provides a detailed graphical view of gene-term relationships. The results show that the genes that had a fold change ratio more than 2 were classified into five functional gene groups. Green represents the positive association between the gene-term; black represents an unknown association.

Table 5.2: The top 10 bio-functions obtained from IPA analysis of the differentially expressed genes.

Top 10 biofunctions in FHL2 knockout mice

	Category	p-value	Molecules
1	Cancer	9.06e-4 - 2.86e-2	Cyp26a1, Lcn2, Bcl6
2	Digestive System Development and Function	9.06e-4 - 9.06e-4	Onecut1
3	Hematological Disease	9.06e-4 - 9.06e-4	Bcl6
4	Hepatic System Development and Function	9.06e-4 - 9.06e-4	Onecut1
5	Immunological Disease	9.06e-4 - 7.22e-3	Bcl6
6	Inflammatory Response	9.06e-4 - 4.26e-2	Lcn2, Bcl6
7	Lipid Metabolism	9.06e-4 - 3.91e-2	Cyp26a1, Saa2
8	Molecular Transport	9.06e-4 - 2.24e-2	Cyp26a1, Saa2
9	Organ Development	9.06e-4 - 3.74e-2	Cyp26a1, Onecut1
10	Organismal Development	9.06e-4 - 1.35e-2	Cyp26a1, Lcn2, Onecut1

Table 5.3: A table showing the top 10 pathways found by 2 fold gene lists as identified by GeneGO Metacore. Light grey shading highlights the statistically significant pathways ($P<0.05$).

	Name	Min(pValue)	Network objects
1	Keratan sulfate metabolism p.1	2.451e-3	3/35
2	Keratan sulfate metabolism p.2	3.348e-3	3/39
3	Neolacto-series GSL Metabolism p.2	1.067e-2	3/59
4	Neolacto-series GSL Metabolism p.2 / Human version	1.067e-2	3/59
5	Neurophysiological process_Olfactory transduction	1.228e-2	1/20
6	Immune response_BCR pathway	3.287e-2	1/54
7	Immune response_IL-17 signaling pathways	3.647e-2	1/60
8	Heme metabolism	5.900e-2	2/98
9	Glycine, serine, cysteine and threonine metabolism	7.302e-2	1/122
10	Glycine, serine, cysteine and threonine metabolism/ Rodent version	7.418e-2	1/124

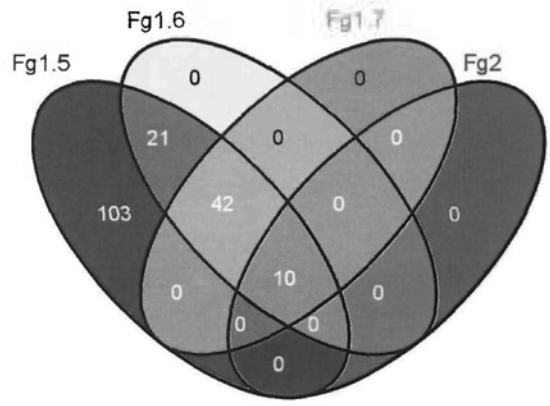

Fig. 5.2: Venn diagram showing the overlapping candidate pathways among the gene lists generated based on fold changes.

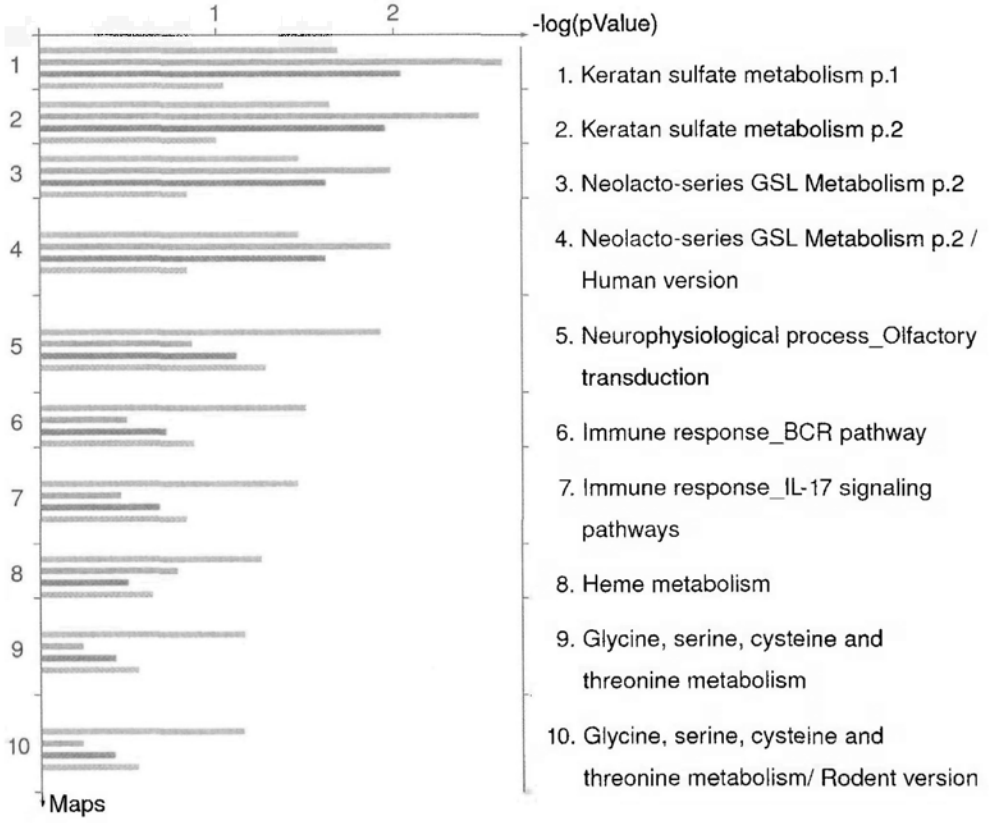

Fig. 5.3: The 10 overlapped pathways among gene lists obtained by GeneGO's Metacore functional ontology enrichment analysis. The results were ranked by p-value. In the figure, orange, blue, red and green color is used to represent the 2 fold, 1.5 fold, 1.6 fold and 1.7 fold conditions respectively.

A

ID	Molecules in Network	Score	Focus Molecules	Top Functions
1	↑ABCC2, ↑ABCC3, ↑**ALAS1**, ↑BCL3, ↓**BCL6**, ↑BTNL2, ↑**CABYR**, ↑CCR8, ↑CD80*, ↑CD200, ↑CXCL9, ↑HMGCR, ↑HTRA2, ↓ICAM1, ↑IL4, ↑IL7, ↑IL25, ↓IL27, ↑IL33, ↓IL1RL1, ↓IRF1*, ↑JAK1, KLRB1C (includes EG:17059), ↑**LCN2**, ↑MAPK14, ↓MMP9, ↓MOG, ↑NR1I2, ↓NR5A2, ↑**ONECUT1***, ↓PTHLH, ↑**SAA2**, ↑SLC29A1, TCRB-V8.3, ↓TNF	11	6	Cellular Development, Hematological System Development and Function, Hematopoiesis
2	↓**ADAD1***, ↓YBX2	2	1	Cellular Development, Reproductive System Development and Function, Protein Synthesis
3	↑NANOG, ↑**ZFP42**	2	1	Cellular Development, Cellular Growth and Proliferation, Embryonic Development

B

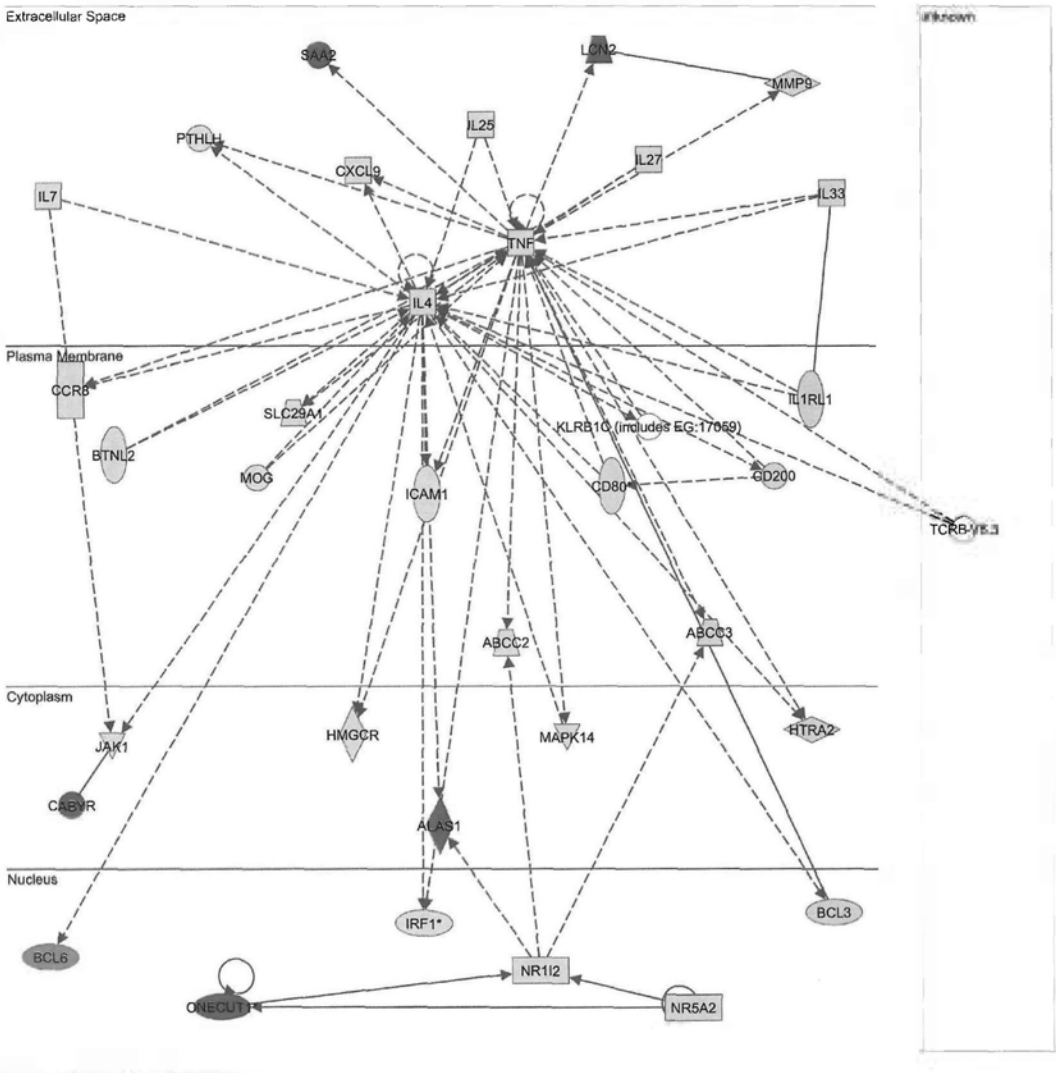

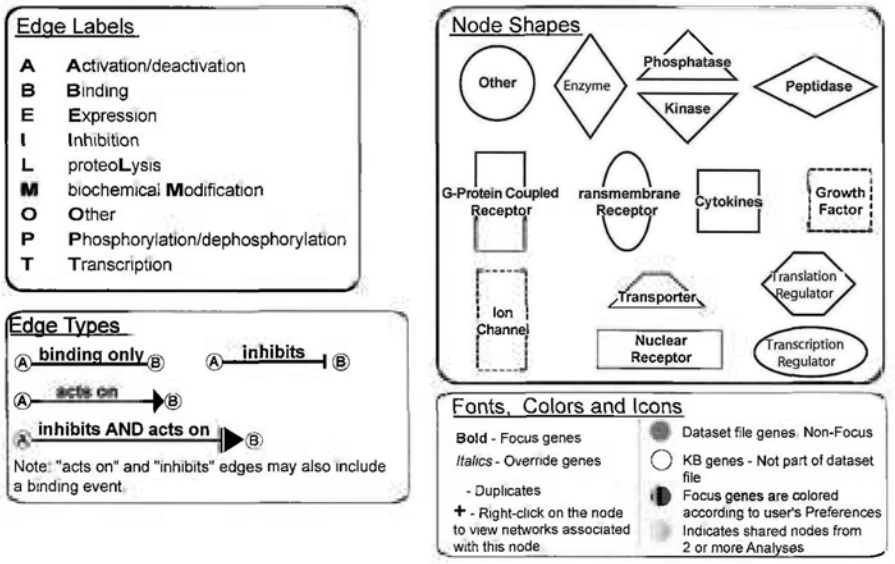

Fig. 5.4: Figure showing the gene interaction network identified using Ingenuity Pathway Analysis (IPA). The software identified only one significant network (panel A). The colored boxed are genes confirmed to be differentially expressed in the microarray dataset. Red indicates upregulated genes, and green indicates downregulated genes (panel B). The legends for IPA generated networks are indicated at the bottom of the figure.

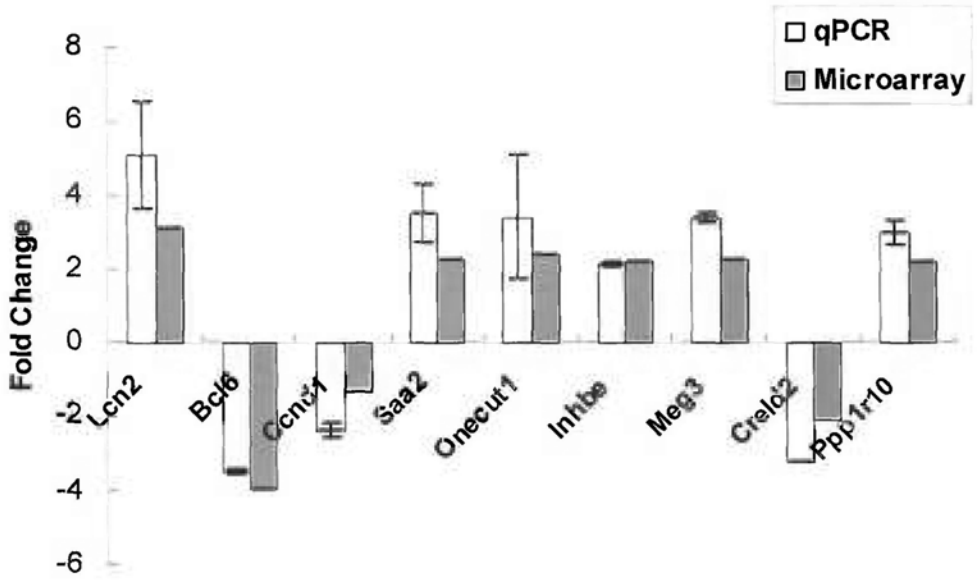

Fig. 5.5: Real-time PCR validation of microarray expression data. The experiments were performed with the pooled samples of 3 mice that had been subjected to microarray analysis. Nine genes showed a consistent pattern of differential gene expression in real-time PCR. Upward and downward pointing bars represent higher or lower expression levels in FHL2 knockout mice compared to those of WT mice. Each bar represents the average value ± SEM of three animals from 2 independent real-time PCR experiments (n=6).

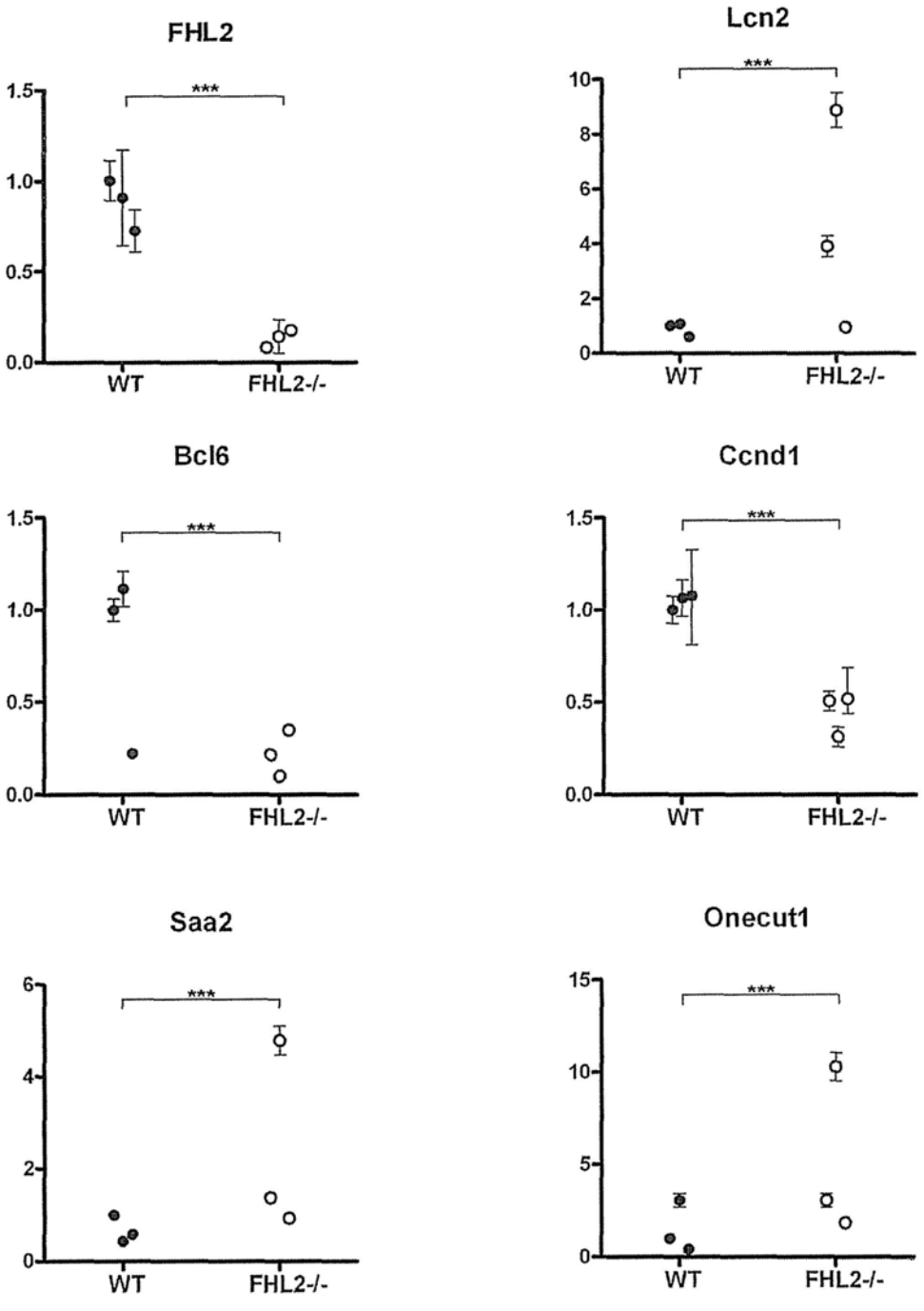
FHL2
***
1.5
1.0
0.5
0.0
WT
FHL2-/-
Lcn2
***
10
8
6
4
2
0
WT
FHL2-/-
Bcl6
***
1.5
1.0
0.5
0.0
WT
FHL2-/-
Ccnd1
***
1.5
1.0
0.5
0.0
WT
FHL2-/-
Saa2
***
6
4
2
0
WT
FHL2-/-
Onecut1
***
15
10
5
0
WT
FHL2-/-

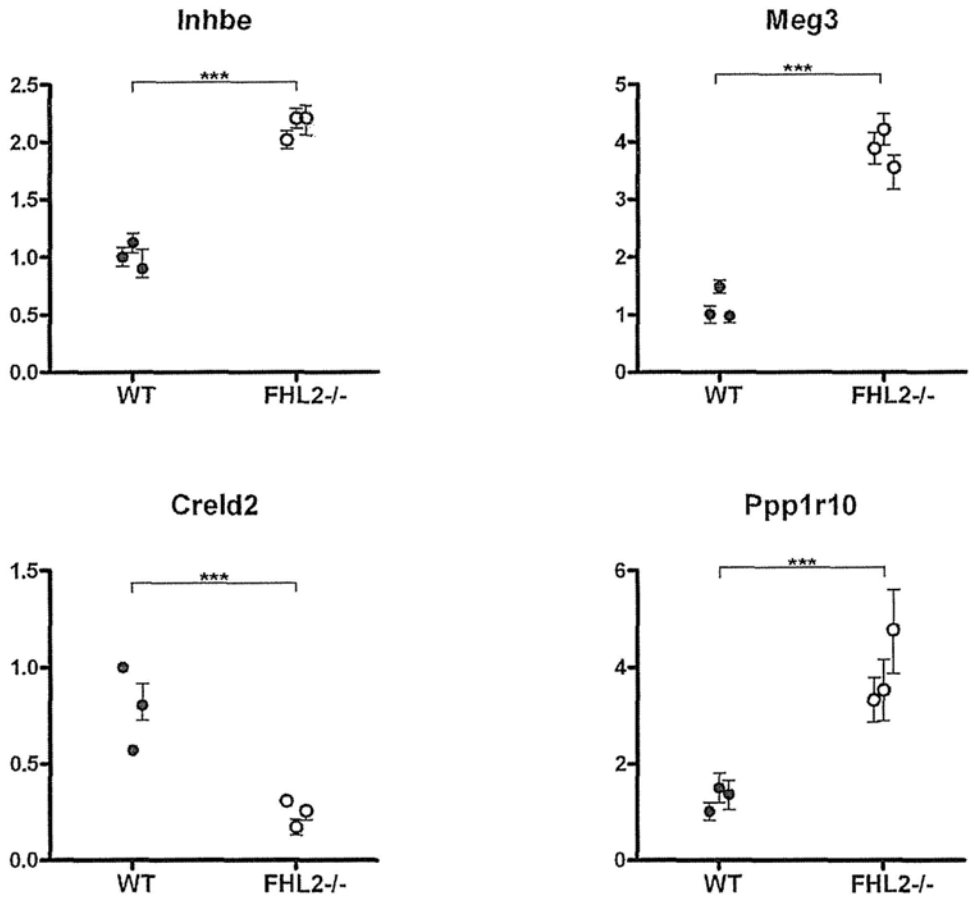

Fig. 5.6: Real-time PCR analysis for comparing gene expression between wild-type and knockout mice. The transcript levels for the indicated genes of individual RNA samples from both wild-type and knockout mice were determined. Each point represents the mean value of individual mouse ± S.D. of two independent experiments performed in triplicate wells. Triple asterisks (***) indicate $P<0.001$ versus control group by two-tailed Mann-Whitney test.

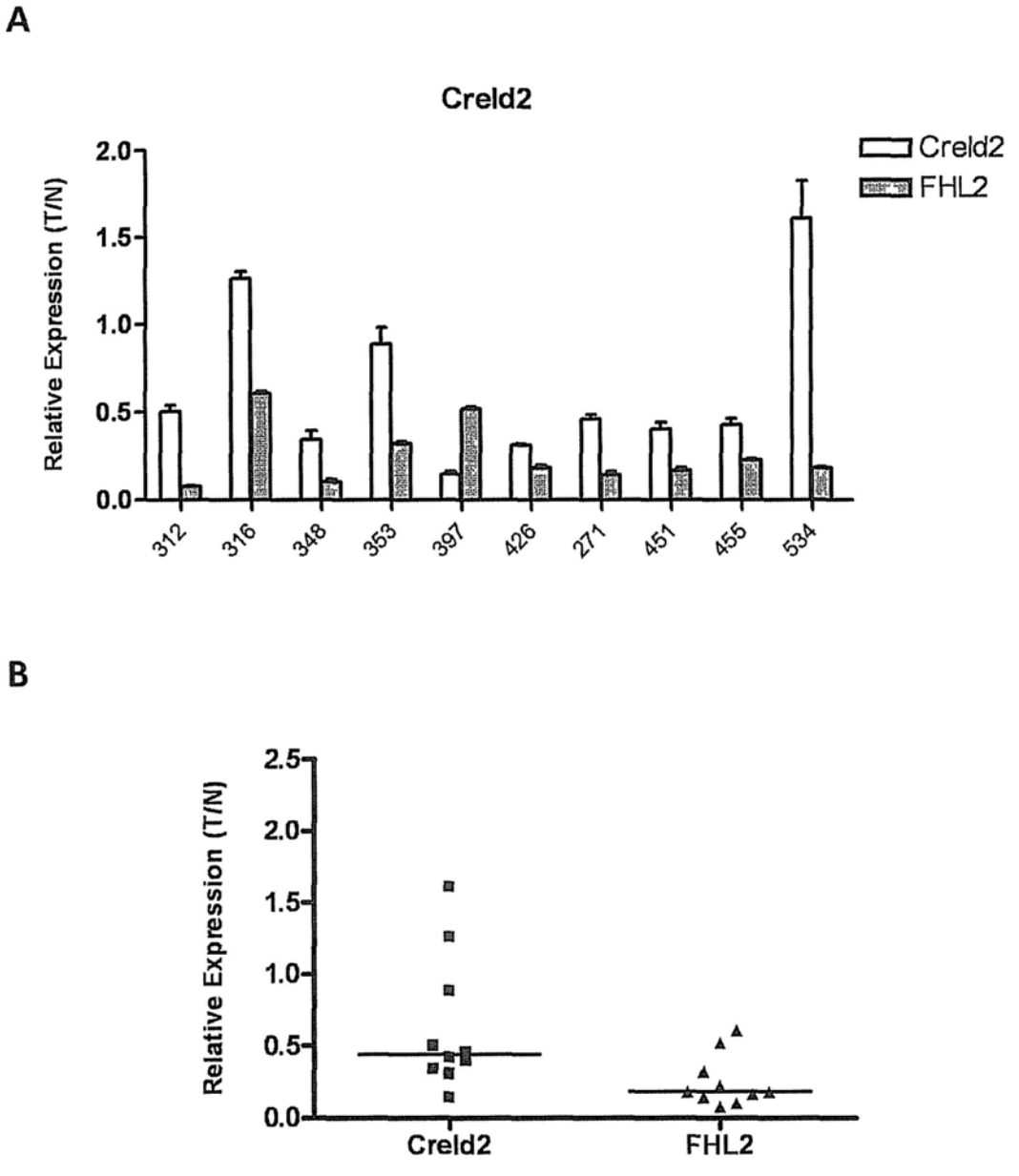

Fig. 5.7: (A) Real-time PCR analysis of Creld2 mRNA expression in samples of human HCC and adjacent normal tissues. Each bar represents the mean ± S.D. of triplicate determinations. **(B)** Dot-plot of the expressions of Creld2 and FHL2 in HCC cancer relative to their non-cancerous counterparts. Creld2 showed significant downregulation in tumor tissues ($P<0.05$).

A

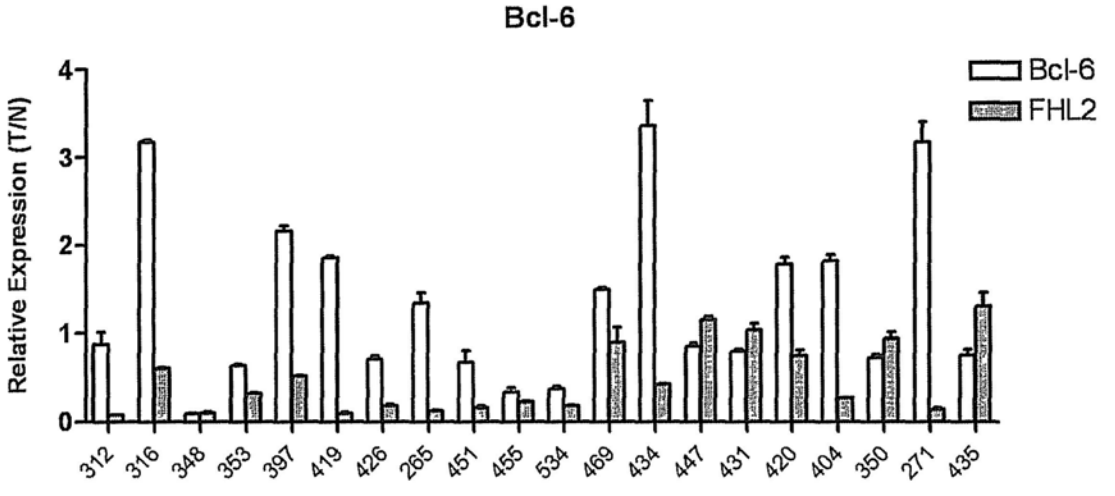
Bcl-6
Bcl-6
FHL2
Relative Expression (T/N)
4
3
2
1
0
312
316
348
353
397
419
426
265
451
455
534
469
434
447
431
420
404
350
271
435

B

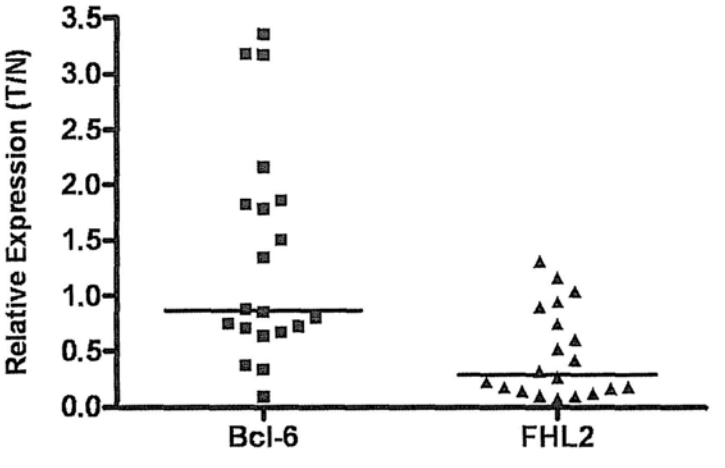
Relative Expression (T/N)
3.5
3.0
2.5
2.0
1.5
1.0
0.5
0.0
Bcl-6
FHL2

C

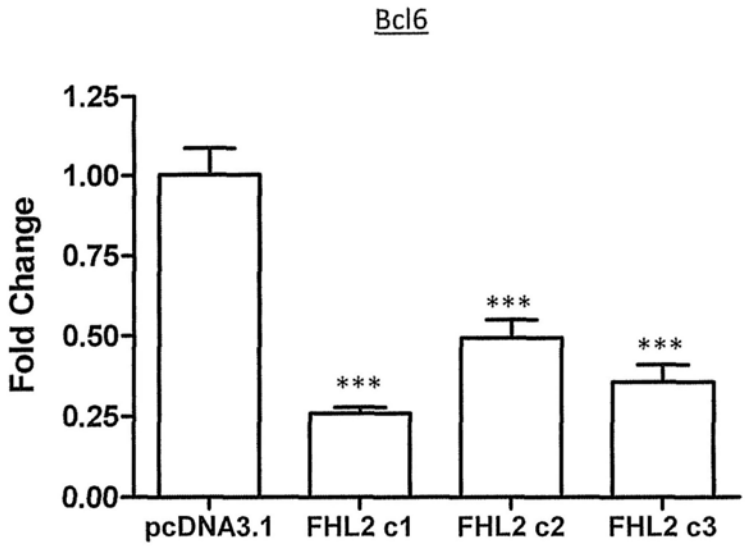

Fig. 5.8: (A) Real-time PCR analysis of Bcl-6 mRNA expression in samples of human HCC and adjacent normal tissues. Each bar represents the mean ± S.D. of triplicate determinations. **(B)** Dot-plot of the expressions of Bcl-6 and FHL2 in HCC cancer relative to their non-cancerous counterparts. There was not a significant downregulation of Bcl-6 in the tumor. **(C)** The Bcl-6 gene expression was influenced by FHL2 overexpression in Hep3B HCC cell line. Data represent mean ± S.D. of three independent experiments each performed in triplicate. ***P<0.001 compared to empty vector control.

Chapter 6

CHARACTERIZATION OF THE ROLE OF FHL1 IN HCC

6.1 Introduction

The highly related family member FHL1 has also been discovered to play a role in cancer development. In the current studies, we characterized another potential cancer target gene FHL1 in HCC. Our study investigated the potential role of FHL1 gene expression in the development of HCC and studied the epigenetic alterations causing the aberrant expression in tumor cells.

6.2 Results

6.2.1 FHL1 is downregulated in liver cancer cell lines and HCC tissues

To determine the FHL1 expression in liver cancer cell lines, real-time PCR was performed using β-actin as an endogenous control. Compared with normal liver cell WRL68, the expression of FHL1 mRNA was significantly downregulated by more than 150 folds in liver cancer cell lines Huh7, Hep3B and HepG2 ($P<0.001$) (Fig. 6.1).

We also measured the expressions of FHL1 and FHL3 gene in the HCC patients by real-time PCR. The results showed that FHL1 transcript was downregulated by more than 2-fold in 29 of 47 tumors (62%) compared to adjacent normal tissues (Fig. 6.2A). Only 2 out of 47 tumors showed >2-fold increase in expression. Median FHL1 expression level in tumors was 36% of the corresponding normal samples (P<0.001) (Fig. 6.2C). On the other hand, FHL3 showed more than 2-fold downregulation in 7 out of 20 tumors (35%) and fold change <1 in 13 out of 20 tumors (Fig. 6.2B). However, the expression was not significantly reduced in tumor tissues (Fig. 6.2C). The median expression of FHL3 in tumors was 61% in comparison with 100% of normal tissues, but not statistically significant (P=0.254).

6.2.2 Relationship between FHL1 expression and clinicopathologic features

The relationship between FHL1 expression levels with different clinical and pathologic parameters was analyzed. The FHL1 expression values of HCC patients were compared with the pathologic parameters. No significant differences in gene expression were found for multiple tumors, tumor size, clinical stages, degree of differentiation and vascular invasion (P>0.05) (Table 6.1A). The only differences were that FHL1 expression levels were lower in moderately (intermediate-grade) and poorly-differentiated HCCs (high-grade tumors) compared with well-differentiated (or low grade) tumors, as well as in the HCC patients with multiple tumors (>=2 tumors) than in single HCC, although these results were not statistically significant (Figs. 6.3A and B). We also conducted survival analysis using the Cox proportional

hazard model but the results did not reveal the relationship between FHL1 expressions and the survival times of patients (Table 6.1B).

6.2.3 Effect of TSA treatment on FHL1 and FHL3 expression

The effect of TSA treatment on gene expression was investigated. There was a marked increase of FHL1 mRNA expression in Huh7, Hep3B, WRL68 and HepG2 cells (3.8- to 170-fold induction) (Fig. 6.4). On the other hand, the expression of FHL3 was significantly reduced in Hep3B and WRL68 cells, but significantly increased in Huh7 cells. The results indicated that the reduced expression of FHL1 may be resulted from histone deacetylation.

6.2.4 Effect of 5-aza-dC on FHL1 and FHL3 expression

To investigate whether DNA methylation is responsible for decreased expression of these genes, the gene expression was measured upon 5-aza-dC treatment. There was a marked increase of FHL1 mRNA expression in Hep3B, MiHA and HepG2 cells (3.3- to 32-fold induction) and a slight increase in L02 cells (1.5-fold) (Fig. 6.5). There was also a significant increase of FHL3 expression in Hep3B, MiHA and HepG2 cells (1.9- to 2.2-fold), but no difference in expression in Huh7 and L02 cells. 5-aza-dC restored both the expression of FHL1 and FHL3.

6.2.5 Analysis of FHL1 promoter methylation

The FHL1 promoter methylation status was determined by bisulfite sequencing analysis. The Methyl Express software v1.0 predicted a CpG island from –1066 to

+934 bp of the FHL1 gene (+1 defined as the TSS). The promoter region of FHL1 between –170 and +421 bp containing 74 CpG sites was analyzed in our study (Fig. 6.6A). The results show that the CpG sites in this region were rarely methylated in all three liver cancer cell lines (Fig. 6.6B), indicating the lack of methylation of FHL1 promoter.

6.3 Discussion

Recent studies suggest that FHL1 plays a role in cancer. Our study demonstrates that downregulation of FHL1 gene expression frequently occurs in HCC. FHL1 may also act like FHL2 as tumor suppressor in HCC.

6.3.1 Study on the expression of FHL1 and its clinical correlation in HCC

Our results demonstrate a significant reduction of FHL1 expression in HCC cell lines and patients, which was consistent with previous study conducted on FHL proteins (Ding *et al.*, 2009b). FHL3 was also shown to be downregulated in HCC, but we have not got significant results perhaps due to the small sample size. There are limited studies about the role of FHL3 in cancer. On the other hand, FHL1 has been shown to be downregulated in many malignancies, including brain, breast, kidney, liver, lung, prostate and skin cancers (Shen *et al.*, 2006). It has been shown that the suppression of FHL1 by Src kinase was required to promote anchorage-independent cell growth and migration for the process of cell transformation (Shen *et al.*, 2006). FHL1 has also been reported to inhibit breast cancer cell growth, and was the result from repression of estrogen-responsive gene transcription (Ding *et al.*, 2009a). Although it has been suggested FHL1 may act as tumor suppressor in HCC, the specific function of FHL1 has not been determined. The precise role of FHL1 and also FHL3 in HCC tumor suppression will need to be clarified.

In this study, we did not find any relationship between FHL1 gene expression and the tumor behavior. The finding was the same as in the previous chapter for FHL2. In other words, the gene expression did not translate into clinical significance in liver cancer. The result is a bit disappointing but understandable. Although not statistically significant in our study, FHL1 expression may be correlated with tumor progression. Low FHL1 expression may be associated with poor differentiation of the tumor. The lack of significant result in some variables (e.g. tumor differentiation and multiple tumors) may be due to the small sample size which may not have enough power. For example, the data set contains limited number of samples from poor and well differentiated tumors (mostly are moderately differentiated). Besides, not all tumor features gave consistent result in gene expression, e.g. tumor staging did not give apparent difference in the gene expression levels. In fact, tumor staging can be affected by factors other than alteration of the genetic materials like the time of diagnosis (the time when the tumor is detected); the gene expression level might only be manifested in the tumor differentiation. For survival analysis, there are even more confounding factors, for example post-operative mortality which had been excluded from the analysis. Besides adequate resection margin is also important. This should also be considered in our case selection.

6.3.2 Epigenetic mechanisms involved in the regulation of FHL1

We then investigated the role of epigenetic mechanisms in the regulation of FHL1 gene expression. It has been reported that promoter hypermethylation was the mechanism of downregulation of FHL1 mRNA in human bladder cancer

(Matsumoto *et al.*, 2010). Increased methylation of CpG islands was often associated with tumor suppressor gene silencing in cancers. In our study, methylation was not observed within the FHL1 promoter region, although the gene expression was upregulated in response to 5-aza-dC. Promoter hypermethylation may not be responsible for decrease of FHL1 expression in HCC cells. The increase in gene expression may be due to an indirect effect of 5-aza-dC. On the other hand, the gene silencing of FHL1 may be regulated by histone deacetylation. We found that only FHL1 gene was consistently upregulated following histone deacetylases inhibition in the four studied hepatoma cells. The mRNA expression of FHL1, but not FHL2 and FHL3, was markedly induced by TSA. Thus, histone modifications may play a role in regulating FHL1 gene expression in liver carcinogenesis. In the present study, the mechanism of TSA-induced gene expression was not examined. Future studies will be conducted to determine whether TSA would involve regulation of transcription at the promoter level or affect the mRNA stability.

In conclusion, we showed the downregulation of FHL1 expression in HCC. Histone modifications may play a role in repressing the FHL1 gene expression in HCC cells. FHL1 may act as a candidate tumor suppressor gene in HCC. Further studies will be necessary to elucidate the functional role of FHL1 in HCC pathogenesis.

Table 6.1: Correlation between FHL1 expression and clinical features

A: Correlation of FHL1 with the various parameters

Variables	Test Statistics		Significance
Multiple Tumour	Mann-Whitney U Asymp. Sig. (2-tailed)	0.7070	NS
Vascular Invasion	Mann-Whitney U Asymp. Sig. (2-tailed)	0.7047	NS
Size >=5cm	Mann-Whitney U Asymp. Sig. (2-tailed)	0.2794	NS
AJCC Staging	Kruskal Wallis ANOVA Asymp. Sig.	0.2712	NS
Tumour Differentiation	Kruskal Wallis ANOVA Asymp. Sig.	0.2241	NS

B: Survival Analysis using Cox-proportional Hazard Model

Variable	B	SE	Wald	df	**Sig.**	Exp(B)	95% CI Exp(B)
FHL1	-0.0906	0.4406	0.0423	1	0.8371	0.9134	0.3851-2.1663

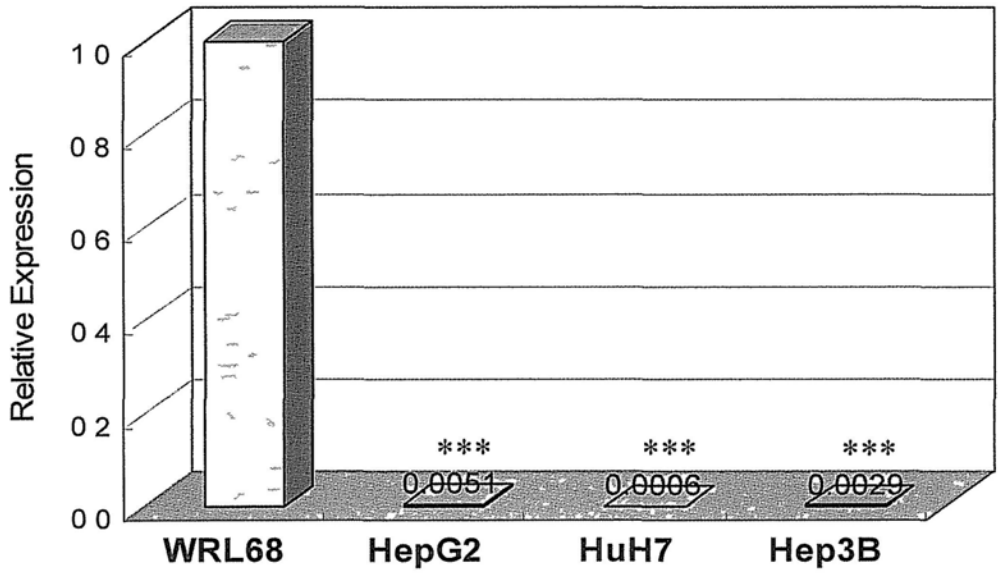

Fig. 6.1: Expression of FHL1 mRNA in HCC cell lines. Results represent the mean of three independent experiments. Triple asterisks indicate $P<0.001$ vs. WRL68. Error bar was too small to be shown.

A

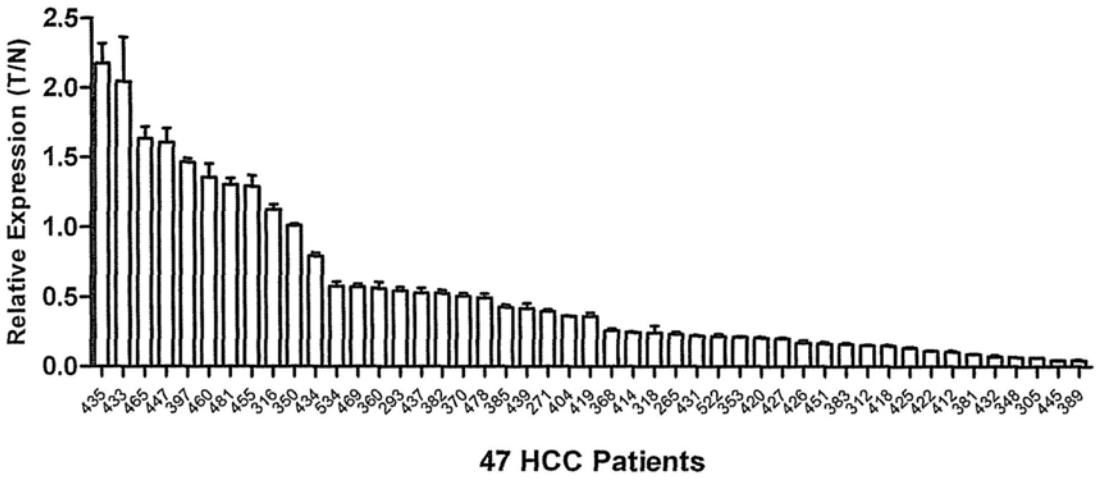
Relative Expression (T/N)
2.5
2.0
1.5
1.0
0.5
0.0
435 433 465 447 397 460 481 455 316 350 434 534 469 360 293 437 382 370 478 385 439 271 404 419 368 414 318 265 431 522 353 420 427 426 451 383 312 418 425 422 412 381 432 348 305 445 389
47 HCC Patients

B

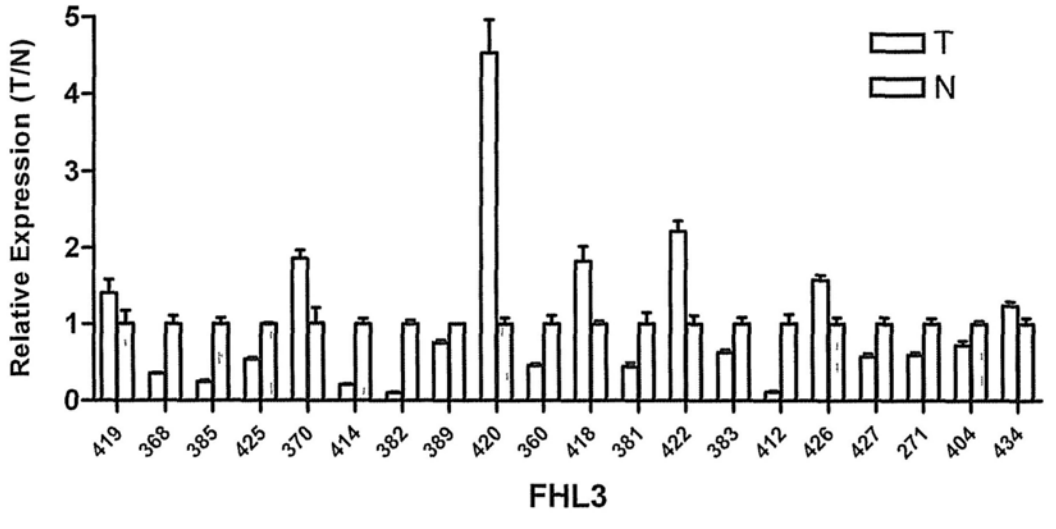
Relative Expression (T/N)
5
4
3
2
1
0
T
N
419 368 385 425 370 414 382 389 420 360 418 381 422 383 412 426 427 271 404 434
FHL3

C

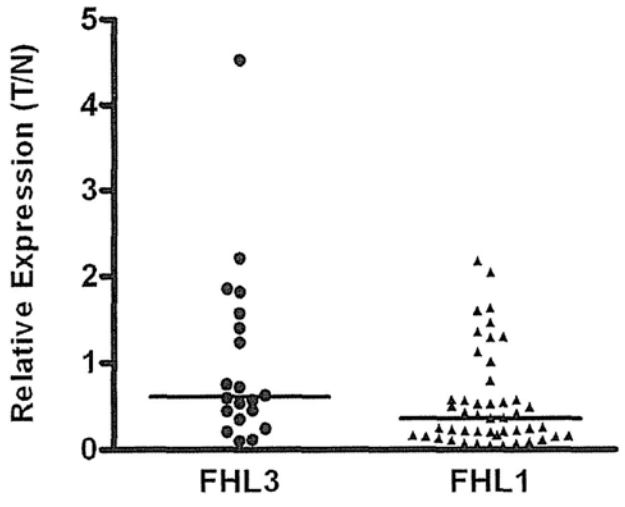

Fig. 6.2: Expression of FHL1 and FHL3 in HCC tumor samples analyzed by quantitative real-time PCR. Each tumor sample was compared with its normal counterpart for **(A)** FHL1 and **(B)** FHL3 mRNA level. Results represent mean ±S.D. of triplicate reactions. **(C)** The overall expressions of FHL1 and FHL3 in tumors were presented in the scatter plot (horizontal line represents the median values). There was significant difference in FHL1 expression compared to nontumor tissue ($P<0.001$).

A

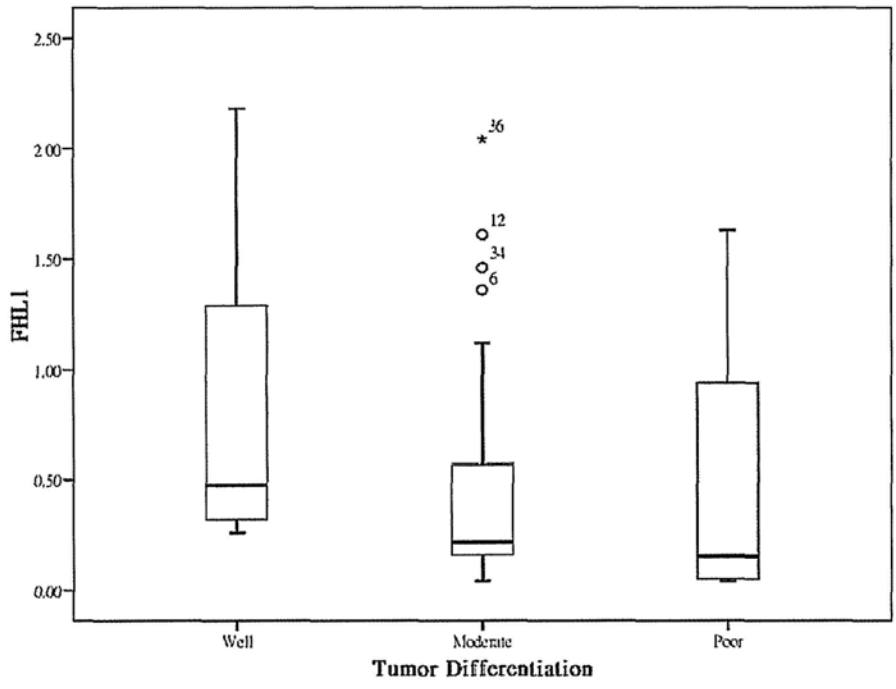
2.50
2.00
1.50
1.00
0.50
0.00
FHL1
36
12
34
6
Well
Moderate
Poor
Tumor Differentiation

B

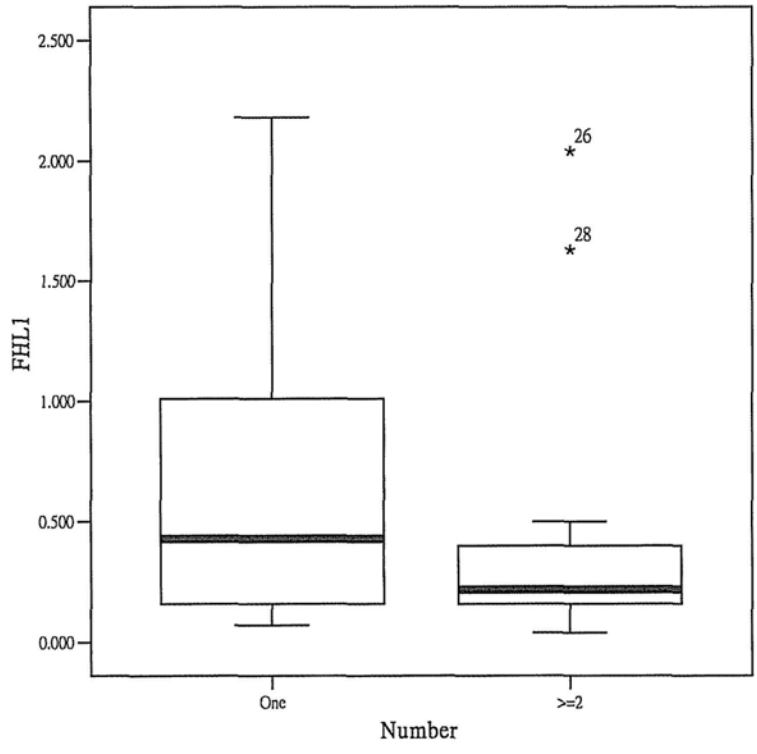
2.500
2.000
1.500
1.000
0.500
0.000
FHL1
26
28
One
>=2
Number

Fig. 6.3: Box plot results of expression of FHL1 in tumor tissues by **(A)** tumor differentiation and **(B)** number of tumors. No statistically significant differences were observed between the groups.

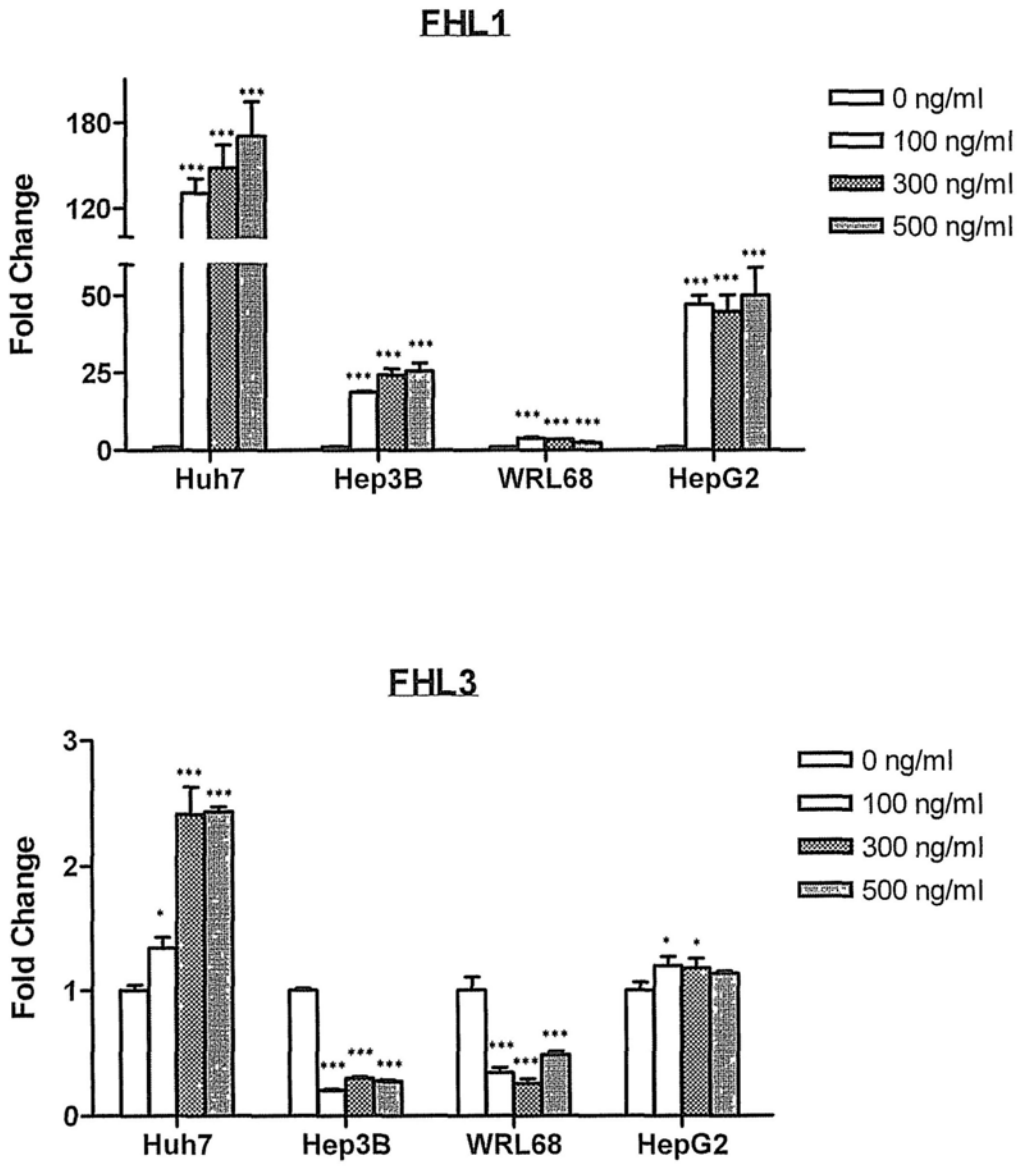

Fig. 6.4: Expression of FHL1 and FHL3 transcripts after treatment with TSA for 24 h. Each bar represents the mean ± S.D. for triplicate wells. Single asterisk "*" indicates p-value < 0.05, double asterisks "**" indicates p-value < 0.01, while triple asterisks "***" indicate p-value < 0.001 with respect to control.

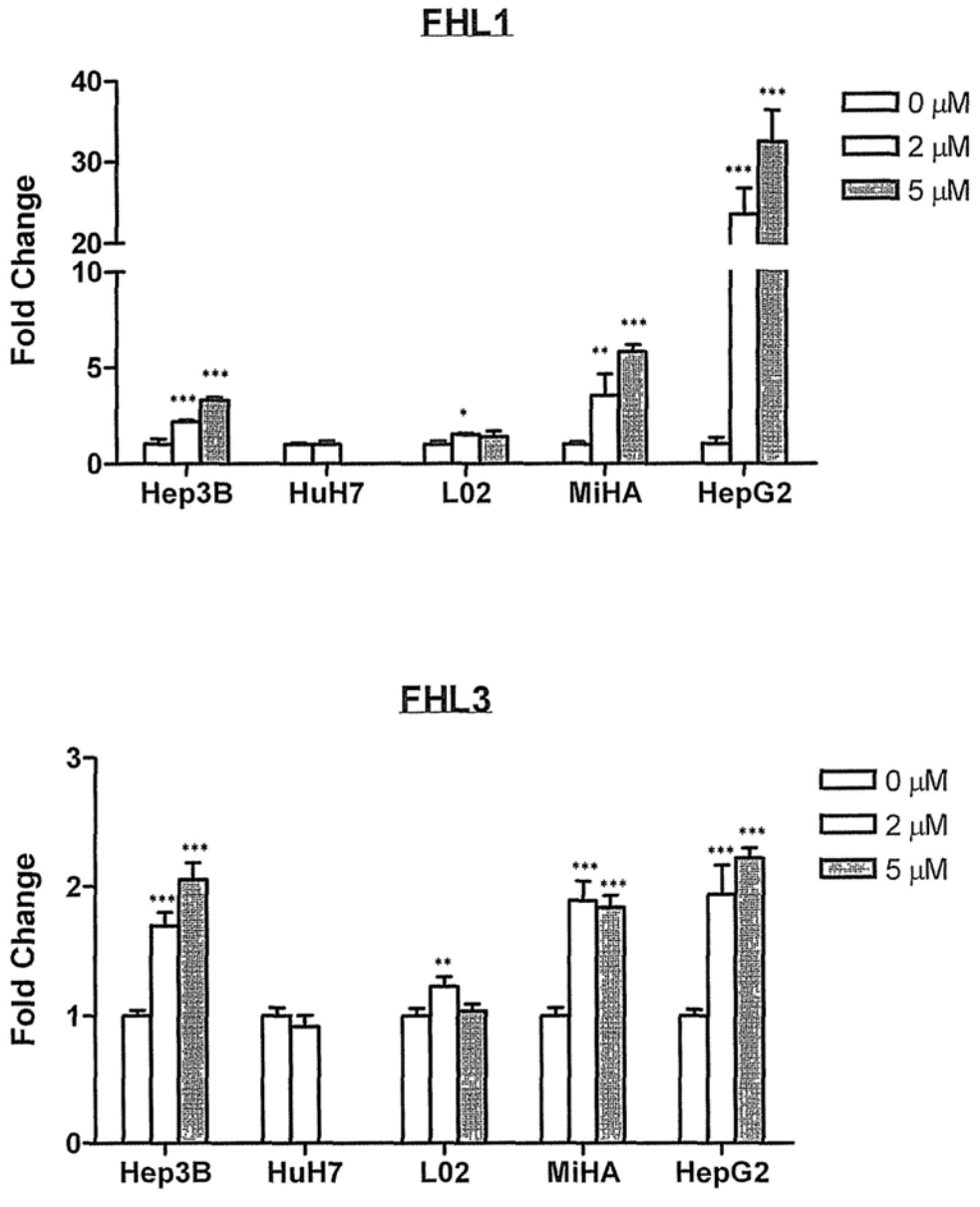

Fig. 6.5: Expression of FHL1 and FHL3 transcripts after 4 days of demethylation treatment with 5-aza-dC. Each bar represents the mean ± S.D. for triplicate wells. Single asterisk "*" indicates p-value < 0.05, double asterisks "**" indicates p-value < 0.01, while triple asterisks "***" indicate p-value < 0.001 with respect to control.

A

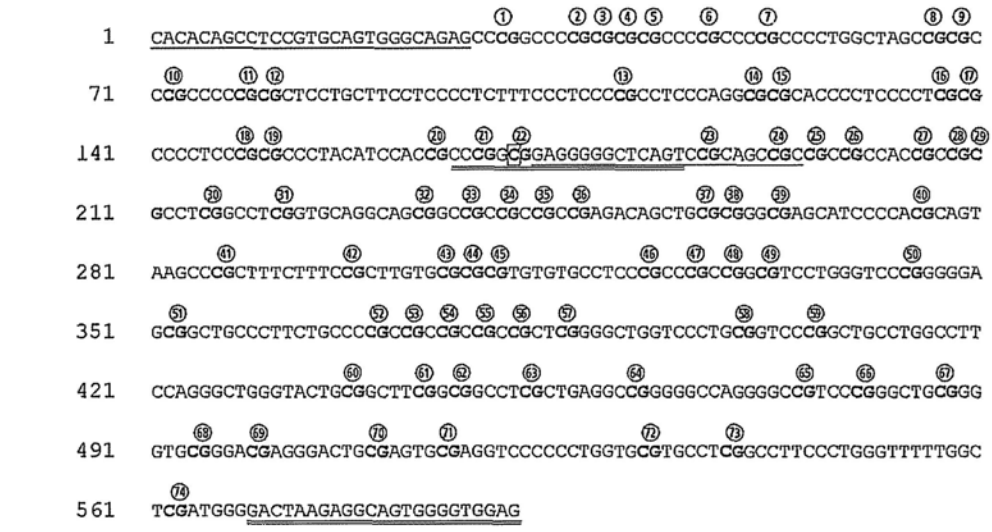
1 CACACAGCCTCCGTGCAGTGGGCAGAGCCCGGCCCCGCGCGCGCCCCGCCCCGCCCCTGGCTAGCCGCGC
71 CCGCCCCCGCGCTCCTGCTTCCTCCCCTCTTTCCCTCCCCGCCTCCCAGGCGCGCACCCCTCCCCTCGCG
141 CCCCTCCCGCGCCCTACATCCACCGCCCGGCCGGAGGGGGCTCAGTCCGCAGCCGCCGCCGCCACCGCCGC
211 GCCTCGGCCTCGGTGCAGGCAGCGGCCGCCGCCGCCGAGACAGCTGCGCGGGCGAGCATCCCCACGCAGT
281 AAGCCCGCTTTCTTTCCGCTTGTGCGCGCGTGTGTGCCTCCCGCCCGCCGGCGTCCTGGGTCCCGGGGGA
351 GCGGCTGCCCTTCTGCCCCGCCGCCGCCGCCGCTCGGGGCTGGTCCCTGCGGTCCCGGCTGCCTGGCCTT
421 CCAGGGCTGGGTACTGCGGCTTCGGCGGCCTCGCTGAGGCCGGGGGCCAGGGGCCGTCCCGGGCTGCGGG
491 GTGCGGGACGAGGGACTGCGAGTGCGAGGTCCCCCCTGGTGCGTGCCTCGGCCTTCCCTGGGTTTTTGGC
561 TCGATGGGGACTAAGAGGCAGTGGGGTGGAG

B

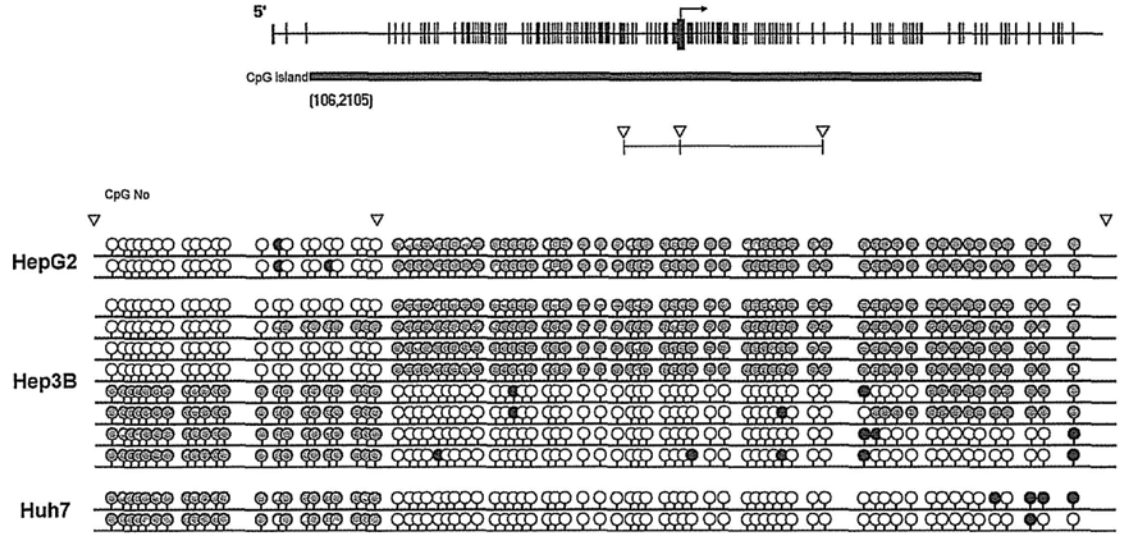
5'
CpG Island
(106,2105)
CpG No
HepG2
Hep3B
Huh7

Fig. 6.6: Bisulfite sequencing results of the FHL1 CpG island. **(A)** The two pairs of primers for bisulfite sequencing were underlined. Position of TSS was indicated by the arrow (shown in B) and the boxed nucleotide. **(B)** Bisulfite-converted DNA from liver cancer cell lines were amplified at the selected region of the FHL1 CpG island and the products cloned and sequenced. The methylation status of each CpG site for each clone was indicated in the lollipop diagram, with filled circles indicating methylated sites and open circles indicating the absence of methylation (gray circles: undetermined).

Chapter 7

CONCLUSION

7.1 Expression and functional studies of FHL2

Background: Hepatocellular carcinoma (HCC) is the fifth most prevalent cancers worldwide and the second most lethal cancer in China. The understanding of gene functions in cancer is essential in the development of molecular targeting therapies of cancer. Recent studies have suggested that the FHL2 plays an important role in tumorigenesis. FHL2 displays tumor promoting or tumor suppressing activities depending on the types of tumor cells. The roles played by FHL2 are therefore particularly intriguing. So far, the precise function of FHL2 in liver tumorigenesis remains unclear. ***Results:*** We show herein that FHL2 gene expression is downregulated in the majority of HCC patient samples and in addition three HCC cell lines. Using stable overexpression clones of FHL2 in human HCC Hep3B cells, we show that FHL2 inhibits the HCC cell proliferation through cell cycle regulation by decreasing cyclin D1 expression while increasing the expressions of cyclin-dependent kinase inhibitors p21 and p27. FHL2 overexpression also inhibits migration and invasion of HCC cells through EMT-mediated pathway, as shown by reduction of mesenchymal marker vimentin and induction of epithelial marker

E-cadherin. The effects of FHL2 overexpression on apoptosis are also examined. There is an increase of Bcl-2 and Bcl-xL protein levels in response to FHL2 overexpression and this correlates to a decrease of cell death and apoptosis induction towards doxorubicin. ***Conclusions:*** Taken together, both the antiapoptotic and antiproliferative functions of FHL2 are shown in this study, which suggests the intriguing functions for this protein in cancers.

7.2 Study on transcription regulation of FHL2 gene

In this study, we characterized the different alternative spliced transcripts of *FHL2* by *in silico* analysis and RT-PCR analysis. A novel transcript variant was identified and shown to be expressed in many cell lines and tissues. The two different promoters utilized by *FHL2* indicated there may be tissue-specific regulation of *FHL2*. The present study revealed a reduced expression of *FHL2* mRNA levels in a majority of the human HCC tissues examined. The potential promoter region as well as its methylation status was investigated. *FHL2* itself was not regulated by methylation. To explore the regulation of promoter, we generated a series of deletions mutants of the 5' flanking region of *FHL2* gene and showed that the fragment from -138 to +292 in the promoter have positive regulatory effect. The bioinformatic analysis identified putative binding sites of five transcription factors. Of these TFs, Pax-5 and ZF5 expression was downregulated and correlated with the FHL2 expression in HCC tumor samples, indicating a possible role for these transcription factors in the regulation of *FHL2* expression.

7.3 Microarray analysis of FHL2 knockout mice

In the present studies, we performed microarray analysis of the FHL2 knockout mice to identify new target genes of FHL2. Our data illustrate that FHL2 affects various genes related to cell adhesion and motility, immune function, and transcription factors. Of these genes, Lcn2, Bcl-6 and Creld2 belong to the category of cancer-related genes. We also performed a network analysis of differentially expressed genes using Ingenuity Pathway Analysis. The IPA analysis identified a significant network and IL-4 and TNF-α as the most central genes of the network, which suggests a role for inflammation. We next performed analysis of gene expression in clinical samples to identify genes relevant to human cancer and we identified the altered expression of Bcl-6 and Creld2 genes in HCC.

7.4 FHL1 Studies

We also demonstrated the downregulation of FHL1 expression in HCC. Histone deacetylation may be involved in the repression of the FHL1 gene in HCC. FHL1 may act as a candidate tumor suppressor gene in HCC.

FUTURE WORK

The research presented in this thesis provides the basis for further investigation on various aspects. The following is a list of possible directions of further studies.

(a) Study of the silencing of FHL1 and FHL2 to further establish the tumor suppressive functions of these genes in HCC.
   - Study of the effects of FHL1 and FHL2 gene knockdown in cell proliferation in the normal liver cell lines (e.g. LO-2).
   - Use of FHL1 and FHL2 knockout mice model to study the effects of a gene knockout on tumor susceptibility.

(b) Identification and validation of transcription factors that bind to the FHL2 promoter and regulate the promoter activity in liver cancer cells.

(c) Study of the mechanism of transcriptional activation of the FHL1 gene by the HDAC inhibitor TSA.

(d) Identification and validation of novel tumor suppressor genes with altered expression in HCC.

(e) Study of the interaction partners of FHL2 in the cancer cells to identify the mechanism by which FHL2 inhibits cancer growth.

REFERENCES

Acloque H, Adams MS, Fishwick K, Bronner-Fraser M, Nieto MA. (2009). Epithelial-mesenchymal transitions: the importance of changing cell state in development and disease. *J Clin Invest* **119**:1438-1449.

Amann T, Egle Y, Bosserhoff AK, Hellerbrand C. (2010) FHL2 suppresses growth and differentiation of the colon cancer cell line HT-29. *Oncol Rep* **23**:1669-1674.

Aravalli RN, Steer CJ, Cressman ENK. (2008) Molecular mechanisms of hepatocellular carcinoma. *Hepatology* **48**: 2047-2063.

Bach I. (2000). The LIM domain: regulation by association. *Mech Dev* **91**:5-17.

Bai S, Kitaura H, Zhao H, Chen J, Müller JM, Schüle R, Darnay B, Novack DV, Ross FP, Teitelbaum SL. (2005). FHL2 inhibits the activated osteoclast in a TRAF6-dependent manner. *J Clin Invest* **115**:2742-2751.

Bhattacharjee A, Richards WG, Staunton J, Li C, Monti S, Vasa P, Ladd C, Beheshti J, Bueno R, Gillette M, Loda M, Weber G *et al.* (2001). Classification of human lung carcinomas by mRNA expression profiling reveals distinct adenocarcinoma subclasses. *Proc Natl Acad Sci U S A* **98**:13790-13795.

Blum HE. (2005). Hepatocellular carcinoma: therapy and prevention. *World J Gastroenterol* **11**:7391-7400.

Carr IM, Valleley EM, Cordery SF, Markham AF, Bonthron DT. (2007). Sequence analysis and editing for bisulphite genomic sequencing projects. *Nucleic Acids Res* **35**: e79.

Cartharius K, Frech K, Grote K, Klocke B, Haltmeier M, Klingenhoff A, Frisch M, Bayerlein M, Werner T. (2005). MatInspector and beyond: promoter analysis based on transcription factor binding sites. *Bioinformatics* **21:**2933-2942.

Catlett-Falcone R, Landowski TH, Oshiro MM, Turkson J, Levitzki A, Savino R, Ciliberto G, Moscinski L, Fernández-Luna JL, Nuñez G, Dalton WS, Jove R. (1999). Constitutive activation of Stat3 signaling confers resistance to apoptosis in human U266 myeloma cells. *Immunity* **10**:105-115.

Chan KK, Tsui SK, Lee SM, Luk SC, Liew CC, Fung KP, Waye MM, Lee CY. (1998). Molecular cloning and characterization of FHL2, a novel LIM domain protein preferentially expressed in human heart. *Gene* **210**:345-350.

Chen D, Xu W, Bales E, Colmenares C, Conacci-Sorrell M, Ishii S, Stavnezer E, Campisi J, Fisher DE, Ben-Ze'ev A, Medrano EE. (2003). SKI activates Wnt/beta-catenin signaling in human melanoma. *Cancer Res* **63**:6626-6634.

Chiba T, Yokosuka O, Fukai K, Kojima H, Tada M, Arai M, Imazeki F, Saisho H. (2004). Cell growth inhibition and gene expression induced by the histone deacetylase inhibitor, trichostatin A, on human hepatoma cells. *Oncology* **66**:481-491.

Cho H, Kim JH. (2009). Lipocalin2 expressions correlate significantly with tumor differentiation in epithelial ovarian cancer. *J Histochem Cytochem* **57**:513-521.

Chu PH, Bardwell WM, Gu Y, Ross J Jr, Chen J. (2000a). FHL2 (SLIM3) is not essential for cardiac development and function. *Mol Cell Biol* **20**:7460-7462.

Chu PH, Ruiz-Lozano P, Zhou Q, Cai C, Chen J. (2000b). Expression patterns of FHL/SLIM family members suggest important functional roles in skeletal muscle and cardiovascular system. *Mech Dev* **95**:259-265.

Chun E, Lee KY. (2004). Bcl-2 and Bcl-xL are important for the induction of paclitaxel resistance in human hepatocellular carcinoma cells. *Biochem Biophys Res Commun* **315**:771-779.

Cottle DL, McGrath MJ, Cowling BS, Coghill ID, Brown S, Mitchell CA. (2007). FHL3 binds MyoD and negatively regulates myotube formation. *J Cell Sci* **15**:1423-1435.

Dai DJ, Lu CD, Lai RY, Guo JM, Meng H, Chen WS, Gu J. (2005). Survivin antisense compound inhibits proliferation and promotes apoptosis in liver cancer cells. *World J Gastroenterol* **11**:193-199.

Dannenberg LO, Edenberg HJ. (2006). Epigenetics of gene expression in human hepatoma cells: expression profiling the response to inhibition of DNA methylation and histone deacetylation. *BMC Genomics* **7**:181.

Davuluri RV. (2003). Application of FirstEF to find promoters and first exons in the human genome. *Curr Protoc Bioinformatics* Chapter 4:Unit 4.7.

Ding L, Niu C, Zheng Y, Xiong Z, Liu Y, Lin J, Sun H, Huang K, Yang W, Li X, Ye Q. (2009a). FHL1 interacts with estrogen receptors and regulates breast cancer cell growth. *J Cell Mol Med* Epub ahead of print.

Ding L, Wang Z, Yan J, Yang X, Liu A, Qiu W, Zhu J, Han J, Zhang H, Lin J, Cheng L, Qin X *et al.* (2009b). Human four-and-a-half LIM family members suppress tumor cell growth through a TGF-beta-like signaling pathway. *J Clin Invest* **119**:349-361.

Donato F, Tagger A, Gelatti U, Parrinello G, Boffetta P, Albertini A, Decarli A, Trevisi P, Ribero ML, Martelli C, Porru S, Nardi G. (2002). Alcohol and hepatocellular carcinoma: the effect of lifetime intake and hepatitis virus infections in men and women. *Am J Epidemiol* **155**:323-331.

Du X, Hublitz P, Günther T, Wilhelm D, Englert C, Schüle R. (2002). The LIM-only coactivator FHL2 modulates WT1 transcriptional activity during gonadal differentiation. *Biochim Biophys Acta* **1577**:93-101.

El-Serag HB, Rudolph KL. (2007). Hepatocellular carcinoma: epidemiology and molecular carcinogenesis. *Gastroenterology* **132**:2557-2576.

Farazi PA, DePinho RA. (2006). Hepatocellular carcinoma pathogenesis: from genes to environment. *Nat Rev Cancer* **6**:674-687.

Fernández CA, Yan L, Louis G, Yang J, Kutok JL, Moses MA. (2005). The matrix metalloproteinase-9/neutrophil gelatinase-associated lipocalin complex plays a role in breast tumor growth and is present in the urine of breast cancer patients. *Clin Cancer Res* **11**:5390-5395.

Fernandez de Mattos S, Essafi A, Soeiro I, Pietersen AM, Birkenkamp KU, Edwards CS, Martino A, Nelson BH, Francis JM, Jones MC, Brosens JJ, Coffer PJ *et al.* (2004). FoxO3a and BCR-ABL Regulate cyclin D2 Transcription through a STAT5/BCL6-Dependent Mechanism. *Mol Cell Biol* **24**:10058-10071.

Fimia GM, De Cesare D, Sassone-Corsi P. (2000). A family of LIM-only transcriptional coactivators: tissue-specific expression and selective activation of CREB and CREM. *Mol Cell Biol* **20**: 8613-8622.

Fryknäs M, Wickenberg-Bolin U, Göransson H, Gustafsson MG, Foukakis T, Lee JJ, Landegren U, Höög A, Larsson C, Grimelius L, Wallin G, Pettersson U *et al.* (2006). Molecular markers for discrimination of benign and malignant follicular thyroid tumors. *Tumour Biol* **27**:211-220.

Gabriel B, Mildenberger S, Weisser CW, Metzger E, Gitsch G, Schüle R, Müller JM. (2004). Focal adhesion kinase interacts with the transcriptional coactivator FHL2 and both are overexpressed in epithelial ovarian cancer. *Anticancer Res* **24**:921-927.

Gamen S, Anel A, Pérez-Galán P, Lasierra P, Johnson D, Piñeiro A, Naval J. (2000). Doxorubicin treatment activates a Z-VAD-sensitive caspase, which causes deltapsim loss, caspase-9 activity, and apoptosis in Jurkat cells. *Exp Cell Res* **258**:223-235.

Gangavarapu KJ, Olbertz JL, Bhushan A, Lai JC, Daniels CK. (2008). Apoptotic resistance exhibited by dexamethasone-resistant murine 7TD1 cells is controlled independently of interleukin-6 triggered signaling. *Apoptosis* **13**:1394-1400.

Gardiner-Garden M, Frommer M. (1987). CpG islands in vertebrate genomes. *J Mol Biol* **196**:261-282.

Genini M, Schwalbe P, Scholl FA, Remppis A, Mattei MG, Schafer BW. (1997). Subtractive cloning and characterization of DRAL, a novel LIM-domain protein down-regulated in rhabdomyosarcoma. *DNA Cell Biol* **16**:433-442.

Gewirtz DA. (1999). A critical evaluation of the mechanisms of action proposed for the antitumor effects of the anthracycline antibiotics adriamycin and daunorubicin. *Biochem Pharmacol* **57**:727-741.

Glaser KB, Staver MJ, Waring JF, Stender J, Ulrich RG, Davidsen SK. (2003). Gene expression profiling of multiple histone deacetylase (HDAC) inhibitors: defining a common gene set produced by HDAC inhibition in T24 and MDA carcinoma cell lines. *Mol Cancer Ther* **2**:151-163.

Greten TF, Korangy F, Manns MP, Malek NP. (2009). Molecular therapy for the treatment of hepatocellular carcinoma. *Br J Cancer* **100**:19-23.

Guo XZ, Shao XD, Liu MP, Xu JH, Ren LN, Zhao JJ, Li HY, Wang D. (2002). Effect of bax, bcl-2 and bcl-xL on regulating apoptosis in tissues of normal liver and hepatocellular carcinoma. *World J Gastroenterol* **8**:1059-1062.

Guo Z, Zhang W, Xia G, Niu L, Zhang Y, Wang X, Zhang Y, Jiang B, Wang J. (2010). Sp1 upregulates the four and half lim 2 (FHL2) expression in gastrointestinal cancers through transcription regulation. *Mol Carcinog* **49:**826-836.

Hebbes TR, Thorne AW, Crane-Robinson C. (1988). A direct link between core histone acetylation and transcriptionally active chromatin. *EMBO J* **7**:1395-1402.

Heemers HV, Regan KM, Dehm SM, Tindall DJ. (2007). Androgen induction of the androgen receptor coactivator four and a half LIM domain protein-2: evidence for a role for serum response factor in prostate cancer. *Cancer Res* **67**:10592-10599.

Hill AA, Riley PR. (2004). Differential regulation of Hand1 homodimer and Hand1-E12 heterodimer activity by the cofactor FHL2. *Mol Cell Biol* **24:**9835-9847.

Huang da W, Sherman BT, Lempicki RA. (2009). Systematic and integrative analysis of large gene lists using DAVID bioinformatics resources. *Nat Protoc* **4**:44-57.

Huang da W, Sherman BT, Tan Q, Collins JR, Alvord WG, Roayaei J, Stephens R, Baseler MW, Lane HC, Lempicki RA. (2007). The DAVID Gene Functional Classification Tool: a novel biological module-centric algorithm to functionally analyze large gene lists. *Genome Biol.* **8**:R183

Ito T, Shiraki K, Sugimoto K, Yamanaka T, Fujikawa K, Ito M, Takase K, Moriyama M, Kawano H, Hayashida M, Nakano T, Suzuki A. (2000). Survivin promotes cell proliferation in human hepatocellular carcinoma. *Hepatology* **31**:1080-1085.

Jariwala U, Prescott J, Jia L, Barski A, Pregizer S, Cogan JP, Arasheben A, Tilley WD, Scher HI, Gerald WL, Buchanan G, Coetzee GA *et al.* (2007). Identification of novel androgen receptor target genes in prostate cancer. Mol Cancer **6**:39.

Johannessen M, Møller S, Hansen T, Moens U, Van Ghelue M. (2006). The multifunctional roles of the four-and-a-half-LIM only protein FHL2. *Cell Mol Life Sci* **63**:268-284.

Johnson ME, Howerth EW. (2004). Survivin: a bifunctional inhibitor of apoptosis protein. *Vet Pathol* **41**:599-607.

Kel AE, Gossling E, Reuter I, Cheremushkin E, Kel-Margoulis OV, Wingender E. (2003). MATCH: A tool for searching transcription factor binding sites in DNA sequences. *Nucleic Acids Res* **31**:3576-3579.

Kinoshita M, Nakagawa T, Shimizu A, Katsuoka Y. (2005). Differently regulated androgen receptor transcriptional complex in prostate cancer compared with normal prostate. *Int J Urol* **12**:390-397.

Kleiber K, Strebhardt K, Martin BT. (2007). The biological relevance of FHL2 in tumour cells and its role as a putative cancer target. *Anticancer Res* **27**:55-61.

Kong Y, Shelton JM, Rothermel B, Li X, Richardson JA, Bassel-Duby R, Williams RS. (2001). Cardiac-specific LIM protein FHL2 modifies the hypertrophic response to beta-adrenergic stimulation. *Circulation* **103**:2731–2738.

Kusaba M, Nakao K, Goto T, Nishimura D, Kawashimo H, Shibata H, Motoyoshi Y, Taura N, Ichikawa T, Hamasaki K, Eguchi K. (2007). Abrogation of constitutive STAT3 activity sensitizes human hepatoma cells to TRAIL-mediated apoptosis. *J Hepatol* **47**:546-555.

Labalette C, Nouët Y, Sobczak-Thepot J, Armengol C, Levillayer F, Gendron MC, Renard CA, Regnault B, Chen J, Buendia MA, Wei Y. (2008). The LIM-only protein FHL2 regulates cyclin D1 expression and cell proliferation. *J Biol Chem* **283**:15201-15208.

Labalette C, Renard CA, Neuveut C, Buendia MA, Wei Y. (2004). Interaction and functional cooperation between the LIM protein FHL2, CBP/p300, and β-catenin. *Mol Cell Biol* **24**:10689-10702.

Lam EW, Francis RE, Petkovic M. (2006). FOXO transcription factors: key regulators of cell fate. *Biochem Soc Trans* **34**:722-726.

Lee S, Lee HJ, Kim JH, Lee HS, Jang JJ, Kang GH. (2003). Aberrant CpG island hypermethylation along multistep hepatocarcinogenesis. *Am J Pathol* **163**:1371-1378.

Lee SM, Li HY, Ng EK, Or SM, Chan KK, Kotaka M, Chim SS, Tsui SK, Waye MM, Fung KP, Lee CY. (1999). Characterization of a brain-specific nuclear LIM domain protein (FHL1B) which is an alternatively spliced variant of FHL1. *Gene* **237**:253-263.

Lee SM, Tsui SK, Chan KK, Garcia-Barcelo M, Waye MM, Fung KP, Liew CC, Lee CY. (1998). Chromosomal mapping, tissue distribution and cDNA sequence of four-and-a-half LIM domain protein 1 (FHL1). *Gene* **216**:163-170.

Leng X, Ding T, Lin H, Wang Y, Hu L, Hu J, Feig B, Zhang W, Pusztai L, Symmans WF, Wu Y, Arlinghaus RB. (2009). Inhibition of lipocalin 2 impairs breast tumorigenesis and metastasis. *Cancer Res* **69**:8579-8584.

Li HY, Ng EK, Lee SM, Kotaka M, Tsui SK, Lee CY, Fung KP, Waye MM. (2001). Protein-protein interaction of FHL3 with FHL2 and visualization of their interaction by green fluorescent proteins (GFP) two-fusion fluorescence resonance energy transfer (FRET). *J Cell Biochem* **80**:293-303.

Li M, Wang J, Ng SS, Chan CY, Chen AC, Xia HP, Yew DT, Wong BC, Chen Z, Kung HF, Lin MC. (2008). The four-and-a-half-LIM protein 2 (FHL2) is overexpressed in gliomas and associated with oncogenic activities. *Glia* **56**:1328-1338.

Li X, Jia Z, Shen Y, Ichikawa H, Jarvik J, Nagele RG, Goldberg GS. (2008). Coordinate suppression of Sdpr and Fhl1 expression in tumors of the breast, kidney, and prostate. *Cancer Sci* **99**:1326-1333.

Lüpertz R, Chovolou Y, Unfried K, Kampkötter A, Wätjen W, Kahl R. (2008). The forkhead transcription factor FOXO4 sensitizes cancer cells to doxorubicin-mediated cytotoxicity. *Carcinogenesis* **29**:2045-2052.

Makki MS, Heinzel T, Englert C. (2008). TSA downregulates Wilms tumor gene 1 (Wt1) expression at multiple levels. *Nucleic Acid Res* **36**:4067-4078.

Martin BT, Kleiber K, Wixler V, Raab M, Zimmer B, Kaufmann M, Strebhardt K (2007). FHL2 regulates cell cycle-dependent and doxorubicin-induced p21Cip1/Waf1 expression in breast cancer cells. *Cell Cycle* **6**:1779-1788.

Martin B, Schneider R, Janetzky S, Waibler Z, Pandur P, Kühl M, Behrens J, von der Mark K, Starzinski-Powitz A, Wixler V. (2002). The LIM-only protein FHL2 interacts with beta-catenin and promotes differentiation of mouse myoblasts. *J Cell Biol* **159**:113-122.

Matsumoto M, Kawakami K, Enokida H, Toki K, Matsuda R, Chiyomaru T, Nishiyama K, Kawahara K, Seki N, Nakagawa M. (2010). CpG hypermethylation of human four-and-a-half LIM domains 1 contributes to migration and invasion activity of human bladder cancer. *Int J Mol Med* **26**:241-247.

McLoughlin P, Ehler E, Carlile G, Licht JD, Schäfer BW. (2002). The LIM-only protein DRAL/FHL2 interacts with and is a corepressor for the promyelocytic leukemia zinc finger protein. *J Biol Chem* 277:37045-37053.

Méndez O, Martín B, Sanz R, Aragüés R, Moreno V, Oliva B, Stresing V, Sierra A. (2006). Underexpression of transcriptional regulators is common in metastatic breast cancer cells overexpressing Bcl-xL. *Carcinogenesis* **27**:1169-1179.

Meyer K, Lee JS, Dyck PA, Cao WQ, Rao MS, Thorgeirsson SS, Reddy JK. (2003). Molecular profiling of hepatocellular carcinomas developing spontaneously in acyl-CoA oxidase deficient mice: comparison with liver tumors induced in wild-type mice by a peroxisome proliferator and a genotoxic carcinogen. *Carcinogenesis* **24**:975-984.

Morgan MJ, Madgwick AJ. (1996). Slim defines a novel family of LIM-proteins expressed in skeletal muscle. *Biochem Biophys Res Commun* **225:**632-638.

Morlon A, Sassone-Corsi P. (2003). The LIM-only protein FHL2 is a serum-inducible transcriptional coactivator of AP-1. *Proc Natl Acad Sci USA* **100**:3977-3982.

Muller JM, Isele U, Metzger E, Rempel A, Moser M, Pscherer A, Breyer T, Holubarsch C, Buettner R, Schule R. (2000). FHL2, a novel tissue-specific coactivator of the androgen receptor. *EMBO J* **19:**359-369.

Muller JM, Metzger E, Greschik H, Bosserhoff AK, Mercep L, Buettner R, Schüle R. (2002). The transcriptional coactivator FHL2 transmits Rho signals from the cell membrane into the nucleus. *EMBO J* **21**:736–748.

Müller JM, Isele U, Metzger E, Rempel A, Moser M, Pscherer A, Breyer T, Holubarsch C, Buettner R, Schüle R. (2000). FHL2, a novel tissue-specific coactivator of the androgen receptor. *EMBO J* **19**:359-369.

Ng EK, Lee SM, Li HY, Ngai SM, Tsui SK, Waye MM, Lee CY, Fung KP. (2001). Characterization of tissue-specific LIM domain protein (FHL1C) which is an alternatively spliced isoform of a human LIM-only protein (FHL1). *J Cell Biochem* **82**:1-10.

Oh-hashi K, Koga H, Ikeda S, Shimada K, Hirata Y, Kiuchi K. (2009). CRELD2 is a novel endoplasmic reticulum stress-inducible gene. *Biochem Biophys Res Commun* **387**:504-510

Olie RA, Simões-Wüst AP, Baumann B, Leech SH, Fabbro D, Stahel RA Zangemeister-Wittke U. (2000). A novel antisense oligonucleotide targeting survivin expression induces apoptosis and sensitizes lung cancer cells to chemotherapy. *Cancer Res* **60**:2805-2809.

Pang RW, Poon RT. (2007). From molecular biology to targeted therapies for hepatocellular carcinoma: the future is now. *Oncology* **72**:30-44.

Parkin DM, Bray F, Ferlay J, Pisani P. (2005). Global cancer statistics. *CA Cancer J Clin* **55**:74-108.

Peterson CL. (2002). HDAC's at work: everyone doing their part. *Mol Cell* **9**:921-922.

Philippar U, Schratt G, Dieterich C, Müller JM, Galgóczy P, Engel FB, Keating MT, Gertler F, Schüle R, Vingron M, Nordheim A. (2004). The SRF target gene Fhl2 antagonizes RhoA/MAL-dependent activation of SRF. *Mol Cell* **16**:867-880.

Pinto AE, André S, Silva G, Vieira S, Santos AC, Dias S, Soares J. (2009). BCL-6 oncoprotein in breast cancer: loss of expression in disease progression. *Pathobiology* **76**:235-242.

Purcell NH, Darwis D, Bueno OF, Müller JM, Schüle R, Molkentin JD. (2004). Extracellular signal-regulated kinase 2 interacts with and is negatively regulated by the LIM-only protein FHL2 in cardiomyocytes. *Mol Cell Biol* **24**:1081-1095.

Qiao L, Wang Y, Pang R, Wang J, Dai Y, Ma J, Gu Q, Li Z, Zhang Y, Zou B, Lan HY, Wong BC. (2009). Oncogene functions of FHL2 are independent from NF-κBIα in gastrointestinal cancer. *Pathol Oncol Res* **15**:31-36.

Sakashita K, Mimori K, Tanaka F, Kamohara Y, Inoue H, Sawada T, Hirakawa K, Mori M. (2008). Clinical significance of loss of Fhl1 expression in human gastric cancer. *Ann Surg Oncol* **15**:2293-2300.

Sambrook J., Fritsch EF, Maniatis T. (1989). *Molecular cloning: A laboratory manual*, 2nd edition. Cold Spring Harbor Laboratory Press, Cold Spring Harbor, New York.

Scholl FA, McLoughlin P, Ehler E, de Giovanni C, Schäfer BW. (2000). DRAL is a p53-responsive gene whose four and a half LIM domain protein product induces apoptosis. *J Cell Biol* **151**:495-506.

Shathasivam T, Kislinger T, Gramolini AO. (2010). Genes, proteins and complexes: The multifaceted nature of FHL family proteins in diverse tissues. *J Cell Mol Med* in-press.

Shen Y, Jia Z, Nagele RG, Ichikawa H, Goldberg GS. (2006). SRC uses Cas to suppress Fhl1 in order to promote nonanchored growth and migration of tumor cells. *Cancer Res* **66**:1543-1552.

Shi H, Gu Y, Yang J, Xu L, Mi W, Yu W. (2008). Lipocalin 2 promotes lung metastasis of murine breast cancer cells. *J Exp Clin Cancer Res* **27**:83.

Soini Y, Chia SC, Bennett WP, Groopman JD, Wang JS, DeBenedetti VM, Cawley H, Welsh JA, Hansen C, Bergasa NV, Jones EA, DiBisceglie AM *et al.* (1996). An aflatoxin-associated mutational hotspot at codon 249 in the p53 tumor suppressor gene occurs in hepatocellular carcinomas from Mexico. *Carcinogenesis*

17:1007-1012.

Stenger JE, Xu H, Haynes C, Hauser ER, Pericak-Vance M, Goldschmidt-Clermont PJ, Vance JM. (2005). Statistical Viewer: a tool to upload and integrate linkage and association data as plots displayed within the Ensembl genome browser. *BMC Bioinformatics* **6**:95.

Stilo R, Leonardi A, Formisano L, Di Jeso B, Vito P, Liguoro D. (2002). TUCAN/CARDINAL and DRAL participate in a common pathway for modulation of NF-kappaB activation. *FEBS Lett* **521**:165-169.

Sun J, Yan G, Ren A, You B, Liao JK. (2006). FHL2/SLIM3 decreases cardiomyocyte survival by inhibitory interaction with sphingosine kinase-1. *Circ Res* **99**: 468-476.

Taira M, Evrard JL, Steinmetz A, Dawid IB. (1995). Classification of LIM proteins. *Trends Genet* **11**:431-432.

Takehara T, Liu X, Fujimoto J, Friedman SL, Takahashi H. (2001). Expression and role of Bcl-xL in human hepatocellular carcinomas. *Hepatology* **34**:55-61.

Tanahashi H, Tabira T. (2000). Alzheimer's disease-associated presenilin 2 interacts with DRAL, an LIM-domain protein. *Hum Mol Genet* **9**:2281-2289.

Teigan AB and Molund M. (2004). Mutation analysis of the FHL2 gene in human prostate and mammae cancer (Master thesis). Available from Munin open research archive at the University of Tromsø.

Thiery JP. (2003). Epithelial-mesenchymal transitions in development and pathologies. *Curr Opin Cell Biol* **15**:740-746.

Thiery JP. (2002). Epithelial-mesenchymal transitions in tumour progression. *Nat Rev Cancer* **2**:442-454.

Thomas MB, Abbruzzese JL. (2005). Opportunities for targeted therapies in hepatocellular carcinoma. *J Clin Oncol* **23**:8093-8108.

Van Lint C, Emiliani S, Verdin E. (1996). The expression of a small fraction of cellular genes is changed in response to histone hyperacetylation. *Gene Expr* **5**:245-253.

Wan S, Yim AP, Wong CK, Arifi AA, Yip JH, Ng CS, Waye MM, Lam CW. (2002). Expression of FHL2 and cytokine messenger RNAs in human myocardium after cardiopulmonary bypass. *Int J Cardiol* **86**:265-272.

Wang J, Yang Y, Xia HH, Gu Q, Lin MC, Jiang B, Peng Y, Li G, An X, Zhang Y, Zhuang Z, Zhang Z *et al.* (2007). Suppression of FHL2 expression induces cell differentiation and inhibits gastric and colon carcinogenesis. *Gastroenterology* **132**:1066-1076.

Wei Y, Renard CA, Labalette C, Wu Y, Lévy L, Neuveut C, Prieur X, Flajolet M, Prigent S, Buendia MA. (2003). Identification of the LIM protein FHL2 as a coactivator of beta-catenin. *J Biol Chem* **278**:5188-5194.

Wixler V, Hirner S, Müller JM, Gullotti L, Will C, Kirfel J, Günther T, Schneider H, Bosserhoff A, Schorle H, Park J, Schüle R *et al.* (2007). Deficiency in the LIM-only protein Fhl2 impairs skin wound healing. *J Cell Biol* **177**:163-172.

Workman JL, Kingston RE. (1998). Alteration of nucleosome structure as a mechanism of transcriptional regulation. *Annu Rev Biochem* **67**:545-579.

Yamashita Y, Shimada M, Harimoto N, Rikimaru T, Shirabe K, Tanaka S, Sugimachi K. (2003). Histone deacetylase inhibitor trichostatin A induces cell-cycle arrest/apoptosis and hepatocyte differentiation in human hepatoma cells. *Int J Cancer* **103**:572-576.

Yan J, Zhu J, Zhong H, Lu Q, Huang C, Ye Q. (2003). BRCA1 interacts with FHL2 and enhances FHL2 transactivation function. *FEBS Lett* **553**:183-189.

Yang Y, Hou H, Haller EM, Nicosia SV, Bai W. (2005). Suppression of FOXO1 activity by FHL2 through SIRT1-mediated deacetylation. *EMBO J* **24**:1021-1032.

Yan J, Zhu J, Zhong H, Lu Q, Huang C, Ye Q. (2003). BRCA1 interacts with FHL2 and enhances FHL2 transactivation function. *FEBS Lett* **553**:183-189.

Venturelli S, Armeanu S, Pathil A, Hsieh CJ, Weiss TS, Vonthein R, Wehrmann M, Gregor M, Lauer UM, Bitzer M. (2007). Epigenetic combination therapy as a tumor-selective treatment approach for hepatocellular carcinoma. *Cancer* **109**:2132-2141.

Yu J. (2010). Epigenetic inactivation of *paired box gene 5* is associated with poor prognosis in gastric cancer patients. Presented at School of Biomedical Sciences Research Day on June 15, 2010.

Yu HG, Ai YW, Yu LL, Zhou XD, Liu J, Li JH, Xu XM, Liu S, Chen J, Liu F, Qi YL, Deng Q *et al.* (2008). Phosphoinositide 3-kinase/Akt pathway plays an important role in chemoresistance of gastric cancer cells against etoposide and doxorubicin induced cell death. *Int J Cancer* **122**:433-443.

Zhang R, Ma L, Zheng M, Ren J, Wang T, Meng Y, Zhao J, Jia L, Yao L, Han H, Li K, Yang A. (2010). Survivin knockdown by short hairpin RNA abrogates the growth of human hepatocellular carcinoma xenografts in nude mice. *Cancer Gene Ther* **17**:275-288.

Zhang W, Jiang B, Guo Z, Sardet C, Zou B, Lam CS, Li J, He M, Lan HY, Pang R, Hung IF, Tan VP *et al.* (2010). Four and a half LIM protein 2 (FHL2) promotes invasive potential and epithelial-mesenchymal transition in colon cancer. *Carcinogenesis* **31**:1220-1229.

Zhang YJ, Wu HC, Shen J, Ahsan H, Tsai WY, Yang HI, Wang LY, Chen SY, Chen CJ, Santella RM. (2007). Predicting hepatocellular carcinoma by detection of aberrant promoter methylation in serum DNA. *Clin Cancer Res* **13**:2378-2384.

Supplementary Table S1: Below is a list of the genes significantly altered in FHL2 knockout mice compared to wild-type littermates. Genes with over 2 fold difference were classified into functional categories according to their gene ontology (GO) terms.

Categories	Accession no.	Gene name	Symbol	Function	Fold change (vs. WT)
Binding	NM_031368	Bone gamma-carboxyglutamate protein, related sequence	Bglap-rs1	Calcium ion binding	-2.491
	NM_029720	Cysteine-rich with EGF-like domains 2	Creld2	Calcium ion binding	-2.099
	NM_027687	Calcium-binding tyrosine-(Y)-phosphorylation regulated fibrous sheath protein	Cabyr	Calcium ion binding	3.340
	NM_009744	B-cell leukemia/lymphoma 6	Bcl6	Nucleic acid binding	-3.939
	NM_009556	Zinc finger protein 42	Zfp42	Nucleic acid binding	2.363
	NM_175934	Protein phosphatase 1, regulatory subunit 10	Ppp1r10	Nucleic acid binding	2.190
	NM_008262	One cut domain, family member 1	Onecut1	DNA binding	2.407
	NM_011314	Serum amyloid A2	Saa2	Protein binding	2.248
	NM_029726	Triadin	Trdn	Protein binding	-2.364
	X70423	Immunoglobulin heavy chain (gamma polypeptide)	Ighg	Antigen binding	2.157
	NM_008386	Insulin I	Ins1	Hormone activity	-2.279
	NM_008382	Inhibin beta E	Inhbe	Hormone activity	2.171
Catalytic Activity	NM_020559	Aminolevulinic acid synthase 1	Alas1	Heme biosynthesis	2.452
	NM_007811	Cytochrome P450, family 26, subfamily a, polypeptide 1	Cyp26a1	Monooxygenase activity	2.141
	NM_010000	Cytochrome P450, family 2, subfamily b, polypeptide 9	Cyp2b9	Oxidation reduction	2.047

	ENSMUST00000108128	Adenosine deaminase domain containing 1 (testis specific)	Adad1	RNA binding	-2.142
	NM_007887	Deubiquitinating enzyme 1	Dub1	Ubiquitin thiolesterase activity	-1.869
	NM_023850	Carbohydrate (keratan sulfate Gal-6) sulfotransferase 1	Chst1	Sulfotransferase activity	-2.210
	NM_001013376	Ribonuclease P/MRP 38 subunit (human)	Rpp38	Ribonuclease P activity	2.151
	NM_146256	4-hydroxyphenylpyruvate dioxygenase-like	Hpdl	4-hydroxyphenylpyruvate dioxygenase activity	-2.138
Enzyme Regulator Activity	NM_175934	Protein phosphatase 1, regulatory subunit 10	Ppp1r10	Regulation of catalytic actvity	2.190
	NM_027687	Calcium-binding tyrosine-(Y)-phosphorylation regulated fibrous sheath protein	Cabyr	Signal transduction	3.340
Transcription Regulator Activity	NM_009744	B-cell leukemia/lymphoma 6	Bcl6	Nucleic acid binding	-3.939
	NM_175934	Protein phosphatase 1, regulatory subunit 10	Ppp1r10	Transcription	2.190
	NM_008262	One cut domain, family member 1	Onecut1	Liver Development	2.407
Molecular Transducer Activity	NM_147001	Olfactory receptor 172	Olfr172	Signal transducer activity	2.579
	NM_146811	Olfactory receptor 910	Olfr910	Signal transducer activity	1.551
	NM_146730	Olfactory receptor 1095	Olfr1095	Signal transducer activity	1.947
Electron Carrier Activity	NM_007811	Cytochrome P450, family 26, subfamily a, polypeptide 1	Cyp26a1	Electron carrier activity	2.141

Transporter Activity	NM_008491	Lipocalin 2	Lcn2	Transporter activity	3.125
Miscellaneous	NM_175204	Proteasome (prosome, macropain) subunit, beta type, 11	Psmb11	Protein catabolic process	2.020
	NM_029662	Major facilitator superfamily domain containing 2	Mfsd2	Transport	3.584
Unclassified (Unknown)	NM_026613	Coiled-coil domain containing 34	Ccdc34	---	2.163
	ENSMUST00000069293	Dynein, axonemal, heavy chain 7B	Dnahc7b	---	-2.136
	NR_003633	Maternally expressed 3	Meg3		2.262
	XR_032419	Predicted gene, EG435727	EG435727	---	2.931
	XR_032980	Predicted gene, OTTMUSG00000007905	OTTMUSG00000007905	---	2.941
	NM_175442	RIKEN cDNA A630033H20 gene	A630033H20Rik	---	2.121
	NR_003646	RIKEN cDNA 4921511C20 gene	4921511C20Rik	---	-2.514
	NM_001081643	X-linked lymphocyte-regulated 3B	Xlr3b	---	2.093
	NM_021365	X-linked lymphocyte-regulated 4B	Xlr4b	---	4.277
	NM_183094	X-linked lymphocyte-regulated 4C	Xlr4c	---	4.459

Supplementary Table S2: Details characteristics of HCC patients analyzed in the present study

Code	Sex	Age	Largest size	Tumor Size	HBV	AJCC Stage	Differentiation	Vascular Inv	Cirrhosis
265	F	63	1.2	<5	positive	I	well	negative	positive
271	M	46	5	>=5	positive	IIIA	moderate	negative	positive
293	M	45	4.5	<5	positive	I	moderately differentiated	negative	negative
305	M	68	2	<5	positive	II	mod to poorly	negative	negative
312	M	70	5.5	>=5	negative	I	moderately	negative	negative
316	M	74	3.5	<5	negative	I	well to moderately	negative	positive
318	M	33	2.5	<5	positive	I	moderate	negative	negative
348	F	41	2.5	<5	positive	I	moderate	negative	positive
350	M	72	7	>=5	negative	I	moderately differentiated	negative	negative
353	M	73	4.5	<5	negative	I	moderately differentiated	positive	positive
360	F	45	3.4	<5	positive	I	moderate	negaitve	negative
370	M	43	13.2	>=5	positive	III	moderate	positive	positive
383	M	43	3.5	<5	positive	IIIB	moderate	negative	positive
385	M	52	3	<5	positive	I	well	negative	negative
397	M	63	3.5	<5	negative	I	moderate	negative	positive
404	M	74	6	>=5	positive	IIIB	moderately differentiated	negative	negative
412	M	27	5	>=5	positive	I	moderate	negative	negative
414	F	72	5.2	>=5	positive	II	poor	negative	positive
418	M	59	7	>=5	positive	I	moderate	negative	negative
419	F	78	5.3	>=5	negative	I	moderately well	negative	negative
420	M	59	5.8	>=5	positive	I	well to moderate	negative	negative
422	M	42	3	<5	positive	I	moderate to well	negative	negative

425	M	38	10.5	>=5	positive	I	moderate	negative	negative
426	M	45	7.5	>=5	positive	IIIA	moderate	negative	positive
427	M	53	3	<5	positive	I	well to moderate	negative	negative
432	M	33	10	>=5	positive	IIIA	moderate to poor	negative	negative
433	M	40	6.5	>=5	positive	IIIA	well to moderate	positive	positive
434	F	45	10	>=5	positive	I	well	negative	negative
435	M	60	6.4	>=5	positive	I	moderately	negative	negative
437	M	50	4	<5	positive	I	moderate	negative	negative
439	M	40	2.3	<5	positive	I	poor to moderate	negative	positive
445	M	60	none	none	negative	missing	moderately differentiated	negative	positive
447	F	71	3	<5	positive	I	well to moderate	negative	positive
451	F	60	4	<5	positive	I	moderate	negative	positive
455	M	57	3.8	<5	positive	I	well differentiated	negative	positive
460	M	70	5.9	>=5	positive	I	moderately differentiated	negative	negative
465	M	58	6.5	>=5	negative	IIIA	poorly differentiated	negative	positive
469	F	67	5.5	>=5	negative	I	moderate	negative	positive
478	M	64	2.8	<5	positive	I	moderately	negative	positive
481	M	49	9	>=5	positive	I	moderate	negative	negative
522	F	42	3.5	<5	positive	I	moderate	negative	positive
534	F	45	6	>=5	positive	II	moderately	positive	negative